THE UNIVERSITY OF QUEENSLAND

A U S T R A L I A

Development of a lipoid microbubble formulation and *in vitro* evaluation assisted by ultrasound

Daniel Mobasseri

Doctor of Pharmacy (Pharm.D.)

A thesis submitted for the degree of Master of Philosophy at

The University of Queensland in 2018

School of Pharmacy

Abstract

The pursuit of targeted drug delivery leading to improved efficacy, mitigated side effects and desirable therapeutic outcomes has drawn much interest in recent decades. In this context this research aimed to develop a lipoid microbubble (LMB) platform, which upon application of ultrasound (US) cavitates the LMBs releasing energy pulses in the form of micro-jets and shockwaves facilitating penetration of drug into tissues. The energy released following cavitation of micron-sized, echogenic vesicles is purported to have potential in enhancing localized cellular uptake of drug and/or increase the depth of penetration of drug into tissue.

In this research novel, for the first time, a reproducible method for preparation of ciprofloxacin filled US-responsive LMBs (CLMB) with high loading efficiency (i.e. $\cong 90\%$) and extended *in vitro* stability was developed and optimized. Moreover, a range of US parameters, namely frequency, duration, power and duty cycle were optimized to ensure negligible hyperthermic effects on the LMBs and surrounding media. To study the effects of cavitation, LMBs were first prepared and mixed with a low viscosity Carbopol®-based gel infused with rhodamine B, a red water-soluble dye, which was then applied to agarose models of varying rigidity/permeability. Optimized US was then applied to the gel and dye penetration into agarose films was measured. One of the main challenges observed in this study was the gradual unassisted diffusion of dye into the agarose films hindering an accurate measurement of depth of penetration as potentiated by US. Therefore, a Franz cell diffusion apparatus-based study was designed/performed next, to further investigate the effect of LMB cavitation on penetration of dye across a 3.5 kDa molecular weight cut-off SnakeSkin™ dialysis membrane, using the aforementioned optimized US parameters. The results did not show any improvements in penetration of dye across agarose barrier models compared to the control arms.

Next, bacteria time kill studies were designed/performed to test if the LMBs synergistically increase the efficacy of the fluoroquinolone antibiotic, ciprofloxacin on *Pseudomonas aeruginosa*, which commonly colonises burns/chronic wounds. The results did not show any synergistic bactericidal effects of the cavitation in the presence of ciprofloxacin. Next, another study using Trypan blue, an agent impermeable to bacteria, was trialled to ascertain whether cavitation facilitated its penetration into the aforementioned bacteria. However, the recorded absorbance correlating to intracellular Trypan blue fell below the limit of detection in this assay, and an inconclusive result was recorded.

From the collection of studies presented in this thesis limitations in the low intensity US device in imparting effective dye permeation/drug delivery became apparent. In light of this,

access to and development of a more versatile US unit is required in order to prove the applicability of US-assisted drug delivery from LMBs. It is expected this could be facilitated through a set-up comprising of an oscilloscope, hydrophone, and high-speed camera, which would pave the way for effective monitoring of the cavitation effects of LMBs assisted by a tunable US device.

Declaration by author

This thesis is composed of my original work, and contains no material previously published or written by another person except where due reference has been made in the text. I have clearly stated the contribution by others to jointly-authored works that I have included in my thesis.

I have clearly stated the contribution of others to my thesis as a whole, including statistical assistance, survey design, data analysis, significant technical procedures, professional editorial advice, financial support and any other original research work used or reported in my thesis. The content of my thesis is the result of work I have carried out since the commencement of my higher degree by research candidature and does not include a substantial part of work that has been submitted to qualify for the award of any other degree or diploma in any university or other tertiary institution. I have clearly stated which parts of my thesis, if any, have been submitted to qualify for another award.

I acknowledge that an electronic copy of my thesis must be lodged with the University Library and, subject to the policy and procedures of The University of Queensland, the thesis be made available for research and study in accordance with the Copyright Act 1968 unless a period of embargo has been approved by the Dean of the Graduate School.

I acknowledge that copyright of all material contained in my thesis resides with the copyright holder(s) of that material. Where appropriate I have obtained copyright permission from the copyright holder to reproduce material in this thesis and have sought permission from co-authors for any jointly authored works included in the thesis.

<u>Publications during candidature</u>

No publications

<u>Publications included in this thesis</u>

No publications included

Contributions by others to the thesis

No contributions by others.

Statement of parts of the thesis submitted to qualify for the award of another degree

None.

Research Involving Human or Animal Subjects

No animal or human subjects were involved in this research.

Acknowledgements

Keywords

Lipoid microbubble, ultrasound (US), cavitation, penetration depth, agarose model, barrier model, echogenicity, stability, ciprofloxacin

Australian and New Zealand Standard Research Classifications (ANZSRC)

ANZSRC code: 111504, Pharmaceutical Sciences, 80%

ANZSRC code: 110801, Medical Bacteriology, 20%

Fields of Research (FoR) Classification

FoR code: 1115, Pharmacology and Pharmaceutical Sciences, 80%

FoR code: 1108, Medical Microbiology, 20%

Contents

Table of figures:

Chapter 1: literature review

1. Introduction

The main aim of this research was to develop stable LMBs, derived from lipoid-based particles (i.e. liposomes), and investigate if their US mediated cavitation could assist drug delivery/efficacy in wound models. While having a complete discussion about clinical applications of lipoid based particles is beyond the scope of the thesis, the focus of this chapter is to first review some of the successful lipoid particles and their clinical applications (i.e. optimizing the pharmacokinetics of drugs for better therapeutic outcomes). Then the discussion further continues by explaining chronic wounds, current treatments and the potential of different carrier systems to better manage and treat wounds. At the end of this chapter, LMBs and their clinical applications have been elaborated.

1.1. Lipoid based drug delivery systems in clinic

Despite a plethora of new techniques being available in the design and development of drug molecules, the success rate in proceeding to the clinic remains low. Therefore, one of the emerging strategies to improve systemic treatments is to alter the pharmacokinetics (PK) and pharmacodynamics (PD) of classic drugs with the aid of carrier systems. Successful delivery of a molecule to its site of action is the cornerstone of modern treatments and remains a challenge particularly following systemic treatment with drugs having a high volume of distribution (V_d). The correlation between the expected effect(s) of the drug and the severity of its side effect(s) invariably dictates the loading/maintenance dose for a given condition in the development of each treatment (1).

In the case of chemotherapeutics many lack specificity for the proposed site of action resulting in both healthy and cancerous cells being affected, which leads to debilitating side effects. Nano carrier systems, with ability to preferentially deliver and trap chemotherapeutics in tumour site thus minimising the exposure of healthy tissues to the cytotoxic drugs, are proposed as ideal vectors tomitigate the incidence and severity of side effects (2). The phenomenon is referred to as the enhanced permeation and retention (EPR) effect, which is due to the immature vasculature system in tumours (Figure 1-1). That said, in the context of cancer treatment even when employing a carrier system to deliver a drug, chemotherapy is far from perfect in clinical settings (e.g. cardiotoxicity in treatment with Doxil® (3) and/or peripheral neuropathy in treatment with Abraxane® (4)). The complex vasculature of a tumour can lead to unpredictable drug deposition, while lymphatic drainage is an often-overlooked parameter (5).

Healthy microvasculature

Tumour microvasculature

Tumour microvasculature

Healthy microvasculature

Tumour microvasculature

Healthy microvasculature

Tumour microvasculature

Tumour Cell

Healthy Cell

Collagen

T cells

Red blood cells

B cells

Drug filled liposome
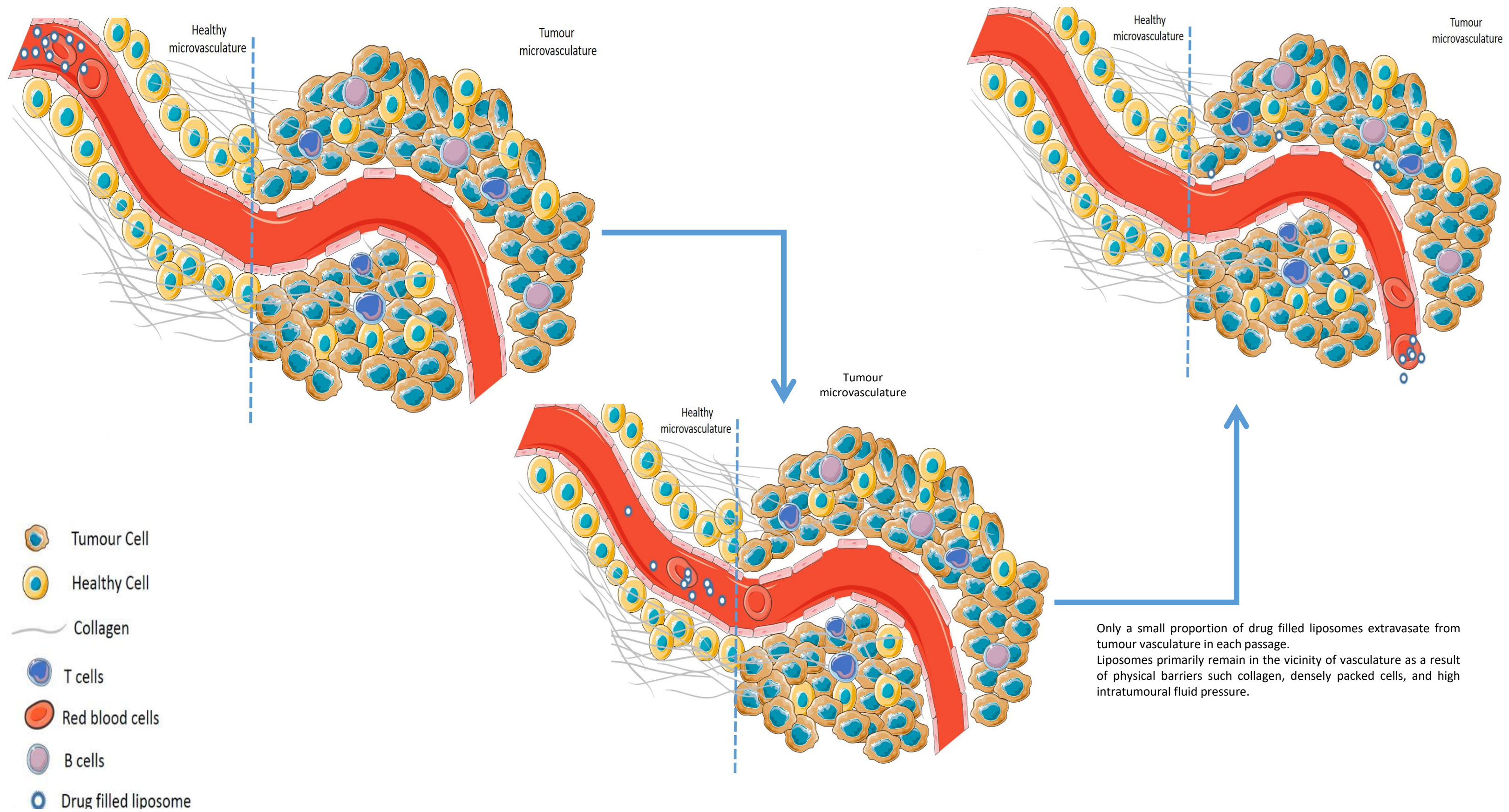
Only a small proportion of drug filled liposomes extravasate from tumour vasculature in each passage.
Liposomes primarily remain in the vicinity of vasculature as a result of physical barriers such collagen, densely packed cells, and high intratumoural fluid pressure.

Figure 1-1: Enhanced permeation and retention (EPR) effect: The cells inside the vasculature system are simplified for a better demonstration. Images are taken from Servier Medical Art (http://smart.servier.com/)

Another example in enhancing the therapeutic efficacy of classic drugs using lipoids is liposomal amphotericin B (AmBisome®). Compared to conventional amphotericin, this FDA approved product has higher fungicidal effects and a better toxicity profile (i.e. less nephrotoxicity and infusion-related reactions) (6), which is due to a higher affinity of the liposomes (containing amphotericin B) for the fungi cell membrane compared to free drug (7).

DepoFoam® is another successful lipid based drug delivery platform with local applications (i.e. infiltration administration) in which spherical micron sized lipoid particles together form multi-vesicular honeycomb-like structures (Figure 1-2) (8). The aforesaid scaffold provides numerous internal aqueous chambers with ability to store and slow-release the core drug. Bupivacaine, a local anaesthetic of the amide type, has been successfully reformulated using the aforementioned platform to induce longer anaesthesia (i.e. EXPAREL®) obviating the need for post-surgery administration of opioids, especially in patients undergoing haemorrhoidectomy (9).
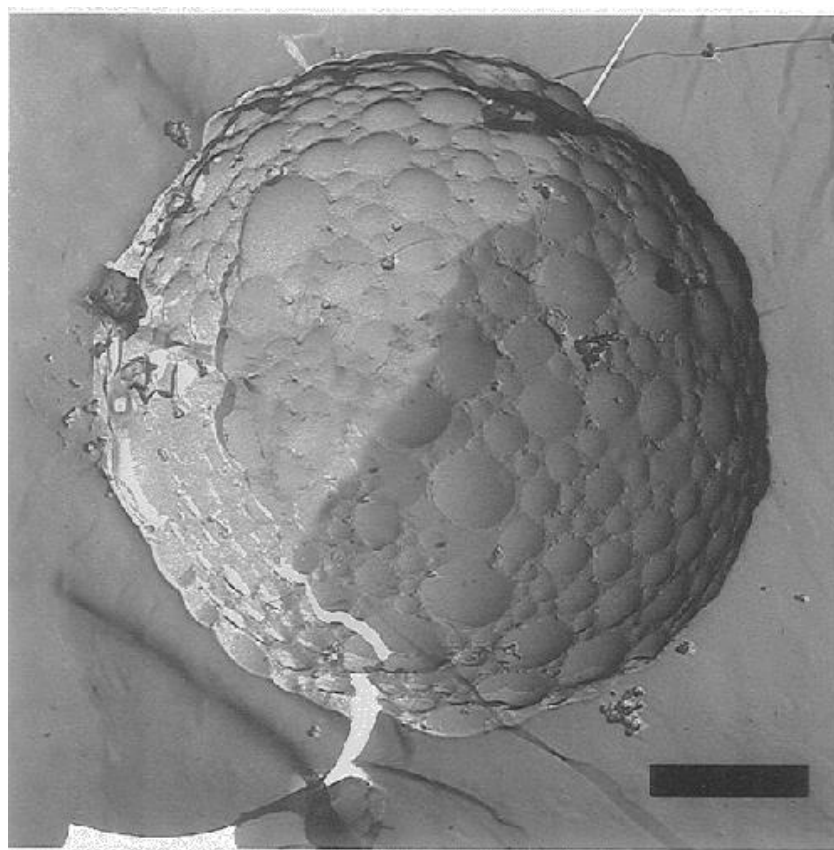
Figure 1-2: Electron micrograph showing the honeycomb structure of a freeze-fractured multivesicular liposomes in DepoFoam®, Reprinted with permission from (8) Copyright (1996) American Chemical Society

1.2. Challenges in the design of nanosized carriers with systemic applications

The use of nanomaterials to improve the PK/PD profile leading to better therapeutic outcomes faces a range of challenges from design (e.g. formulation from lab to industry) to clinical (e.g. different response in different patients) perspectives. Therefore, a multi-faceted approach considering all the aforesaid challenges is benchmark for the successful design and translation of nanomedicine. Despite significant advancements in nanomedicine, high toxicity in preclinical studies arising from the nanocarrier itself or undesirable pharmacodynamics delays the development of new generation nanocarriers (10). Detection of nanomaterials by the immunity system and/or their clearance from the body are other challenges in this regard and should be taken into consideration during developing nanoparticle based carrier systems for the purpose of systemic treatments (11). For example, a solute smaller than 10 nm is rapidly cleared from blood by the kidneys whereas micronize particles (12) are detected and eliminated by organs of the reticuloendothelial system (e.g. spleen, liver) (10).

1.3. Liposomes – from preparation to systemic application

Liposomes were first described by Bangham et al. in 1965 (13-15) as phospholipid-based amphipathic molecules with two ends: a hydrophilic head (phospho-) and a hydrophobic tail (-lipid) (Figure 1-3 A, B). In aqueous media, they together form bilayered-spheroid-like structures with an inner aqueous core (i.e. liposome) (Figure 1-3 C) (16, 17).
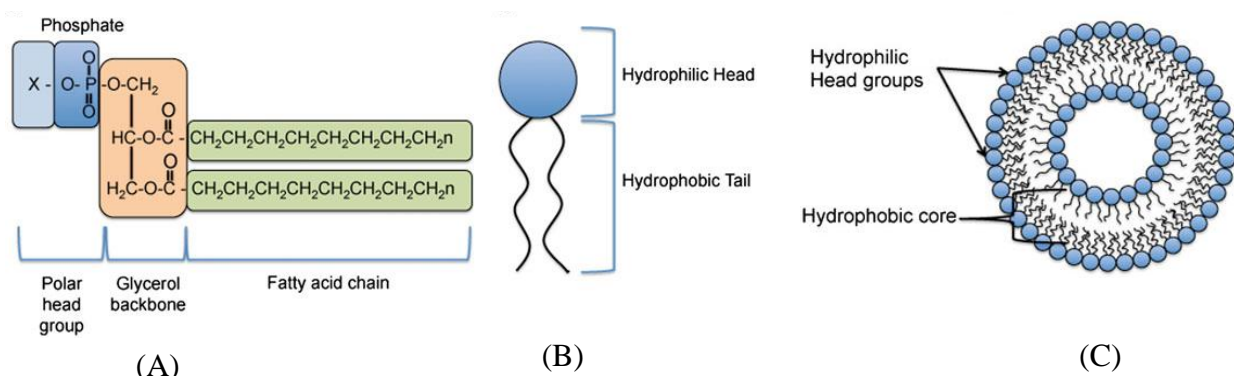
Figure 1-3: Molecular structure of phospholipid (A, B) and array of phospholipids in bilayer membrane of liposome (C). Adapted/Translated with permission from (17) copyright (2013)

Anthracyclines, such as doxorubicin, are a chemotherapeutic class widely used in combination with other chemotherapeutics in the treatment of different cancers such as ovarian cancer, AIDS-related Kaposi's sarcoma and haematological malignancies (18). However,

debilitating side effects derived from these compounds have limited their use and administration. For example, it has been shown around 10% of patients treated with doxorubicin present with cardiac related problems up to 10 years after receiving chemotherapy (19). Doxil®, a US-FDA approved doxorubicin liposomal formulation (20), is widely administered in treatment of Kaposi sarcoma in patients with compromised immunity system (e.g. AIDS) (21, 22). As mentioned earlier, tumour vasculature has higher permeability whilst normal tissues are nurtured by vessels with tight capillary junctions. In this case, the nano-sized liposomes prevents preferential penetration and deposition into tissues other than the tumour site, which is known as passive targeting highlighted earlier in this chapter (23, 24) (please see Figure 1-1).

One of the main challenges in the formulation of liposomes, is to retain the intra-liposomal hydrophilic drugs before administration. The challenge has led to the use of fluid membrane tightening materials, in particular cholesterol in bilayer membrane (25-27). However, lack of ability to retain hydrophobic drugs is still known as an inherent drawback in this carrier system. The liposomal membrane is similar to biological membranes in molecular composition allowing hydrophobic molecules freely cross the bilayer membrane. This has prevented liposomes from being a suitable carrier system for hydrophobic drugs such as paclitaxel (28). Table 1-1 briefly shows some commercial formulations based on lipid(29).

To date, different methods have been developed for the preparation of liposomes, and a summary of these along with their advantages and disadvantages are shown in Table 1-2.

Table 1-1: US-FDA approved liposome/lipid based formulations, reproduced with permission from (29)

Brand name	Administration route	The containing drug	Size/type of particle	Drug form/ storage period	Lipid composition	Indication	Ref.
Ambisome®	Intravenous (IV)	Amphotericin B	Liposome	Powder/36 months	HSPC/DSPG/ Cholesterol and amphotericin B (2:0.8:1:0.4 molar ratio)	Severe fungal infections	(30-32)
Abelcet®	IV	Amphotericin B	Lipid complex	Suspension/ 24 months	DMPC/DMPG (7:3 molar ratio)	Sever fungal infections	(33)
Amphotec®	IV	Amphotericin B	Lipid complex	Powder/24 months	Cholesteryl sulphate	Sever fungal infections	(34)
DaunoXome®	IV	Daunorubicin	Liposome	Emulsion/12 months	DSPC/Cholesterol	Blood tumours	(32, 35, 36)
Doxil®	IV	Doxorubicin	PEGylated liposome	Suspension/20 months	HSPC, cholesterol, and PEG 2000-DSPE (56:39:5 molar ratio)	Kaposi's sarcoma, Ovarian/breast cancer	(32, 37, 38)
Lipo-dox®	IV	Doxorubicin	PEGylated liposome	Suspension/36 months	DSPC, cholesterol, and PEG 2000-DSPE (56:39:5 molar ratio)	Kaposi's sarcoma, Ovarian/breast cancer	(39)
Myocet®	IV	Doxorubicin	Liposome	Powder/18 months	EPC and cholesterol (55:45 molar ratio)	Combination therapy with cyclophosphamide in metastatic breast cancer	(32, 38, 40)
Visudyne®	IV	Verteporfin	Liposome	Powder/48 months	EPG and DMPC (3:5 molar ratio)	Age-related macular degeneration, pathologic myopia, ocular histoplasmosis	(41, 42)
Depocyt®	Spinal	Cytarabine	Liposome	Suspension/18 months	Cholesterol, Triolein, DOPC, and DPPG (11:1:7:1 molar ratio)	Neoplastic meningitis and lymphomatous meningitis	(32, 43)
DepoDur®	Epidural	Morphine sulphate	Liposome	Suspension/24 months	Cholesterol, Triolein, DOPC, and DPPG (11:1:7:1 molar ratio)	Pain management	(44, 45)
Epaxal®	Intramuscular	Inactivated hepatitis A virus (strain RG-SB)	Liposome	Suspension/36 months	DOPC and DOPE	Hepatitis A	(46)
Inflexal V®	Intramuscular	Inactivated hemaglutinine of Influenza virus strains A and B	Liposome	Suspension/12 months	DOPC and DOPE	Influenza	(47)

Method	Advantage	Disadvantage	Ref.
Lipid film hydration	Simple and quick production method	Formation of polydisperse multilamellar vesicles	(48)
Reverse phase evaporation	Production of bulky liposomes with high entrapment capacity, easy to scale up	The use of organic solvent	(48, 49)
Detergent removal	High entrapment efficiency	Preparation issues, bio-macromolecule denaturation caused by detergent	(50)
The ethanol injection method	Simplicity of the method, fast preparation with good reproducibility, negligible lipid degradation and/or oxidative alterations	Use of organic solvent in manufacturing process, low encapsulation efficiency, diluted liposomes	(51-53)
Proliposome-liposome method	Simple and practical technique, high entrapment efficiency, suitable for various drugs with different water and alcohol solubilities	Scaling up issues, the use of organic solvent	(52, 54)

In general, loading the liposomes with drug molecules of interest is another challenge in the production procedure. This step is termed "remote loading" because encapsulation of drug happens after the formation of vesicles (28).The efficiency of loading step can be calculated via the following equation:

$$\% \: Loading \: efficiency = \frac{The \: amount \: of \: drug \: entrapped \: inside \: the \: liposome}{The \: total \: amount \: of \: drug \: added \: to \: the \: solution} \times 100$$

The most common technique used for remote loading is to precipitate the drug inside the vesicle via (55-57):

1. Establishment of transmembrane pH gradients;
2. Using a proton-generating dissociable salt such as ammonium sulphate (Figure 1-4) (58).
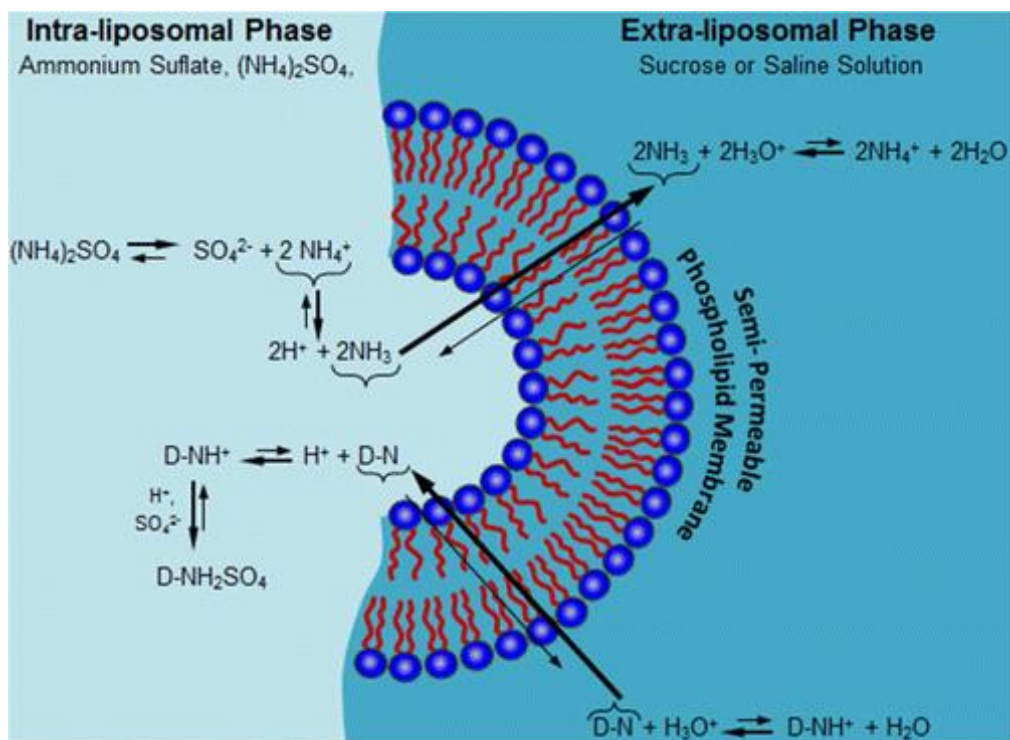
Figure 1-4: Chemical mechanism of remote loading of drug into liposomes, entrapment of drug molecules inside liposomes occurs via conjugation with sulphate ions, the remote loading is performed at 10 °C above the transition temperature of the phospholipids in the bilayer membrane, reprinted with permission from (58) copyright (2016) American Chemical Society

Mononuclear phagocytic (MP) cells constantly detect exogenous particles and clear them from the body. Therefore, liposomes , being an exogenous particle, can be identified and rapidly cleared from the blood circulation by these cells(59-61). Hence, in order to prevent this , polyethylene glycol (PEG) is widely used and incorporated onto lipid bilayers to disguise liposomes from MP cells (32).

As mentioned previously, an ideal drug carrier for cancer chemotherapy sustains the release of chemotherapeutics while accumulating in tumour site (see chapter 1.1) (62, 63). Liposomal formulations have shown better therapeutic efficacy compared to their conventional formulations (64) by having lower side effects (65), improved tumour targeting (66), longer half-life of the drug (67) and slow drug releasing properties (68).

1.4. Chronic wounds

Chronic wounds are long lasting non healing wounds which are generally classified to: diabetic foot ulcers, pressure ulcers and vascular ulcers (69). Several pathophysiological factors have been postulated to be responsible for failure of these wounds to heal including: persistent inflammation caused by local hypoxia, presence of microbial biofilms resistant to antibiotics, and lack of respond to reparative stimuli by dermal and/or epidermal cells (70, 71).

Chronic wounds are reported to place a significant burden (i.e. $\cong$ A\$2.8 billion) on Australian healthcare system and the estimated cost is anticipated to increase by the growing aging population (72). Therefore, from an economical aspect, there is a substantial need for design and develop of new treatment platform(s) which can accelerate the healing procedure in these wounds hence reducing the cost(s) of treatment while increasing the patients' comfort.

1.4.1. Management of chronic wounds

The success rate in treatment of these wounds relies on choosing the right strategies to concurrently address the aetiology and the underlying cause in these wounds. Accordingly, the first approach in the management of chronic wounds is to diagnose and identify the cause of delay in healing. The next step is to cover as many aspects as possible in these wounds via a multidisciplinary patient-centred approach (73).

1.4.2. Wound debridement

Arguably, surgical treatment (also known as sharp debridement) is considered as the most efficient treatment strategy for chronic wounds which can accelerate the healing of these wounds via remove of necrotic tissue, senescent cells, and biofilms (74). However, one setback in debridement is the delay of healing caused by excessive sharp debridement (69). Alternatively, the following non-surgical debridement are performed in patients who cannot undergo surgery (74):

- Mechanical debridement: using hydrotherapy, wound irrigation and negative pressure wound therapy
- Enzymatic debridement: using debriding enzymes such as collagenase
- Biologic debridement: using sterilized maggots which would selectively attack and digest the necrotic tissue while secreting bactericidal enzymes

1.4.3. Wound dressings

Today, a wide range of wound dressings are available for the treatment of these wounds such as gauzes, films, hydrogels, hydrocolloids, alginates, hydrofibres, and foams (75). Ideal dressings for these wounds are the ones with ability to cover as many aspects as possible such as: removing the excess exudates while maintaining the moist, preventing contaminants to enter the wound bed, having no discomfort for patient on its removal, leaving no debris behind in wound bed after removal, mitigating pain, and negligible allergic reactions(76). Given the

complex pathophysiology of these wounds, none of the currently marketed dressings have been able to cover all the aforesaid aspects simultaneously in such wounds.

ENLUXTRA™ is a smart wound dressing with unique properties due to its proprietary smart polymers embedded with hydrogels. The dressing senses and responds to the 'changing' wound via absorbing exudates from wound zones while hydrating other dry zones (77).

Figure 1-5 briefly describes the principles involved in the management of chronic wounds (78).

Figure 1-5: Principles in the management of chronic wounds (78)

1.4.4. Antibiotics in chronic wound management

Inadequate blood perfusion in chronic wounds prevents sufficient delivery of intravenously administered antibiotic(s) to the bacteria in the wound. Therefore, having the advantage of delivering a bolus dose directly to the intended site with negligible off-target toxicities of topical antibiotics is a preferred (79). However, despite sustained delivery in topical antibiotics, tightly packed polymeric matrices (i.e. biofilms) around the present bacteria creates another major obstacle against drug delivery to the bacteria in these wounds (80) and is deemed to play a crucial role in delay of healing via:

- Blocking the delivery of therapeutic molecule of interest to their target (i.e. the present bacteria)
- Impeding the immune cells reach the present bacteria which would consequently result in constant stimulation of immune system with no considerable therapeutic outcome(s) hence collateral damage of the peri-wound tissue (81).

1.4.5. Nanotechnology in chronic wounds

Despite a myriad of nanomaterials have been tested to enhance/accelerate the healing course in chronic wounds, silver NPs have been the only successful NPs paving their way to clinic with inherent antimicrobial and anti-inflammatory properties (82). Moreover, a number of NPs with/without intrinsic healing properties are currently under development for this purpose. For example, chitosan-based copper nanocomposites have shown their ability to accelerate healing of wound in rat models via regulating cells, cytokines and growth factors in these wounds (83). In another attempt, gold-NPs-conjugated-nucleic-acids dispersed in Aquaphor® have shown their ability to penetrate into skin and preventing synthesis of ganglioside-monosialic acid 3 synthase, a substance known to impede wound healing, thus accelerating the healing process in these wounds (84).

1.5. LMBs and their potential chemotherapeutic application

LMBs are most typically made from liposomes and an US responsive, echogenic gas. It is shown that the linear oscillation of bubbles induced by US (85) concentrates the US energy on a microscale with ability to rupture lipid membranes in their vicinity (86). Oscillation of bubbles in presence of ultrasound with larger amplitudes is followed by their violent collapse (Figure 1-6) creating a burst release of energy in the form of micro jets and shockwaves (87).
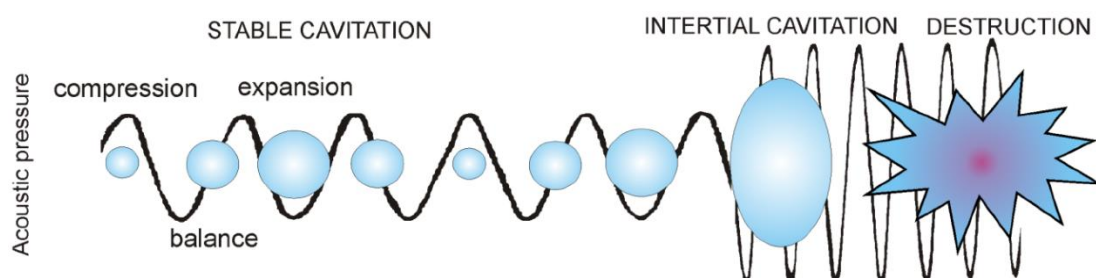
Figure 1-6: US consistently expands and contracts bubbles via compression and rarefaction of the surrounding media, bubble collapses violently once it grows to a particular size, reprinted with permission from (87) copyright 2015

The resulting shockwaves and micro jets from collapse of bubbles have been suggested as potential percutaneous penetration enhancer benefiting drug delivery across the aforesaid barrier (88). The most important parameters playing key role in bubble-US induced oscillation

are: the size of bubbles and nature of the gas inside, US frequency, liquid pressure and liquid density (89, 90). When considering liquid density, it has been reported that in viscous media (e.g. plasma with a viscosity *circa*. 4 cP) wideband emissions from LMBs is far less (i.e. up to 10.2 times) than non-viscous media (e.g. water or saline 0.9%w/v with a viscosity *circa*. 1 cP). Hence, there is an inverse nonlinear correlation between the likelihood of LMB cavitation and the viscosity of the media surrounding LMBs (91)Table 1-3 shows bubbles behaviour in presence of different US frequencies and their potential applications.

Table 1-3: Bubble application and US frequency (90)

Frequency	Bubble behaviour in presence of US	Application	Ref.
20 kHz	Generation of large bubbles and strong shockwaves generated from their collapse	Mechanical agitating applications such as emulsification	(92)
100 to 1000 kHz	Smaller bubbles compared to 20 kHz with higher increase in temperature during cavitation	Sonochemical purposes	(93)
1 MHz and above	Weaker cavitation hence lower toxicity	Medical imaging	(94)

Cavitation caused by US (also termed as acoustic cavitation) in body has been defined/studied (95) whereby the likelihood of cavitation for a particular bubble at different US frequencies relies on different parameters including the US peak negative pressure (96, 97). This burst release of energy, not only can trigger release of drug from the liposomes (via disarrangement of phospholipid molecules in liposomes bilayer membrane) (89, 98), but also increases the cellular uptake of drugs via generation of transitory pores in nearby cellular membranes (99). To date, LMBs and US have been successfully applied to a range of preclinical settings such as gene delivery (100-104) and augmentation of blood flow to muscles in mice (105). Table 1-4 and Table 1-5 show the LMB based diagnostic products and some of the most recent published *in vivo* applications of bubbles and US respectively.

Table 1-4: LMBs products and their clinical applications

Name	Composition	Application	Ref.
Definity®	Dipalmitoylphosphatidylcholine (DPPC), dipalmitoylphosphatidic acid (DPPA), dipalmitolyphosphatidylethanolamine–PEG5000 (DPPE–PEG5000) Octafluoropropane	Echocardiography	(89, 106)
Sonazoid™	Hydrogenated egg phosphatidyl serine (HPSC), perfluorobutane, sucrose	Characterisation of focal liver lesions	(107)
SonoVue®	Macrogol 4000, distearoylphosphatidylcholine (DSPC), dipalmitoylphosphatidylglycerol (DPPG), sodium palmitic acid sulphur hexafluoride	Echocardiography, doppler of vasculature	(108, 109)

Table 1-5: Proposed applications of bubble cavitation

Bubble type	US settings and parameters	Effect(s)	Ref.
Lipoid microbubble	1.3 MHz with a 5-second interval, pulse repetition frequency of 9.3 kHz, mechanical index (MI) of 1.3	Therapeutic US cavitation increased muscle perfusion by 7-fold in normal mice	(105)
Lipoid microbubble	In-house probe with following input parameters: 10-cycle sinusoidal at 620 kHz, MI with planar and concave aperture design were 0.4 and 1.0 respectively	Thrombolysis rate of $0.7\% \pm 0.15\%$ *in vitro* without any use of thrombolytic drugs	(110)
Lipoid bubble	1 MHz, intensity of 2 W/cm² and duty cycle of 50% for 1 min repeated every 2 days in 19 days	Enhanced the gene silencing of siRNA-NBs both *in vitro* and *in vivo*, elevated levels of cancer cell apoptosis	(111)
Microbubbles (SonoVue®, Definity® and USphere®)	0.4 MHz focused US with MI ranging from 0.62 to 1.38	Creating openings in blood brain barrier	(112)
Lipoid microbubbles	9 MHz, MI 1.3, duration = 10 seconds, 10 times repetition	Liposomal -CoQ10 in combination with cavitation of bubbles were able to reverse diabetic nephropathy	(113)

1.6. Ultrasound parameters and its biological effects

US is high frequency inaudible acoustic vibration (i.e. >20 kHz) currently used in clinic for diagnostic and therapeutic purposes. Although a detailed discussion about US transducers is beyond the scope of this chapter, in brief, each probe has a main US emitting compartment made of a piezoelectric crystal or ceramic which converts electricity to mechanical energy via

changes in its size and shape (i.e. convexity to concavity and vice versa) (114). An electricity generator is the other key compartment generating high-frequency alternating currents matching the properties of the transducer's piezoelectric crystal (115).

The general rule of thumb relating to depth of penetration of US is that higher frequencies penetrate tissue to a lesser degree (i.e. 1 MHz penetrates deeper than that of 3 MHz) (116). The phenomenon (also known as dissipation or loss of US energy in the media (117)) is a result of US attenuation caused by reflection, scattering and absorption of the waves by the molecules of the media during the transmission leading to gradual decrease in US intensity in deeper tissues (118). The most known bio-effects observed in application of US are generation of heat(119), increase in cellular drug uptake (120) and gas body activation (i.e. cavitation of stabilized gas within the body) which happens at lower frequencies and higher energies/intensities (121, 122).

The ability of US to cause cavitation is defined by its mechanical index (MI) which can be calculated via the following equation(123):

$$\text{MI} = \frac{PNP}{\sqrt{f}}$$

Where:

PNP: Peak Negative Pressure (or peak rarefaction pressure) which depends on the transducer's piezoelectric crystal.

f: Frequency

Therefore, two different US frequencies with similar *PNP*s would present different MIs. (i.e. lower frequency would have higher mechanical index, thus having more cavitational effects).

$$\frac{MI_1}{MI_2} = \sqrt{\frac{f_2}{f_1}} \; \rightarrow \; \text{If } f_2 > f_1 \rightarrow MI_1 > MI_2$$

Moreover, the effect of the therapeutic US on cells has been tested at various intensities between 0.1-1.5 W/cm^2 (124) while 1.5 W/cm^2 is used to induce hyperthermia in periwound tissue (125).

1.7. Research hypotheses and aims

    1.7.1. Hypotheses

The main aim of this research was to prepare stable LMBs and test if the cavitation of the prepared LMBs could accelerate the healing of wound models via enhancing the delivery of antibiotics. Therefore, it was postulated that:

- Stable, highly echogenic LMBs encapsulating a clinically relevant chemotherapeutic can be prepared with high drug entrapment efficiency and low polydispersity.

- Ultrasound-assisted cavitation of LMBs can increase the penetration of a model agent (dye) into barrier models of infectious disease.

- Enhanced cellular uptake of antibiotic-containing LMBs assisted by ultrasound leads to reduced bacterial burden and consequently presents a platform for improved management of chronic wounds.

    1.7.2. Aims

- To develop a reproducible preparation method for liposomal ciprofloxacin with high loading efficiency and low polydispersity.

- To develop a highly echogenic formulation of liposomal ciprofloxacin using a patented process established by Parekh et al (WO 2018/053601 A1).

- To evaluate the stability of optimized, drug filled LMBs over a 28-day period.

- To perform ultrasound optimization studies to find US parameters able to cavitate the bubbles while having negligible hyperthermia

- To study the effect(s) of the optimised US and LMBs on:
    - Penetration pattern of rhodamine B into/across different barrier models.
    - Antibacterial efficacy of ciprofloxacin HCl on *P. aeruginosa* via time kill study
    - Cellular uptake of Trypan blue by *P. aeruginosa*

2. Development of liposomal-drug formulations with potential for 'on-demand' US-mediated release

As described earlier in section 1.3 above, remote loading is a key step in preparation of drug filled liposomes through which drug molecules are entrapped inside liposomes and can be done via conjugation with sulphate ions. This step (compared to passive loading technique) has advantage of entrapping higher number of drug molecules within the liposomes. Therefore, in order to determine whether drug-filled liposomes can be transformed into LMBs, active remote loading of drug was first chosen and optimised to achieve high drug entrapment. For this purpose, ciprofloxacin, a fluoroquinolone, was chosen based on the literature showing its ability to be remote loaded into liposomes with high loading efficiency (126).

2.1. Materials and methods

DSPC ($M_w \cong 790$ g/mol), DSPEmPEG-2000 ($M_w \cong 2805$ g/mol), Whatman® Nuclepore Track-Etched membranes and polycarbonate extrusion filters were ordered from Avanti®. Ciprofloxacin HCl was purchased from Sigma-Aldrich®. Ammonium sulphate was purchased from chem-supply. Dialysis membrane, 1 mL shell vials and 20 mm aluminium cap, plain, centre hole; Pharma-Fix-Septa, butyl/PTFE, 50° shore A, 3.0mm were purchased from ThermoFisher Scientific. For extrusion of liposomes LIPEX liposome extrusion system equipped with N_2 cylinder was used. Perfluoropropane (PFP) was purchased from Coregas. Sephadex G-50 was purchased from GE healthcare. Shimadzu Nexera-i LC-2040C 3D and a C18 HL 5µL Vision HT column were used for HPLC assay studies. The temperatures of the media were measured using an ISO-LAB "desk-top" digital Thermometer equipped with a probe. For US exposure, a digital Johari US device (JUS2) with dual frequency (i.e. 1 and 3 MHz) and maximum intensity of 3 W/cm^2 was used. Ellex eyecubed™ US unit (Ellex, Adelaide) was used to record echograms. Triethylamine (TEA) and Orthophosphoric acid 85% were purchased from Ajax Finechem. Acetonitrile was purchased from Merck. An Osmomat 3000 was used to measure the osmolality of the media.

2.2. Data analysis

All the data were analysed using GraphPad Prism® 7 and for t-tests and one-way ANOVA, a p-value < 0.05 was considered to be significant.

2.3. Preparation of ciprofloxacin-filled liposomes

Liposomes were prepared using a well-established lipid film hydration preparation method (127). In brief, DSPC and DSPEmPEG-2000 (at molar ratio of 94:6) were dissolved in ethanol.

The organic solvent was then removed by rotary evaporation to form a uniform lipid film in a round bottom flask. The resulting lipid film was left overnight under vacuum to remove all traces of solvent. Next, the lipid film was hydrated using a 135 mM ammonium sulphate solution at 65 ºC for 30 minutes to reach a final lipid solution of 11 mM of giant MLV. Then, they were extruded respectively through 800 and 200 nm polycarbonate filters five times each, using N_2 at high pressure to form unilamellar liposomes (PDI ≤ 0.1) followed by snap cooling of the final liposomes in an ice filled Eski. The external ammonium sulphate buffer was replaced with isosmotic saline (0.9% w/v) via dialysis in 4-8 ºC over 48 hours, to ensure all traces of ammonium sulphate was removed from the external buffer solution. After dialysis, ciprofloxacin HCl (1 mg/mL) was remotely loaded into the liposomes with different loading times (i.e. 5, 10, 20 and 30 minutes); this being performed at a temperature $10^{\circ}C$ higher than the transition temperature of the primary phospholipid (i.e. DSPC) used to prepare the liposomes (i.e. 65 °C). The amount of ciprofloxacin HCl successfully loaded into the liposomes was then quantified using size exclusion chromatography, the technique of which is described later in section 2.5.

2.4. Characterization of ciprofloxacin-filled liposomes

The ciprofloxacin-loaded liposomes were characterised by dynamic light scattering (DLS) technique using a Malvern Zetasizer Nano. A manual measurement protocol employing the following conditions were used to determine the hydrodynamic diameter and PDI through cumulative analysis:

- Temperature 25 ° C with 120 seconds for equilibration time
- For the material: Refractive index (RI) 1.45, absorption 0.010
- Dispersant parameters: 25 ° C, viscosity 0.8910 cP and RI 1.333
- Measurement angle: 173 Backscatter (NIBS default)

2.5. Determination of ciprofloxacin entrapment efficiency in liposomes

To measure the loading efficiency and/or the concentration of liposomal drug, a size exclusion chromatography method was utilised and separation of extra-liposomal and liposomal drug was undertaken using Sephadex® G50 spin columns as previously described in literature (128). Accordingly, fresh in-house Sephadex® columns were made via the following established protocol developed by Torchilin et al: briefly, 1 g Sephadex® G-50 was swelled with 12 mL NaCl 0.9% w/v for 5 hours. The plunger of 1 mL syringe was removed and a small ball of cotton was placed in the barrel to support the Sephadex®. Then, the swelled Sephadex®

was transferred to the barrel and the final column was placed into a 15 mL Falcon tube (Figure 2-1) (128).
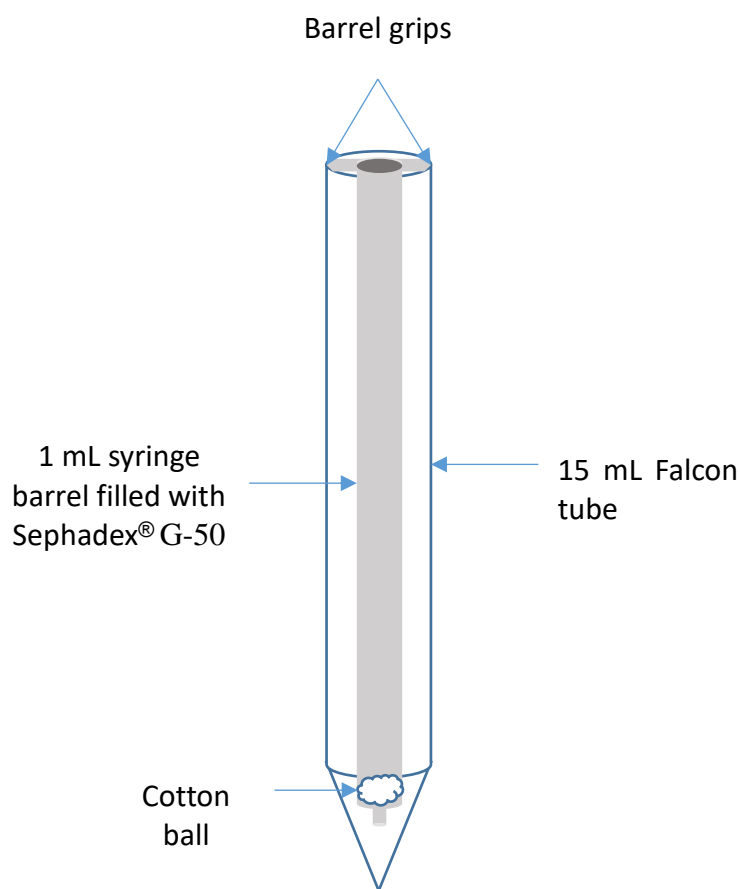
Figure 2-1: Schematic representation of Sephadex® spin column, the plunger of 1mL syringe was removed and the cotton ball inside the barrel was to support the gel, 1g Sephadex® G-50 is swelled with 12 mL saline 0.9% w/w for 5 hours, the barrel was placed inside a 15 mL Falcon tube, the separation is performed by centrifugation of this column for 3 min at 1000 g

The separation of the liposomal ciprofloxacin from the free drug was performed by addition of 100 µL of crude formulation (i.e. containing extra-liposomal and liposomal ciprofloxacin) and 100 µL of normal saline (0.9% w/v) to the prepared Sephadex® column and centrifugation of the column at 1000 g for 3 minutes (Figure 2-2). The eluent was collected and the procedure was repeated twice by adding 200 µL saline each time to the column and repeating the centrifuging process at 1000 g × 3 minutes. All the eluents were collected and diluted 5 times (made up to 1000 µL) and analysed using a Malvern Zetasizer Nano instrument.
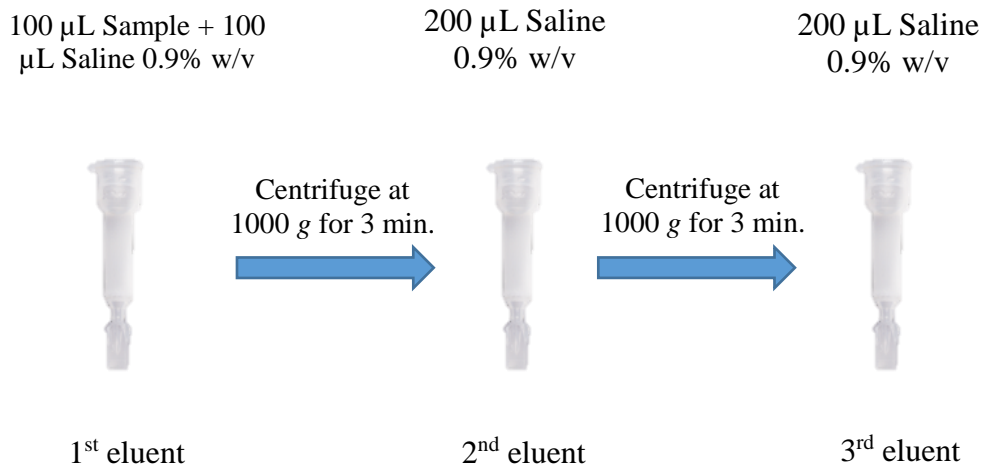
Figure 2-2: Size exclusion chromatography technique for quantification of intraliposomal ciprofloxacin HCl, the first eluent contains the liposomes only whereas the 2nd and 3rd eluent contain drug + liposomes, only the 1st eluent is taken for quantification by HPLC, liposomes are ruptured by Triton X-100, 0.5% v/v before HPLC

The derived count rate, a parameter that correlates with the number of particles scattering light and is measured as kilo counts per second (*KCPS*), was recorded to determine the percentage of liposomes in each wash relative to the total amount of liposomes in the all washes. The following equation was used to calculate the ratio of liposomes in each wash:

$$X_n = \frac{KCPS_n}{KCP_1 + KCP_2 + \cdots + KCP_n}$$

Where:

X_n = Ratio of liposome in the wash number n

$KCPS_n$ = Derived count rate in the wash number n

Once the percentage of liposomes in the first wash was determined the following steps were taken to quantify the amount of liposomal drug (Figure 2-3):
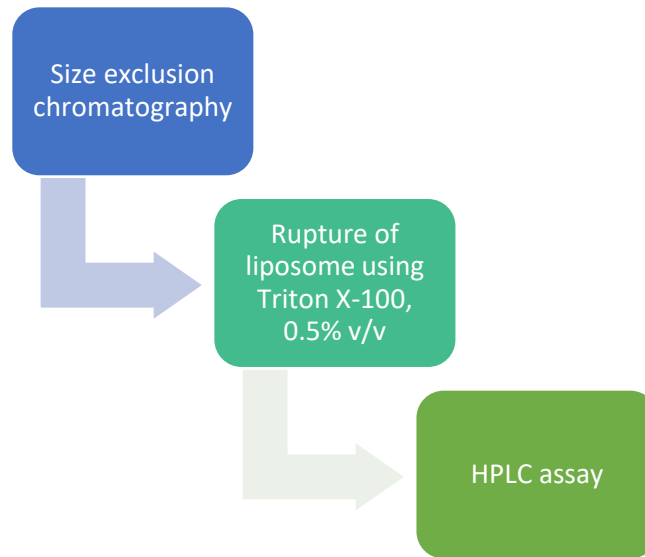
Figure 2-3: Liposomal ciprofloxacin quantification steps

In order to confirm that the separation of free drug from liposomal drug was performed flawlessly the aforesaid experiment was performed using a stock solution of free drug (i.e. ciprofloxacin HCl) with high concentration (i.e. 3000 µg/mL). Since the crude solution does not contain liposomes nor Triton X-100, a UV assay was used to detect the amount of drug in each wash. Figure 2-4 illustrates that the first wash contained mainly liposomal formulation, whereas free drug starts to elute from the second and subsequent washes.
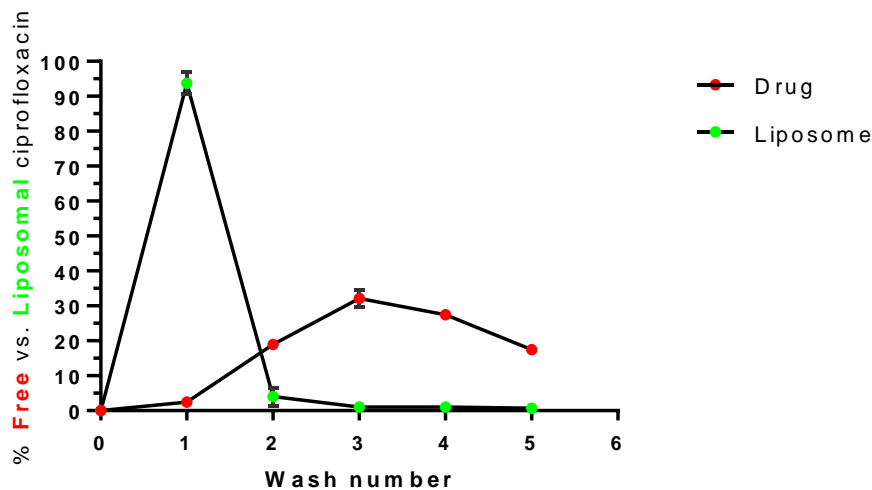
Figure 2-4: Sephadex® studies, percentage of liposomal ciprofloxacin vs. free ciprofloxacin HCl in each eluents from size exclusion chromatography technique, 100 µL of 11mM liposomes + 100 µL saline 0.9% w/v was used as the starting solution for the experiments illustrated in green dots, 200 µL of ciprofloxacin HCl (3000 µg/mL) was used as the starting solution for the drug determination experiments illustrated in red, the gel used in the columns was prepared by swelling 1 g Sephadex® G50 in 12 mL saline 0.9% w/v for 5 hours, the derived count rate was used to determine the percentage of the liposomes in each wash, ciprofloxacin HCl was quantified using UV spectroscopy at 275 nm (n=3 independent experiments, mean ± SD)

Figure 2-5 is ciprofloxacin calibration curve from an in-house HPLC gradient method which was performed at 25 °C and flow rate of 1 mL/min with the following mobile phases based on the USP monograph for ciprofloxacin HCl:

- Mobile phase A: 0.025 M phosphoric acid pH adjusted to 3.0 ± 0.1 with triethylamine.
- Mobile phase B: acetonitrile.
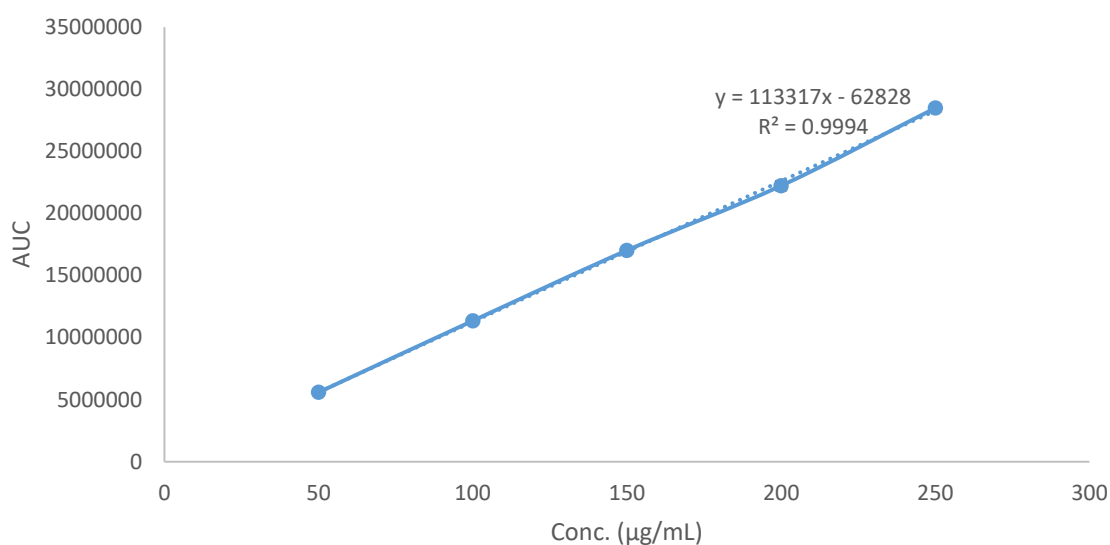
Figure 2-5: Calibration curve for quantification of ciprofloxacin HCl, using HPLC with the following mobile phases: A) 0.025 M phosphoric acid pH adjusted to 3.0 ± 0.1 with triethylamine and B) acetonitrile. The flow rate was 1 mL/min, the column used was Vision HT C18 RP, The UV wavelength was 275 nm, and the column temperature was set to 25 º C (data shown as mean ± SD)

Figure 2-6 depicts the percentage of different remote loading efficiencies achieved from performing the remote loadings with different durations (i.e. 5, 10, 20, and 30 min.). The remote loadings were performed at 65 °C (using a Heidolph® incubator1000) and the liposomes (11mM) were made of DSPC: DSPEmPEG-2000 (94:6).
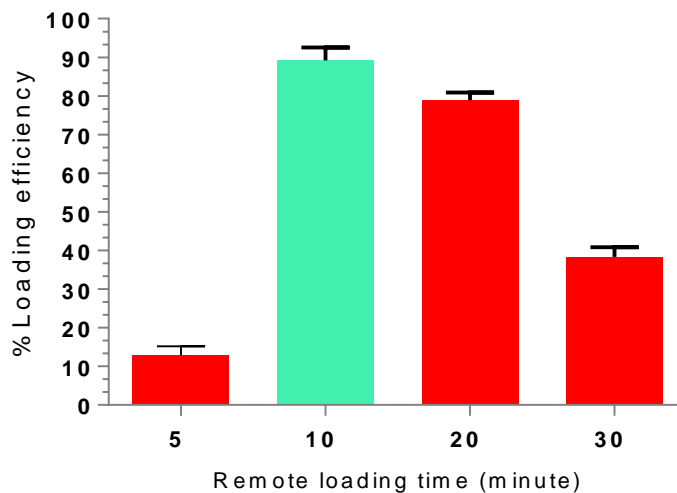
Figure 2-6: % of loading efficiency in ciprofloxacin HCl remote loading technique, comparison between the 4 different remote loading times (i.e.5, 10, 20 and 30 min) performed at 65 ºC using Heidolph® incubator1000, the concentration of lipid solution was 11mM, liposomes were made of DSPC:DSPEmPEG-2000 at molar ratio of 94:6, the lipid film was hydrated by 135 mM ammonium sulphate solution, liposomes were prepared via extrusion and the PDI was ≤ 0.1 for all of the groups, the % of remote loading is determined via size exclusion chromatography assay, the liposomes were ruptured using Triton X-100, 0.5% v/v and the amount of liposomal ciprofloxacin was quantified by HPLC, the remote loading time with the highest % of lading efficiency is coloured in green, (n=3 independent experiments, data shown as mean ± SD)

2.6. Supercharging of liposomes

The ciprofloxacin-filled liposomes were subjected to supercharging with PFP (US contrast agent), this being performed under pressure using an earlier standardized and established protocol (129). Briefly, the liposomal solution (2 mL) was transferred to an air evacuated 9 mL crimp sealed vial. Next, PFP (20mL at 7 psi) was added using a 30 mL Eterna Matic Sanitex syringe equipped with a 25 G hypodermal needle to facilitate entrapment of the contrast agent. To confirm the echogenicity, 50 µL of supercharged formulation was added to 50 mL of isosmotic saline and imaging was performed using an Ellex eyecubed™ US unit (Ellex, Adelaide). As shown in Figure 2-7 below echogenic formulations create contrast which is observed as white noise.
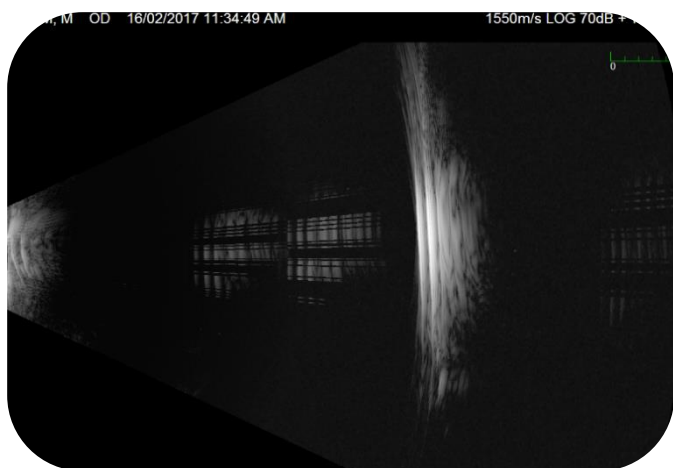
A
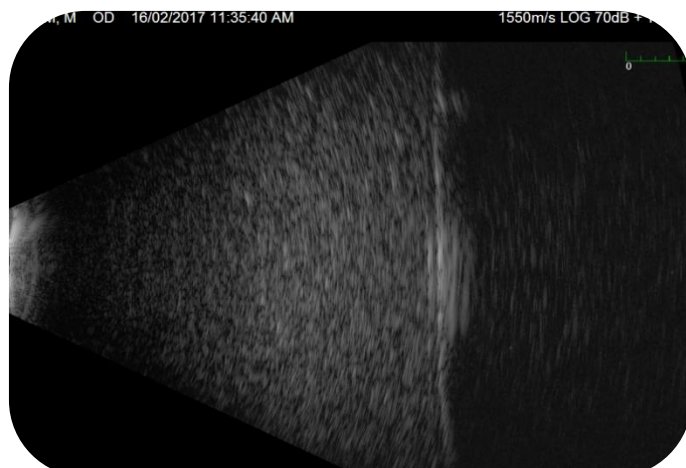
B

Figure 2-7: Echogenicity of 45 mL saline 0.9% w/v before (A) and after addition of 50 μL LMBs (B), LMBs were made of DSPC:DSPEmPEG-2000 (94:6) at 11mM and PFP, the echograms were recorded using 50 mL Falcon tubes at room temperature, the white cloud in the figure A is noise

2.7. Characterization of drug-filled LMBs

2.7.1. Echogenicity studies

It was observed that using the same supercharging protocol, lipoids prepared in iso-osmolar mannitol or sucrose solutions showed no echogenicity whereas lipoids prepared in iso-osmolar sodium chloride or ammonium sulphate became highly echogenic. Figure 2-8 shows that echogenicity was only achieved in solutions containing either saline or ammonium sulphate indicating that presence of such ions in the final formulation is critical to ensuring echogenicity.
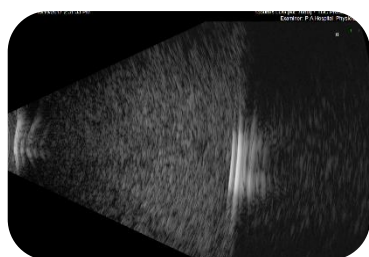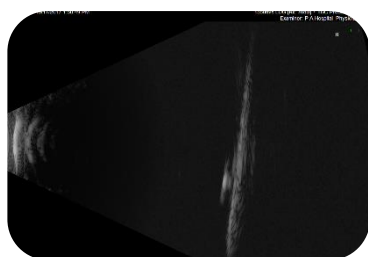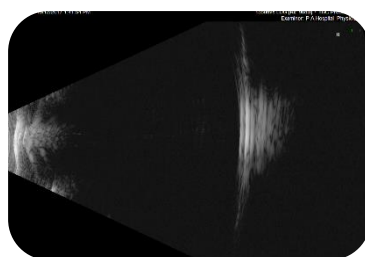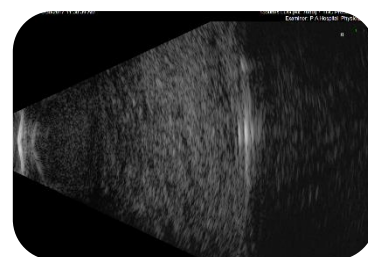
A   B   C   D

Figure 2-8: Echograms of the lipoids (11mM, DSPC:DSPEmPEG-2000 (94:6)) prepared in 4 different media subjected to the same supercharging protocol: A) Ammonium sulphate 135 mM B) Mannitol 10% w/v C) Sucrose 5% w/v D) Sodium chloride 0.9% w/v, for echogenicity studies 50 μL of the lipoid solutions was added to 45 mL of the same hydrating media (e.g. 50 μL of A in 45 mL ammonium sulphate 135 mM), LMBs prepared in mannitol and sucrose (B and C) showed no echogenicity whereas LMBs prepared in ammonium sulphate and sodium chloride (A and D) showed high echogenicity

2.7.2. Microscopic characterization

Electronic microscopy techniques (e.g. TEM/SEM) require sample imaging under high vacuum, which is incompatible with gas filled bubbles leading them to burst under such negative pressures. Therefore, dark field and epifluorescence microscopy as well as optical microscopy were chosen to visualise and image LMBs (Figure 2-9 and Figure 2-10).

For epifluorescence microscope imaging, LMBs were labelled using rhodamine B according to an established protocol (130). In brief, and to avoid self-quenching of rhodamine B, a low concentration of rhodamine B (i.e. ≤2% mol) in 0.9% w/v saline was prepared. Next, 25 µL of the prepared stock was added to 200 µL of the LMBs and then they were imaged using an epifluorescent microscope. The fluorescent labelled micron sized bubbles (arrows in Figure 2-9) indicates the localisation of micron sized hydrophobic gas (PFP) along the lipoid bilayer.
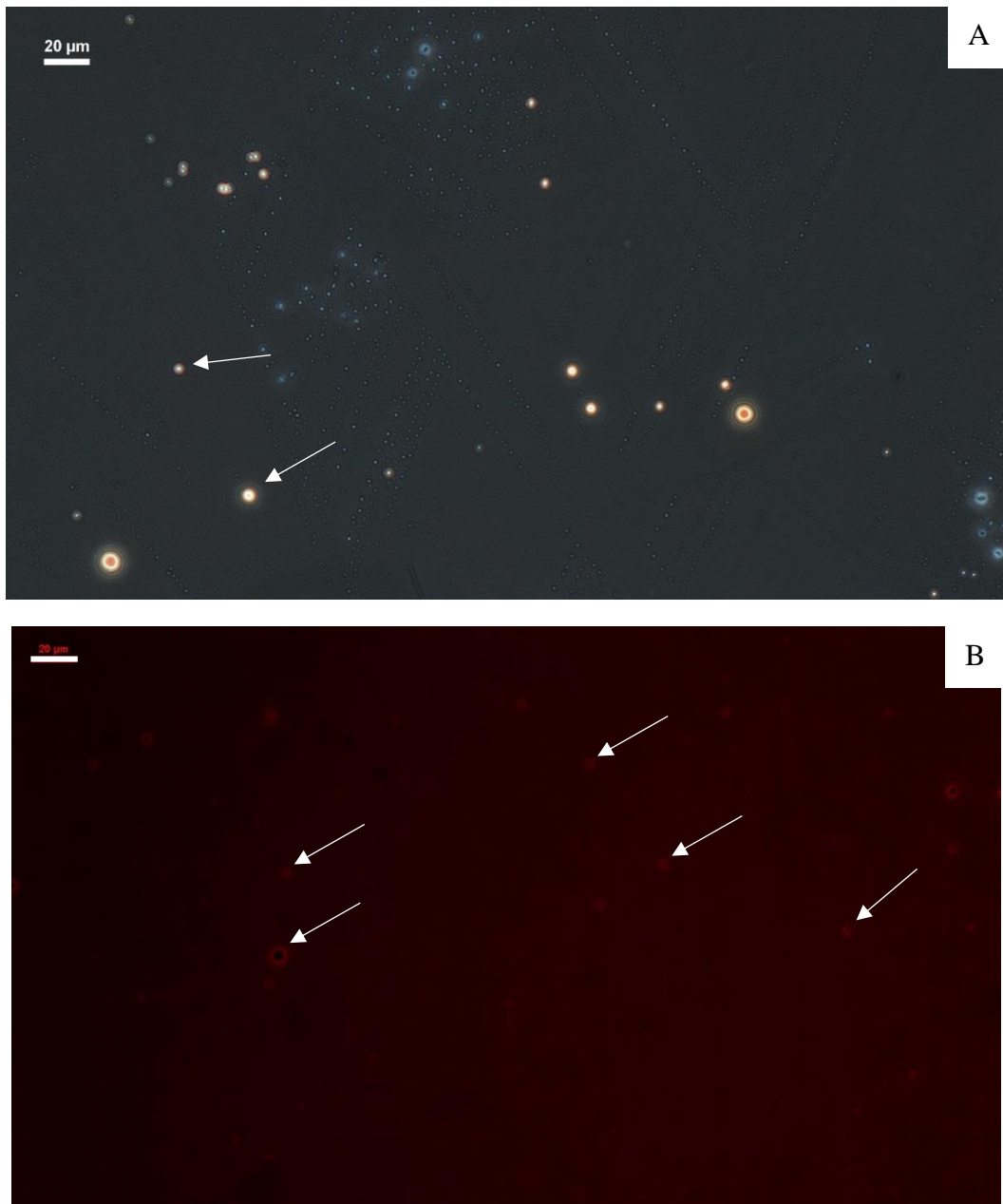
Figure 2-9: Localisation of micron sized hydrophobic gas (PFP) along the lipoid bilayer, dark field microscopy (A) vs. epifluorescence images (B), LMBs (11mM) were made of DSPC:DSPEmPEG-2000 (94:6) and PFP in saline 0.9% w/v and were labelled using rhodamine B, the images were acquired using a 63× objective. (The scale bar represents 20 μm)
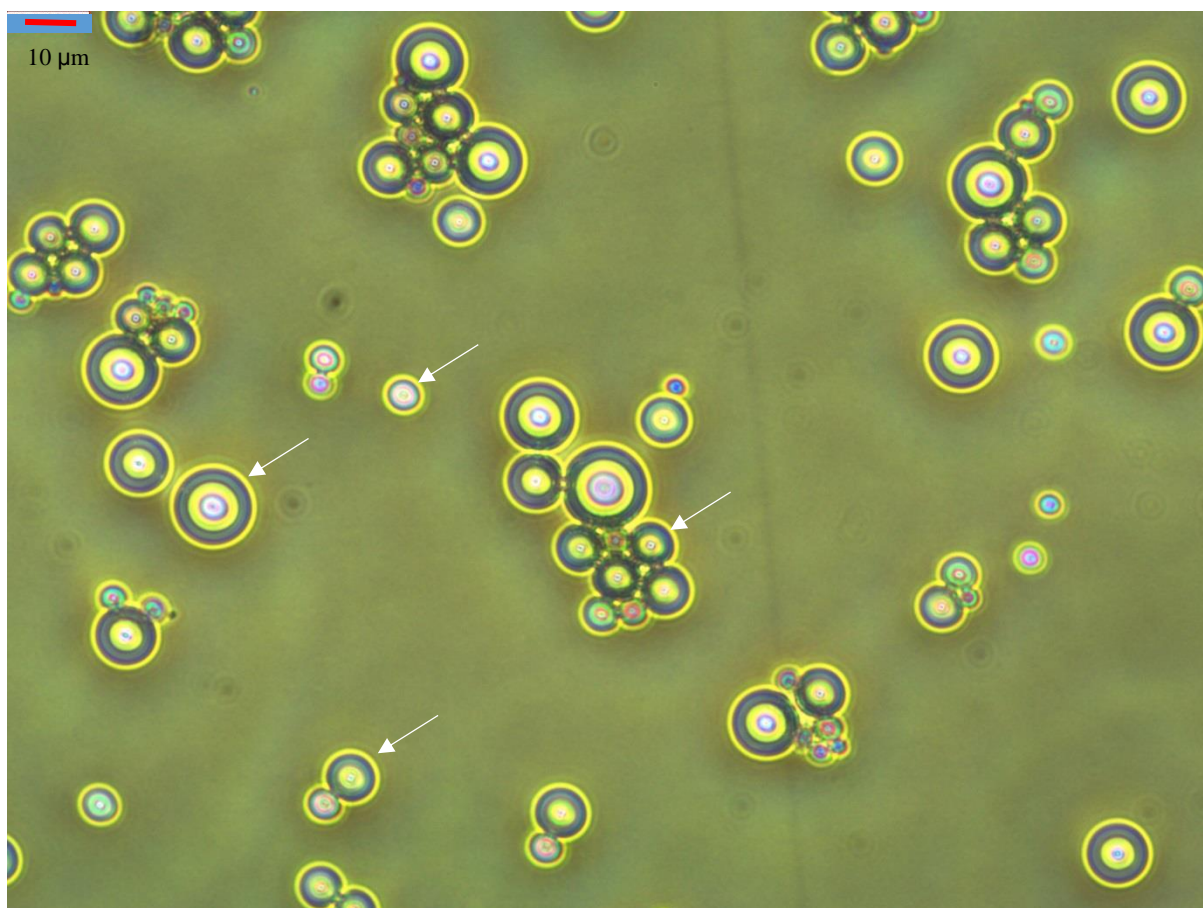
Figure 2-10: Optical microscopy image of LMBs, LMBs (11mM in saline 0.9% w/w) made of DSPC:DSPEmPEG-2000 (94:6) and PFP, (The scale bar represents 10 μm)

2.8. Stability studies

2.8.1. Liposomal drug retention, size and polydispersity index

The optimized CLMBs formulations were monitored every 7 days up to 28 days after their preparation for size, PDI and liposomal drug concentration (Figure 2-11) and the results were compared via a one-way ANOVA test (Dunnett's multiple comparisons test, n=6 for each time point, ns= not significant, p-value > 0.05 indicates non-significance).
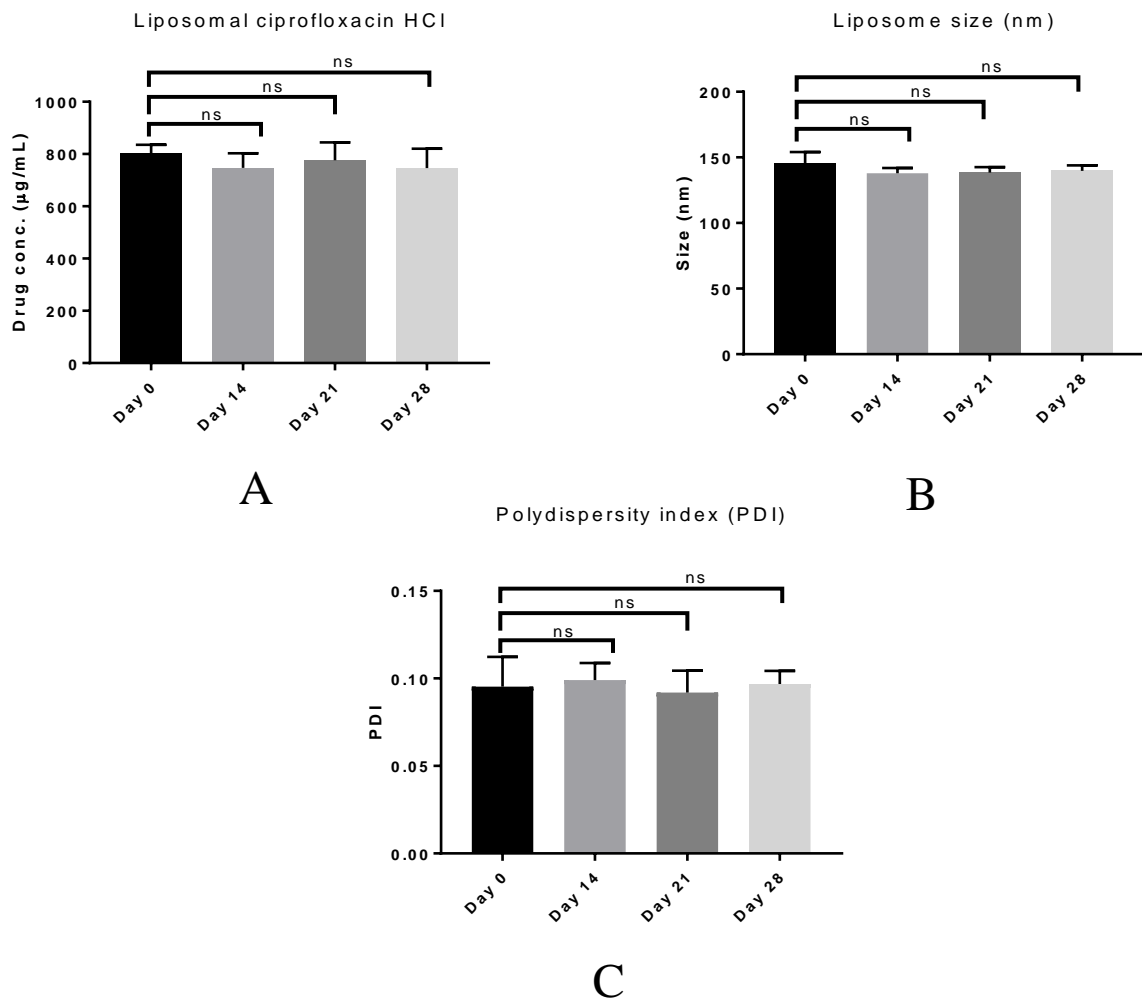
Figure 2-11: 28 day stability study of CLMBs (11mM, DSPC:DSPEmPEG-2000 (94:6), and PFP), The CLMBs were transferred to 1 mL shell vials after the preparation and the vials were closed by inserting the caps, then the caps and the vials were further sealed by parafilm, the storage temperature was 2-8 ºC, A) amount of ciprofloxacin HCl in LMBs, the free drug was separated from liposomal drug using size exclusion chromatography method, LMBs were lysed using Triton X-100, 0.5% v/v and the amount of the liposomal ciprofloxacin HCl was determined by HPLC at 275 nm, (B and C) belong to the size and PDI of LMBs respectively, B and D are from DLS measurements of the eluents from the size exclusion chromatography performed for quantification of the drug, the DLS were performed at 25 °C using cumulative analysis using the following settings: The material parameters: Refractive index (RI) 1.45, absorption 0.010, dispersant parameters: 25 º C, viscosity 0.8910 cP and RI 1.333, measurement angle: 173 backscatter (NIBS default), data presented are mean ± SD, one-way ANOVA (Dunnett's multiple comparisons test, n=6 independent experiments for each time point, ns= not significant, p-value > 0.05

2.8.2. Echogenicity stability studies

Echogenicity of the optimized CLMBs was also recorded every 7 days up to 28 days after their preparation. The results below confirm the echogenic stability of the LMBs over this time course.

Day 0   **Day 7**   **Day 14**   **Day21**   **Day 28**
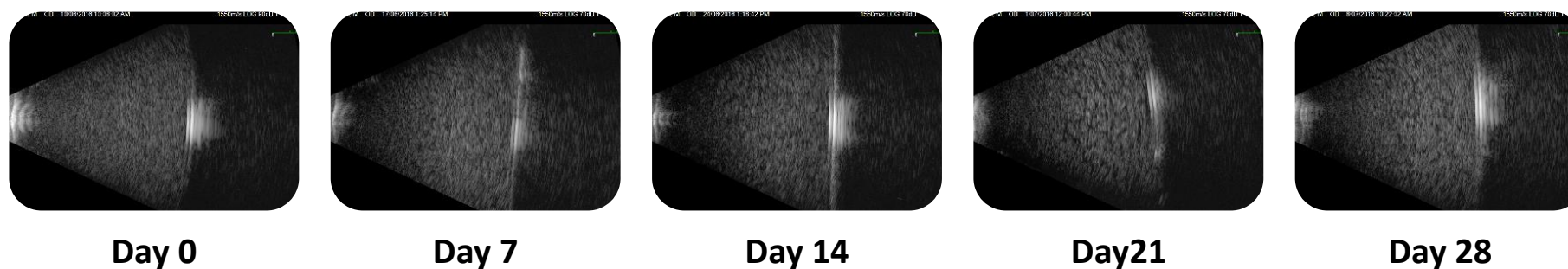
Figure 2-12: Echogenicity of 50 μL LMBs in 45 mL saline 0.9% w/v on the day of preparation (day 0) and 7, 14, 21 and 28 days after the preparation, the echogenicity stability study was performed for all of the 10 prepared LMB formulations mentioned in Table 2-1 , the echograms shown above belong to the sample A from batch 1, the echogenicity was recorded at room temperature, the lipid concentration of the crude LMBs was 11mM and they were made of DSPC:DSPEmPEG-2000 (94:6) and PFP, The LMB solutions were transferred to 1 mL shell vials after the preparation and the vials were closed by inserting the caps, then the caps and the vials were then further sealed by parafilm, the storage temperature was 2-8 ºC

Table 2-1: Echogenicity of 3 different batches (10 samples in total) of CLMBs measured every 7 days over 28 days after their preparation, echograms were recorded after addition of 50 µL to 45 mL saline 0.9% w/v CLMBs, the concentration of the crude LMBs was 11mM and the LMBs were made of DSPC: DSPEmPEG-2000 (94:6) and PFP, The CLMBs were stored in 1 mL shell vials after the preparation and the vials were closed by inserting the caps, then the caps and the vials were further sealed by parafilm, the storage temperature was 2-8 ºC

	Sample name	Day				
		0	7	14	21	28
Batch 1	A	✓	✓	✓	✓	✓
	B	✓	Nil	✓	✓	✓
	C	✓	Nil	Nil	✓	≈✓
Batch 2	A	✓	✓	≈✓	Nil	×
	B	✓	Nil	Nil	✓	×
	C	✓	Nil	Nil	✓	✓
Batch 3	A	✓	✓	✓	✓	≈✓
	B	✓	Nil	✓	✓	✓
	C	✓	Nil	✓	✓	✓
	D	✓	Nil	✓	✓	✓

✓: Echogenic

≈✓: Poorly echogenic

×: Not echogenic

Nil: Not measured

2.9. Optimization of ultrasound parameters

US increases the temperature of the sonicated media/tissue and this hyperthermia depends on different parameters such as frequency, intensity and duration of US exposure. In order to avoid any possible interference caused by hyperthermia in the final results, the following US optimization experiments were performed to optimise US parameters with negligible effect on media's temperature while causing the loss of echogenicity. Accordingly, solutions were sonicated in a 24 well plate and US was applied to each well individually from underneath (Figure 2-13).
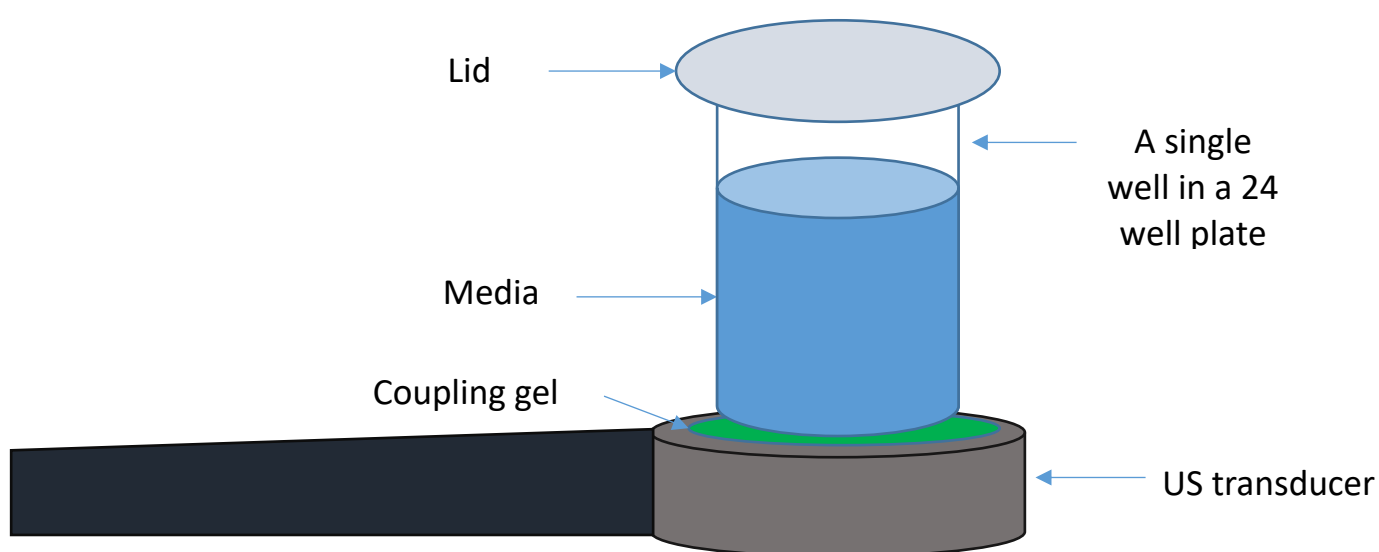
Figure 2-13: US exposure study design: US is applied from underneath of well in a 24 well plate, a coupling gel was used between the US probe and well plate

It was observed that using JUS2 at its highest intensity (i.e. intensity of 2.5 W/cm^2 and 100% duty cycle), any volumes more than 2.25 mL/well (in a 24 well plate) would lead to formation of condensate (as a result of agitation caused by US) on the ceiling of the lid inserted over the samples. This could consequently change the final volume of the samples causing variations between each treatment. Hence, 2.25 mL was chosen as the volume of solution/well for the experiments performed in the aforesaid plate. Moreover, in order to avoid cross exposure of the solutions in wells during US exposure and due to the diameter of the JUS2 probe ($\cong$ 38 mm), only 2 wells (defined in blue in Figure 2-14 A) from each plate were chosen for the experiments. In parallel studies, 10 seconds US exposure was found to be sufficient for the loss of bubbles (Echograms and microscope images confirm the loss of bubbles after US exposure Figure 2-15 and Figure 2-16).
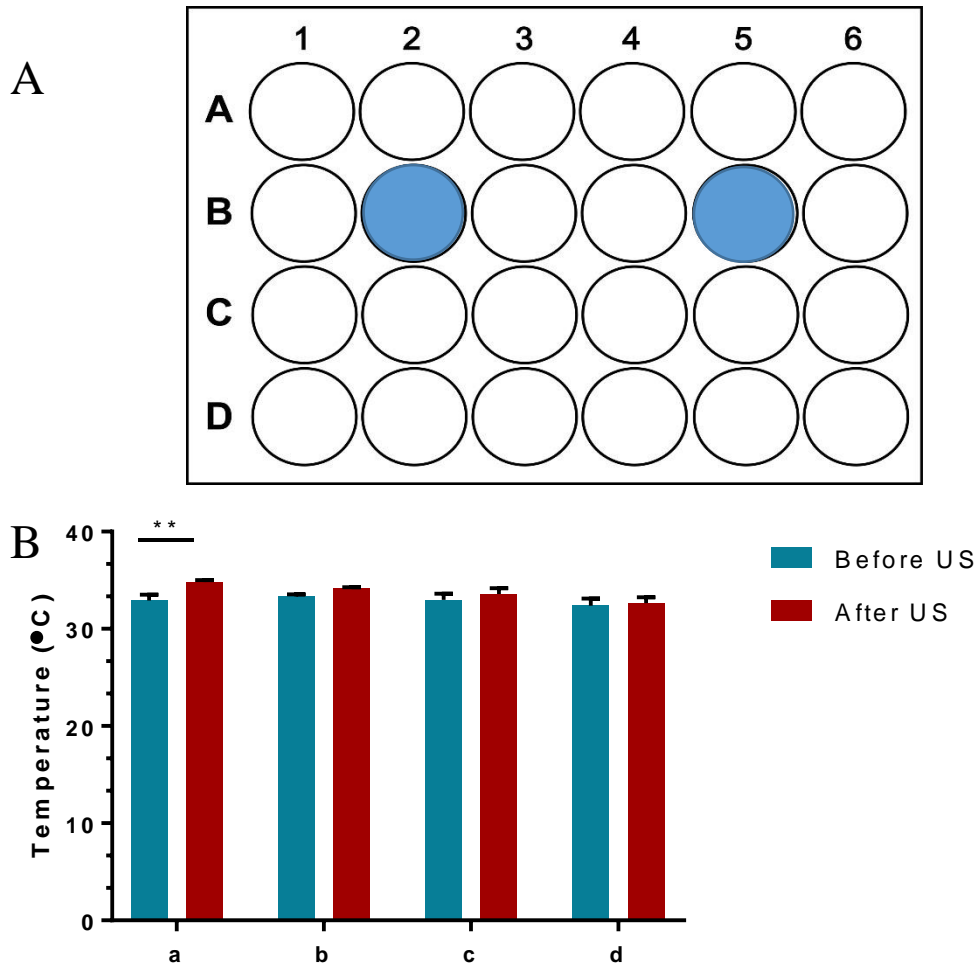
*Figure 2-14: (A) A 24 well plate and the chosen wells for the sonication purposes (i.e. B2 and B5), (B) the effect of 10 seconds US exposure on the temperature of 2.25 mL media (i.e. saline 0.9% w/v) using a) 1 MHz, 100% duty cycle and intensity of 2.5 W/cm², b) 1 MHz, 50% duty cycle and intensity of 3 W/cm², c) 3 MHz, 100% duty cycle and intensity of 2.5 W/cm², d) 3 MHz, 50% duty cycle and intensity of 3 W/cm² , US was applied from underneath of the solutions using JUS2, the experiments were performed in a temperature controlled room at 35°C ± 2 °C, the temperature was measured using a digital thermometer, in the first group (i.e. a) sonication raised the temperature from ≅ 32.9° C to ≅ 34.8 ° C (n=3 independent experiments, mean ± SD, two way ANOVA, Sidak multiple comparison test, ** = significant , p-value < 0.05)*
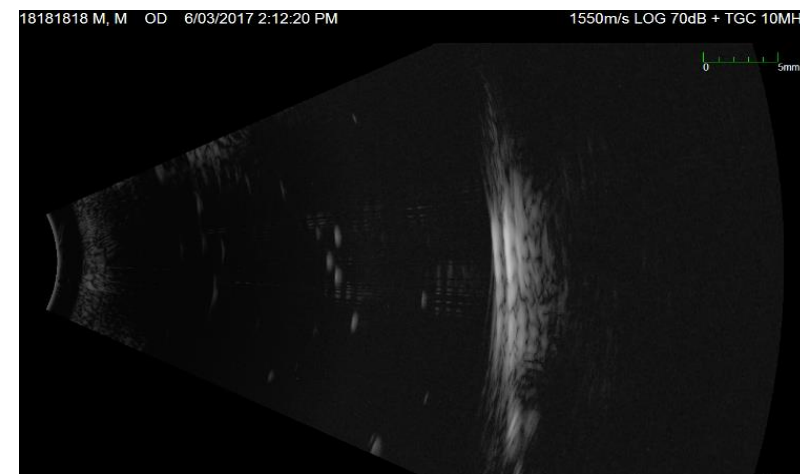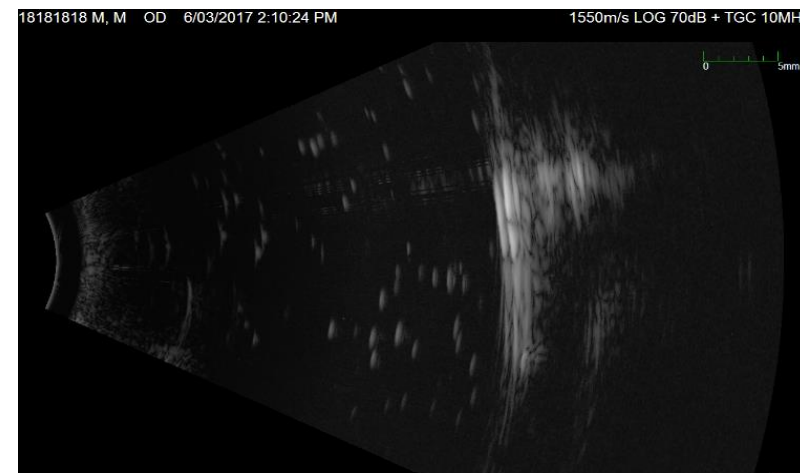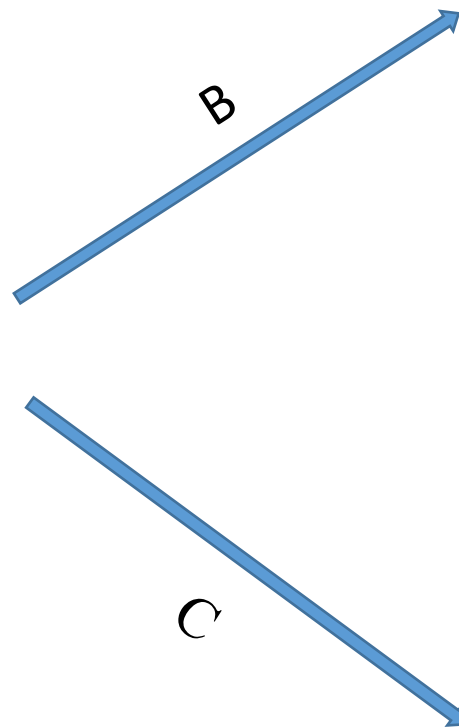
Figure 2-15: Echogenicity of LMBs after application of US using the well plate setup, LMBs (11 mM) were made of DSPC: DSPEmPEG-2000 (94:6) and PFP, echograms were measured in 45 mL saline 0.9% w/v using 50 mL Falcon tubes at room temperature, US parameters were 1MHz 100% duty cycle and intensity of 2.5 W/cm² (A) echogenicity of the solution before US and after (B) 5 seconds and (C) 10 seconds sonication, B and C show the loss of echogenicity after sonication
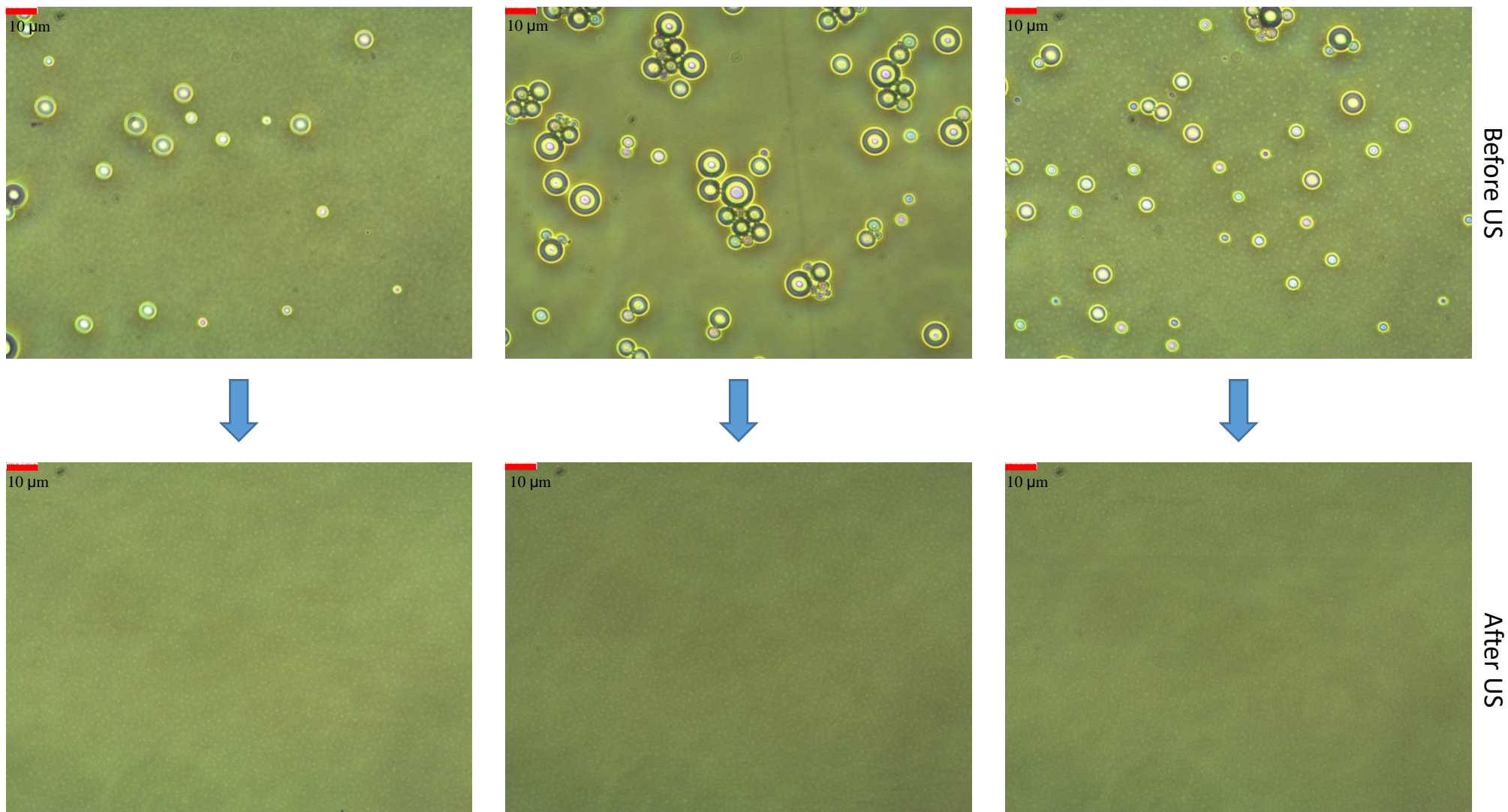
Figure 2-16: Microscope images confirming loss of LMBs after sonication, LMBs (11mM) were made of DSPC: DSPEmPEG-2000 (94:6) and PFP, US parameters were: 1 MHz, 10 seconds, 100% duty cycle and intensity of 2.5 W/cm², the experiments were performed at room temperature using 24 well plate, three independent experiments (The scale bar represents 10 µm)

2.10. Discussion

This chapter describes the formulation and characterisation of CLMBs with an emphasis on analysing their behaviour in the presence of US (i.e. loss of echogenicity). Crude uniform liposomes (i.e. PDI ≤ 0.1) were prepared using extrusion method. The first challenge in this study was finding a proper candidate to remote-load into liposomes. Since the purpose of this study was to enhance the efficacy of topical antibiotics in the treatment of chronic wounds, the antibiotic of interest should have had different specifications such as: A) Being able to be remotely loaded into the liposomes B) Being stable at the temperature required for the remote loading (i.e. 65 °C), C) Being effective on the common bacteria found in chronic wounds (i.e. *P. aeruginosa*), and D) Not irritating the skin at low doses when applied topically (131). Therefore amongst different antibiotics, ciprofloxacin HCl was chosen and the preparation method was optimised to achieve the highest possible loading efficiency. The efficiency of remote loadings in the current study matches those reported in previous studies (i.e. ≅ 90%)(132, 133).

The next challenge in the preparation of CLMBs was to supercharge the prepared ciprofloxacin filled liposomes using an already established supercharging method to achieve final stable CLMBs. For this purpose, the ciprofloxacin filled liposomes were subjected to the aforesaid supercharging protocol and the stability of the final CLMBs was confirmed via a 28-day stability study indicating the successful combine of the two preparation methods.

The last aim of this chapter was to find US parameters capable of cavitating the bubbles while having negligible effects on the temperature of the sonicated media. Hence, LMBs were sonicated using different US parameters and microscopic images of LMBs, echograms and temperature of the sonicated media were recorded before and after the sonication. It was observed that the temperature of the media sonicated using 1 MHz for 10 seconds at 100% duty cycle and intensity of 2.5 W/cm^2 significantly increased (i.e. from ≅ 32.9 °C to ≅ 34.8 °C). However, from clinical perspective, localised induced hyperthermia is a strategy to increase the blood perfusion hence better healing rate in these wounds (134) therefore the observed rise in temperature (i.e. ≅ 1.9 °C) is not considered as clinically significant in this regard.

Chapter 3: *In vitro* evaluation of lipoid microbubbles

3. Introduction - Localised drug delivery using lipoid microbubbles

As discussed previously, persistent infection is postulated to be a key underlying cause of delay in healing of chronic wounds (69). The healing of these wounds are believed to be impeded by the bacteria when their number exceeds 10^5 organism/g of tissue (135). These wounds contain a range of bacteria including *Enterococcus faecalis*, *Staphylococcus aureus*, *P. aeruginosa*, *Proteus spp*, *coagulase-negative staphylococci*, and *anaerobic bacteria* (135). Presence of bacteria at such numbers requires high doses of topical antibiotics. Accordingly, the use of high dose topical antibiotics in treatment of these wounds has been controversial considering the possibility of triggering delayed hypersensitivity reactions, which would consequently exacerbate the patient's condition, and/or developing resistance in bacteria as a result of exposure of the bacteria present in the deep layers of the wound to sub-lethal dose of antibiotics (135, 136).

The objective of the work presented in this chapter was to test if the US assisted cavitation of LMBs can accelerate the healing procedure of these wounds by increasing the efficacy of low dose topical antibiotic against the present infection via:

- Increasing the depth of penetration of the drug in these wounds, therefore exposing the live bacteria present in deep layers of the wounds to higher doses of antibiotics and/or:

- Enhancing the cellular penetration of the drug into the bacteria.

Hence, different experiments were performed to determine the effect(s) of US assisted cavitation of LMBs on:

- The penetration pattern of water-soluble molecules into tissue barrier models: Using two different barrier models, the penetration patterns of rhodamine B across/into these barriers were studied.

- The efficacy of antibiotics: Using optical density and quantitative culture method the antibacterial efficacy of ciprofloxacin HCl on *P. aeruginosa* was studied.

- The penetration of solutes across the cell wall of the bacteria: Using Trypan blue, the amount of dye uptake by *P. aeruginosa* was studied.

3.1. Materials and methods

The LMBs were prepared using the same materials mentioned earlier in chapter two. Agarose was borrowed from Steadman's lab. Rhodamine B was purchased from Sigma Aldrich. 3.5 kDa SnakeSkin™ dialysis membrane was purchased from ThermoFisher SCIENTIFIC. *P. aeruginosa* ATCC® 27853™ was borrowed from CTAB lab. Cationic adjusted

Mueller Hinton (MH) agar and cationic adjusted broth was purchased from BD Life Sciences. A benchtop surgical microscope (i.e. Olympus SZ-3060) equipped with TUCSEN ISH500 microscope camera was used for the dye migration studies. A JUS2 and a XUB-5 ultrasonic bath (with 22.2 W/L and 32 – 38 kHz operating frequency) were used for sonication purposes. Trypan blue solution 0.4% Sigma® was borrowed from Cabot's lab. For the Franz cell diffusion studies, a LOGAN DHC-6T Dry Heat Transdermal System was used. Triethylamine (TEA) UNILAB was purchased from Ajax Finechem. Carbopol® 941 was used for gel preparation. FLUOstar Omega Filter-based multi-mode microplate reader was used for detection of rhodamine B. SPECTROstar Nano absorbance plate reader with cuvette port was used for determination of Trypan blue.

3.2. Data analysis

All the data were analysed using GraphPad Prism® 7 and for t-tests, a p-value < 0.05 was considered to be significant.

3.3. *In vitro* study of lipoid microbubbles cavitation

Shockwaves from cavitation of LMBs might have the potential to benefit drug delivery via enhancing the depth of penetration of drug in localized tissues. Therefore, experiments on different barrier models were designed and performed using LMBs and US to enhance dye migration.

3.3.1. Agarose barrier model

Agarose is reported as a model mimicking open wounds (137). It was observed that among different available water-soluble dyes, rhodamine B acted as the best visual reference for penetration across/into agarose barrier films. The amounts of dye penetration in the agarose disks were imaged using a benchtop surgical microscope (Olympus SZ-3060) equipped with TUCSEN ISH500 microscope camera and a graticule eyepiece. The configuration was calibrated each time before the image recording using a stage micrometre where 1mm was represented by 100 gradated ruled lines 0.01mm apart.

Highly echogenic LMBs were transferred into a gel (Carbopol® 0.5% w/w containing rhodamine B (50 µg/mL), pH adjusted to 6.5 with TEA) and US was applied transiently ($\cong 10$ seconds) to the dye-infused gel and depth of dye penetration into the agar was measured (Figure 3-1 and Figure 3-2).
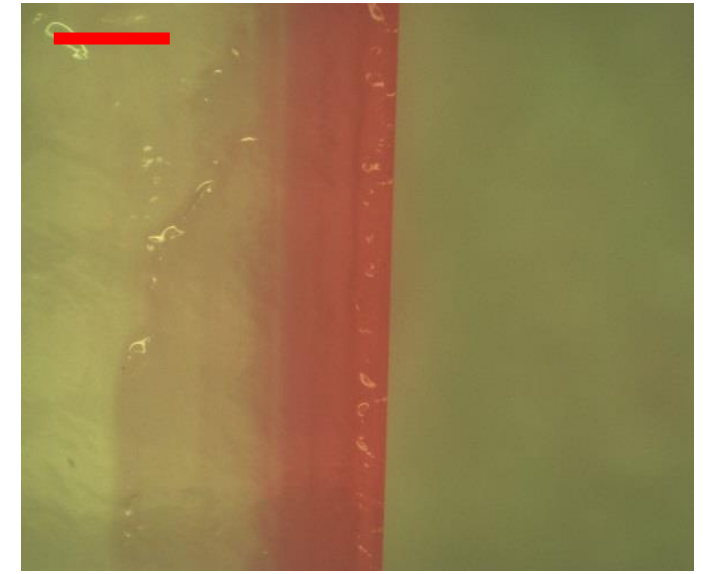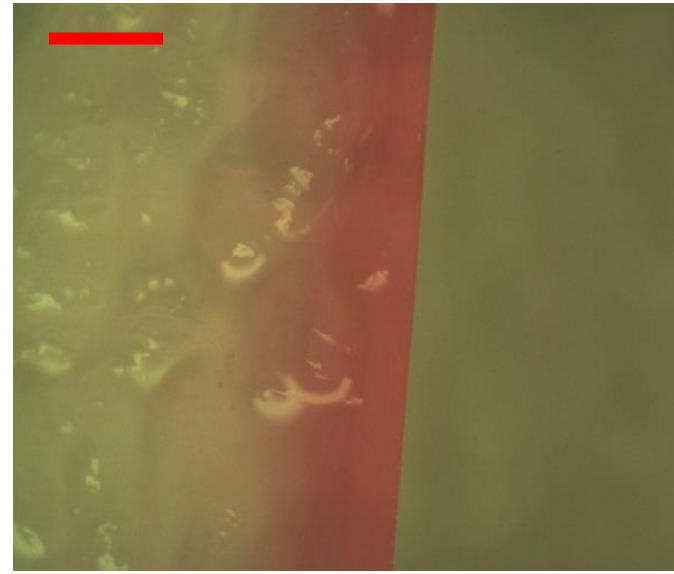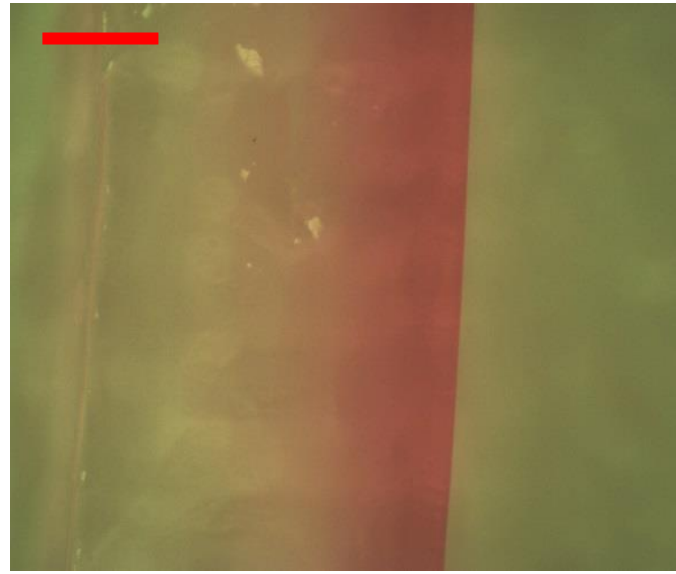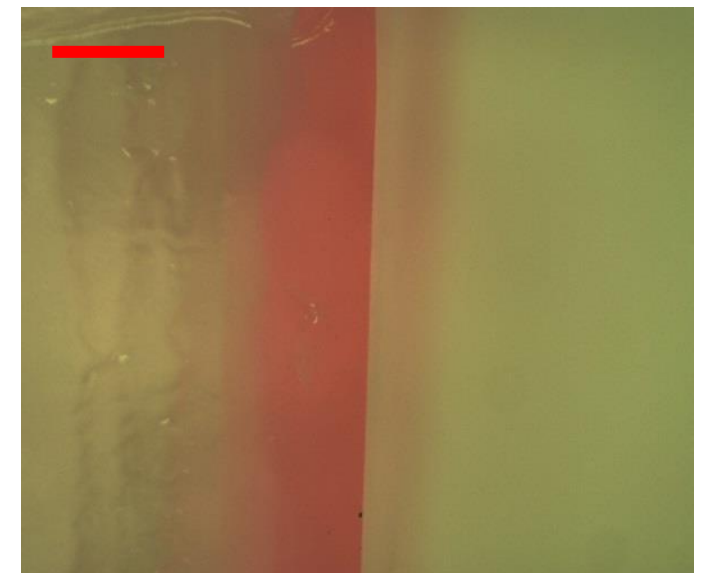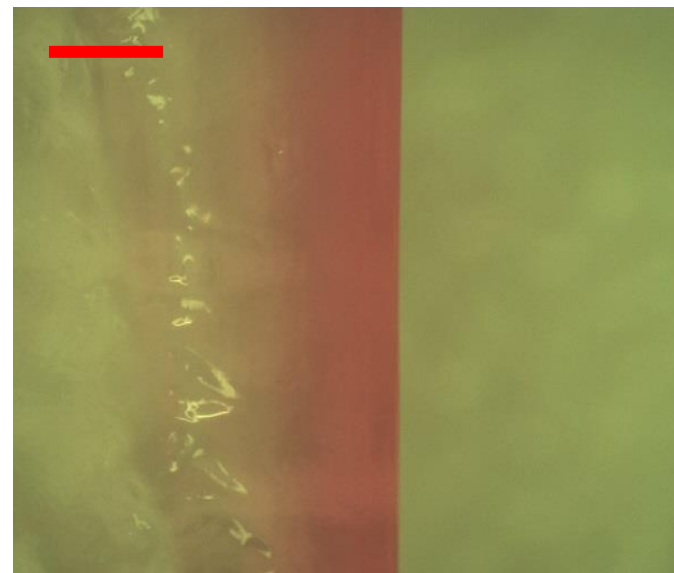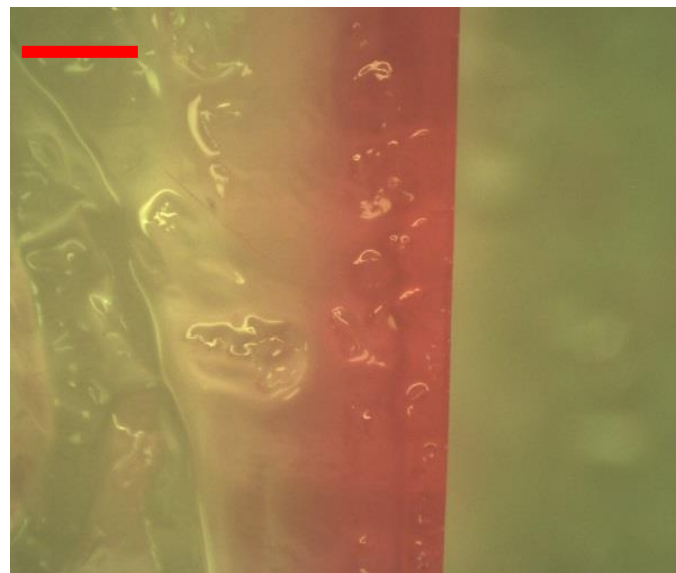
Figure 3-1: Depth of penetration of rhodamine B in agarose 1.5% w/w using Carbopol ® 0.5% w/w containing rhodamine B (50 µg/mL) and the pH was adjusted to 6.5 with TEA, A) no LMBs B) with LMBs (DSPC:DSPEmPEG-2000 94:6 and PFP, the US was applied using JUS2 probe with the following parameters: 1 MHz, 10 seconds, 100% duty cycle and intensity of 2.5 W/cm², three independent experiments (The scale bar represents 100 µm)
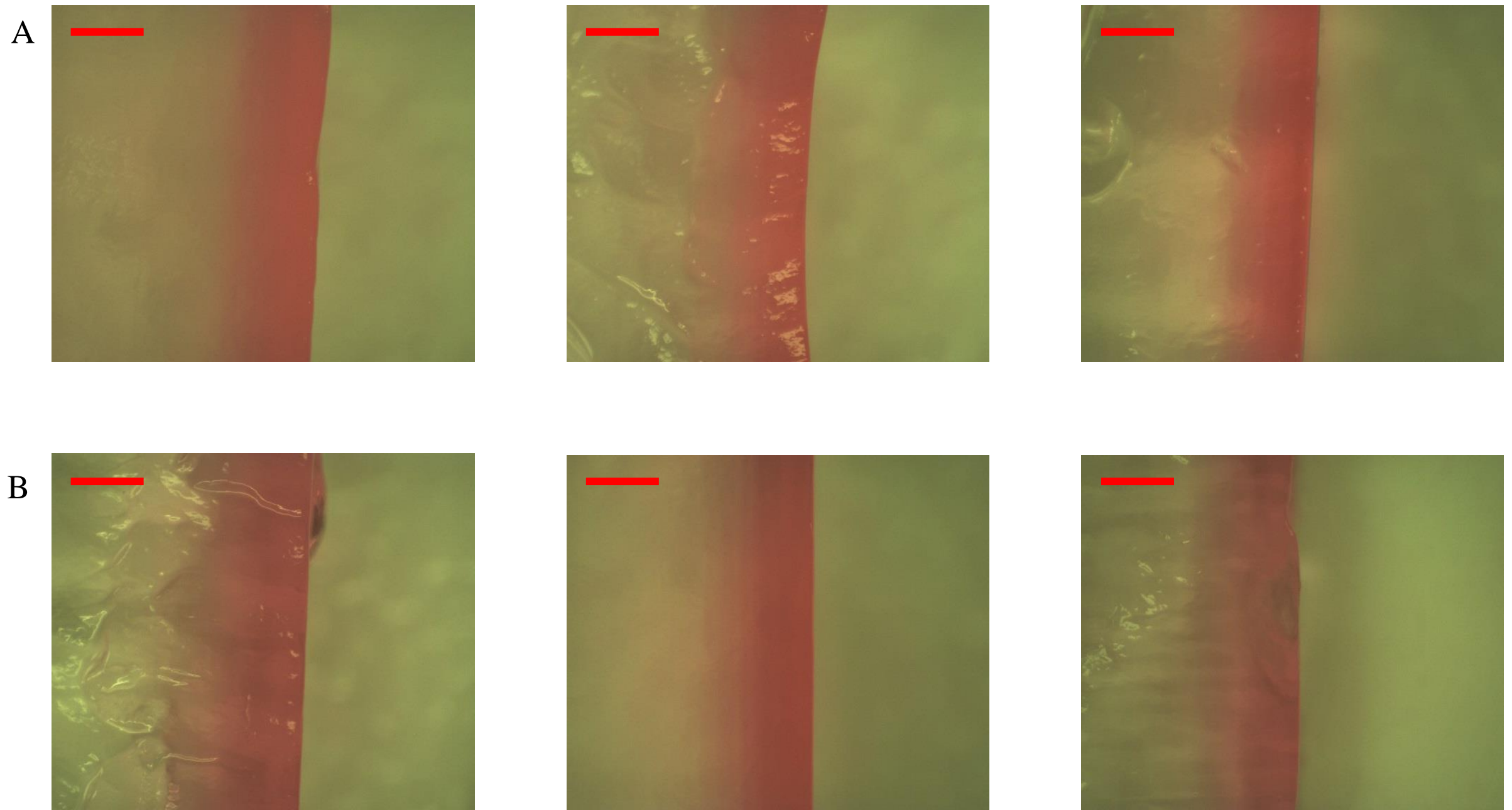
Figure 3-2: Depth of penetration of rhodamine B in agarose 1.5% w/w using Carbopol® gel 0.5% w/w containing rhodamine B (50 µg/mL) and the pH was adjusted to 6.5 with TEA, A) no LMBs B) with LMBs (DSPC:DSPEmPEG-2000, 94:6 and PFP, the US was applied using JUS2 probe with the following parameters: 3 MHz, 10 seconds, 100% duty cycle and intensity of 2.5 W/cm², three independent experiments (The scale bar represents 100 µm)
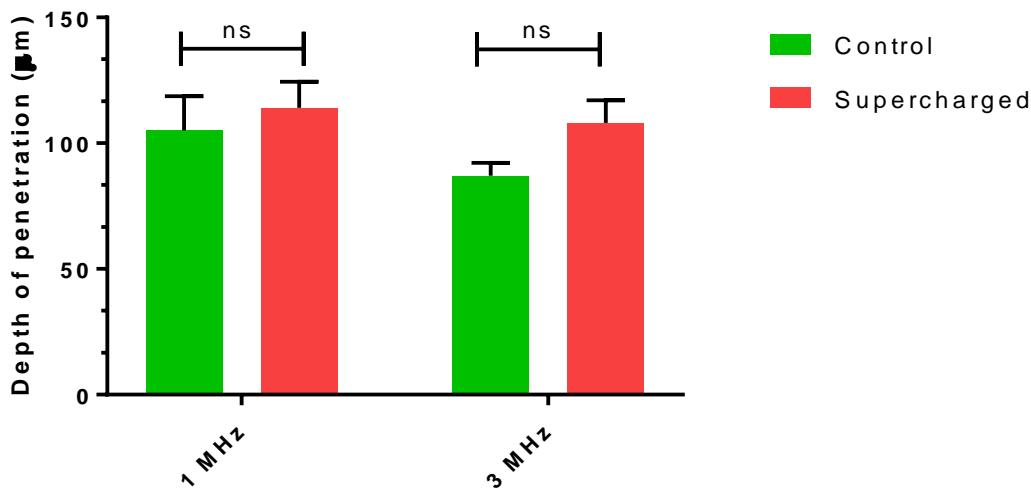
Figure 3-3: Depth of penetration of rhodamine B in agarose disks (1.5% w/w) with and without LMBs, LMBs were made of DSPC:DSPEmPEG-2000 (94:6) in saline 0.9% w/v and PFP, the LMBs were infused in Carbopol® gel 0.5% w/w containing rhodamine B (50 µg/mL) and the pH was adjusted to 6.5 with TEA, the depth of penetration was measured using the calibrated graticule eyepiece, US parameters were: 1 and 3 MHz, 10 seconds, 100% duty cycle and intensity of 2.5 W/cm², n=3 independent experiments, the data shown is mean ± SD, t-test, ns= non-significant, P>0.05
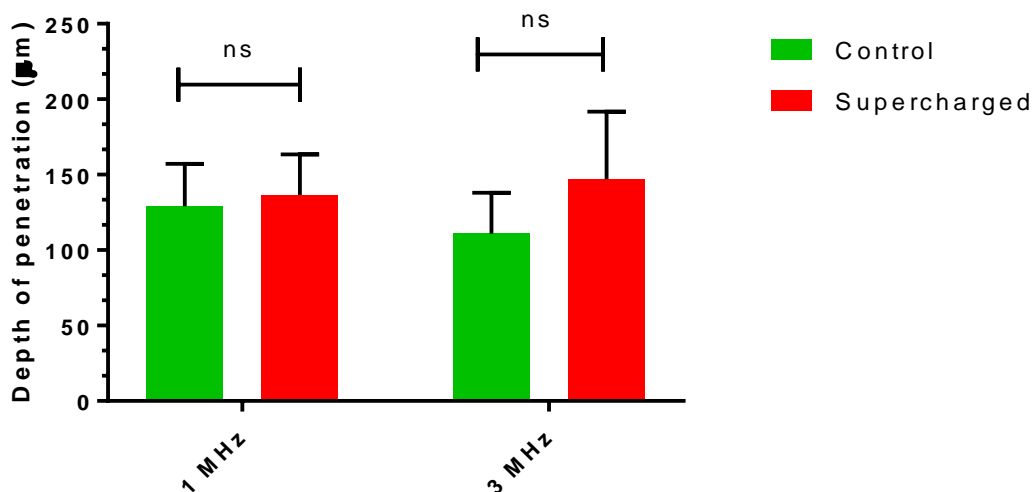
Figure 3-4: Depth of penetration of rhodamine B in agarose disks (1% w/w) with and without LMBs, LMBs were made of DSPC:DSPEmPEG-2000 (94:6) in saline 0.9% w/v and PFP , LMBs were infused in Carbopol® gel 0.5% w/w containing rhodamine B (50 µg/mL) and the pH was adjusted to 6.5 with TEA, the depth of penetration was measured using the calibrated graticule eyepiece, US parameters were: 1 and 3 MHz, 10 seconds, 100% duty cycle and intensity of 2.5 W/cm², the data shown is mean ± SD, n=6 independent experiments, t-test, ns= non-significant, P>0.05

The results above did not show any statistically significant enhancement in the penetration of the dye into the agarose models using JUS2. However, gradual auto-diffusion of rhodamine B into the agarose disks resulting in a fading dye border pattern was a major issue preventing accurate measurements of the dye's depth of penetration into the disks. Hence, a different

barrier model, Franz cell apparatus, was chosen to determine the effect of cavitation on rhodamine B penetration pattern across a semipermeable membrane.

3.3.2. Effect of cavitation on semi permeable membranes

The pulsatile nature of LMB assisted topical drug delivery system requires a barrier model with negligible auto-diffusion of the dye. Therefore, Franz cell apparatus was chosen to determine the effect of cavitation on diffusion of the dye across a semi permeable SnakeSkin™ membrane (Figure 3-5).
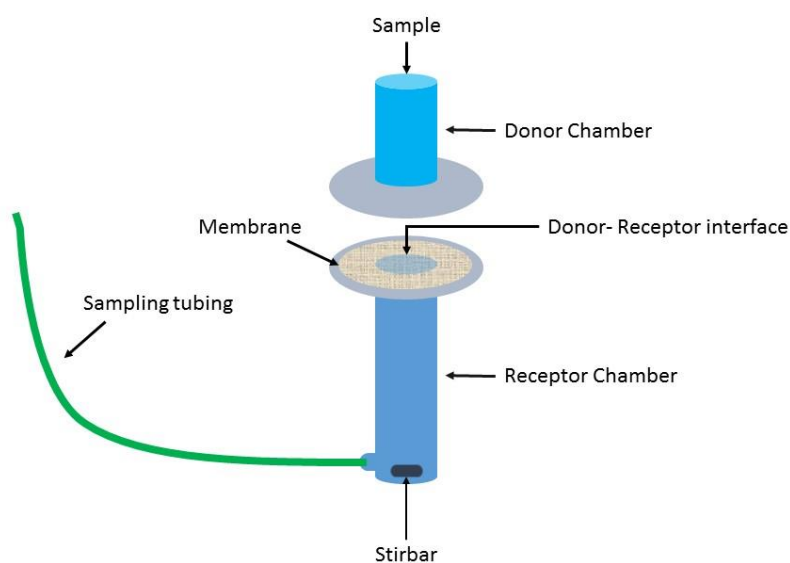
Figure 3-5: Franz cell diffusion apparatus setup for studying the penetration pattern of rhodamine B (50 µg/mL) across a 3.5 kDa SnakeSkin™ dialysis tubing in presence of US assisted cavitation of LMBs, LMBs were made of DSPC: DSPEmPEG-2000 (94:6) and PFP, the experiment was performed at 35°C ± 2°C, samples were taken from the receptor chamber via the sampling tubing

In brief, SnakeSkin™ dialysis tubing with a 3.5 kDa molecular weight cut off was trimmed into circular disks to cover the donor-receptor interface. The donor chamber was clamped to the cell body and the samples were periodically taken from the receptor chamber using a 1 mL syringe. In order to determine the auto diffusion pattern of the dye, 50 µg/mL rhodamine B was placed in the donor chamber and the amount of the dye diffusing into the receptor chamber was measured via sampling of the receptor chamber at 0, 2, 4, 6 and 30 minutes. Next, 100 µL of the collected samples were transferred into a 96 well plate and the fluorescent emissions were recorded using Fluostar omega plate reader (at 544nm for excitation and 620 nm for emission). For cavitation studies, 0.5% w/w Carbopol® gel was infused with 100mL of LMBs and the amount of fluorescence emission in the receptor chamber was recorded after applying 1 and 3

for 10 seconds, 100% duty cycle and intensity of 2.5 W/cm^2. The results are shown below in Figure 3-6.
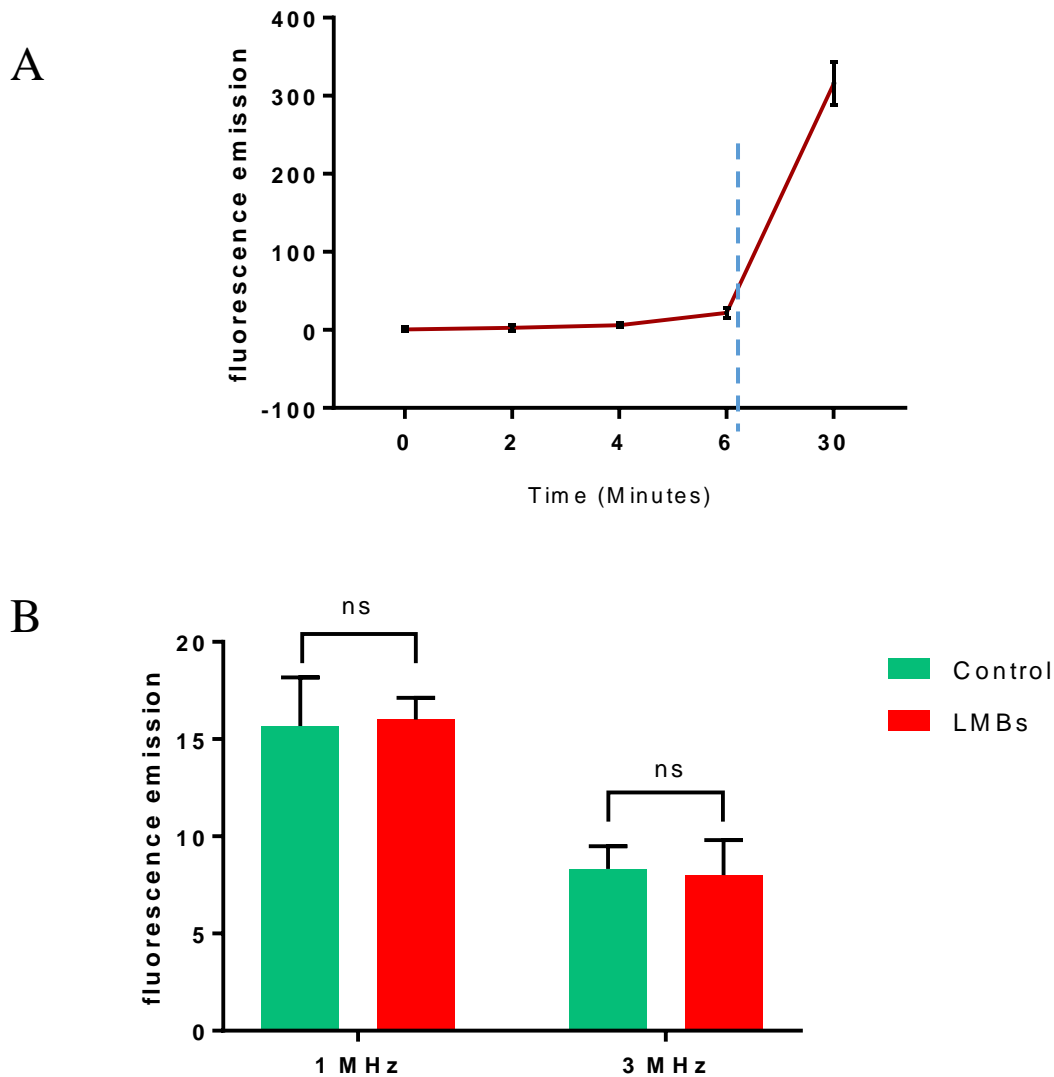
Figure 3-6: Franz cell diffusion apparatus study results performed at 35°C ± 2°C, (A) Auto-diffusion pattern of rhodamine B (50 µg/mL) across a 3.5 kDa SnakeSkin™ dialysis tubing within 30 minutes (B) The fluorescence emissions of the samples taken from the receptor chamber of the Franz cell diffusion apparatus after application of LMBs and US for 10 seconds, 100% duty cycle and intensity of 2.5 W/cm^2, LMBs were made of DSPC:DSPEmPEG-2000 (94:6) and PFP (n ≥ 3 independent experiments, mean ± SD, t-test, ns= non-significant, P>0.05)

The diffusion pattern of rhodamine B (50 µg/mL) in the Franz cell diffusion apparatus study is shown in Figure 3-6 (A). In this experiment, rhodamine B had negligible unassisted diffusion within the first starting minutes of the experiment. Figure 3-6 (B) is the amount of fluorescence emission in the receptor chamber after the US treatment. In this experiment, using LMBs, no significant enhancement in penetration of the dye across the 3.5 kDa dialysis membrane within the range of JUS2 was observed.

3.4. Bacterial time kill studies

As mentioned earlier, persistent infection plays a key role in delaying the healing of chronic wounds. Hence, one of the proposed mechanisms to improve the healing procedure in chronic wounds is to tackle this underlying cause. The earlier barrier models in the current study, did not show any change in penetration rate of rhodamine B using LMBs and US. Therefore, bacterial time kill studies were performed to:

- Determine the efficacy and/or modelling the pharmacodynamics of the LMBs and ciprofloxacin using a sigmoidal dose response curve and identify any potential synergism(s) between the LMBs and the drug.

In order to determine that the nonsterile preparation of LMBs would not result in growth of contaminating organisms affecting the bacterial time kill studies, individual samples (i.e. 200 µL each, from 3 different batches of LMBs solution with no ciprofloxacin), were separately plated on cationic adjusted MH agar plates and were cultured at 37 ° C for 48 hours. After this time, the plates were visually inspected for presence of microorganisms. No colonies were detected visually paving the way for bacterial kill studies.

P. aeruginosa is a gram-negative bacterium susceptible to ciprofloxacin HCl (MIC = 0.5 µg/mL) and is commonly found in chronic wounds (138) therefore, was chosen for the bacterial time kill studies using ciprofloxacin and LMBs.

3.4.1. Optical density

Samples (250 µL) containing bacteria (1×10^8 CFU/mL) were added into 50 mL MH cationic adjusted broth and cultured for 12 hours. Then, 2 mL of the cultured bacteria was aliquoted into the wells and 250 µL of 11mM LMBs containing ciprofloxacin at a final concentration of $0.5 \times$ MIC (i.e. 0.25 µg/mL) was added to each well. US was applied using the parameters below and the Optical density (OD) was measured every 2 hours at 620 nm for 8 hours. The cells were cultured 37 ºC in a Heidolph® 1000 incubator shaker during the experiment.

a. 1 MHz for 10 seconds at 100% duty cycle and intensity of 2.5 W/cm^2
b. 1 MHz for 10 seconds at 50% duty cycle and intensity of 3 W/cm^2
c. 3 MHz for 10 seconds at 100% duty cycle and intensity of 2.5 W/cm^2
d. 3 MHz for 10 seconds at 50% duty cycle and intensity of 3 W/cm^2

Figure 3-7 depicts the OD study results of the bactericidal efficacy of ciprofloxacin on *P. aeruginosa* within the 8 hours after the treatment with US and LMBs.
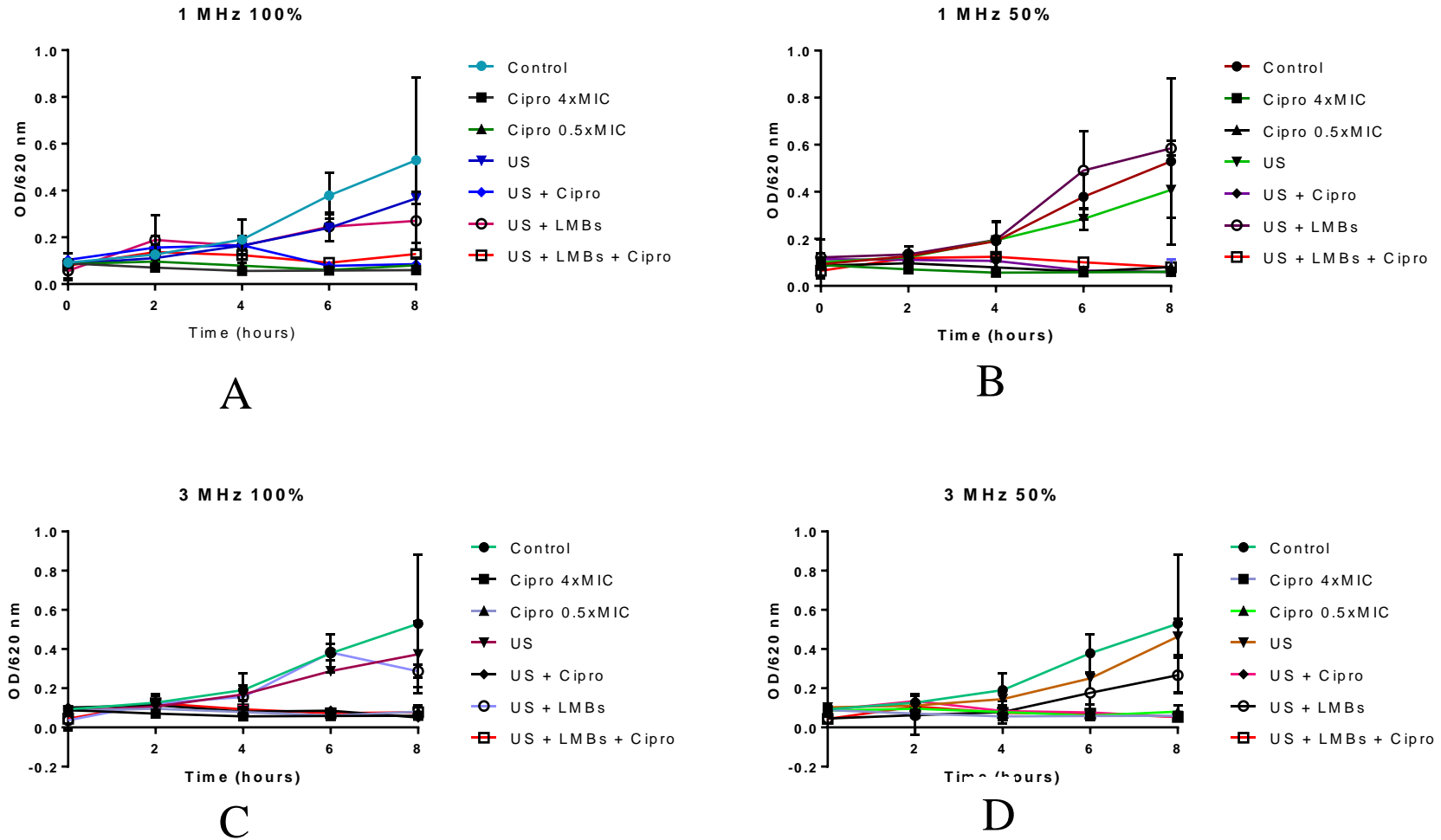
Figure 3-7: Optical density results, time kill study using P. aeruginosa ATCC® 27853™, effect of LMBs+10 sec US on bactericidal activity of ciprofloxacin HCl (0.25 μg/mL), the readings are from before (time=0), and 5 min, 2, 4, 6 and 8 hours after the US treatment, the control group does not contain drug nor LMBs confirming the exponential growth of the bacteria, the interferences caused by LMBs are subtracted from each of the readings in the arms containing LMBs, the US parameters were: A) 1 MHz, 100% duty cycle and intensity of 2.5 W/cm², B) 1 MHz, 50% duty cycle and intensity of 3 W/cm², C) 3 MHz, 100% duty cycle and intensity of 2.5 W/cm², D) 1 MHz, , 50% duty cycle and intensity of 3 W/cm², the cells were cultured at 37 °C in MH cationic adjusted broth (the data shown are mean ±SD)

3.4.2. Colony counting via quantitative culturing

The quantitative culturing (139) protocol used in the current study is detailed in Figure 3-8. In this study, samples containing free ciprofloxacin HCl were washed via centrifugation (9888 *g* for 5 minute) to eliminate bactericidal effect of free ciprofloxacin during the plate culturing.

In order to optimize US parameters for 10 mL solutions used for quantitative culturing assay, a second series of preliminary studies were performed to determine the optimal US parameters which would result in a comprehensive loss of echogenicity in 10 mL samples. Briefly, 10 mL of echogenic medium (i.e. 1 mL LMBs (11mM) + 9 mL saline 0.9% w/v) was transferred to 15 mL Falcon tube and the tube was sealed using nitrile sheath. Next, the tube was inverted and US was applied from below (Figure 3-9). Echograms were recorded before and after US exposure. Surprisingly in this setting, in none of US frequencies (i.e. 1 and 3 MHz) using JUS2 probe, loss of echogenicity was observed. Therefore, a different US generating device (i.e. XUB-5 US bath) was trialled and the loss of echogenicity was confirmed using this device (Figure 3-10). The quantitative culturing results showing the bactericidal efficacy of ciprofloxacin HCl with and without LMBs on *P. aeruginosa* using the optimised US are shown in Figure 3-11.

P. aeruginosa was obtained from the stock

→

The cells were plated on agar for 12-24 hours

→

The cells were suspended in sterile water and compared to McFarland standard to reach a final concentration of ≅ $1.5×10^8$

200 μL was added to each 40 mL of sterile CAMHB and cultured for ≅ 16 hours to reach a final bacterial inoculum of $1x10^8$ CFU/mL. Next, they were mixed in a sterile Schott bottle. 10 mL of sample was aliquoted into each 50 mL Falcon tubes and 1.25mL was removed from each tube.

→

1mL LMBs was added to the treament arm and 1mL sterile 0.9% NaCl was added to the control arm. Then, 250 μL of ciprofloxacin HCl 10 μg/mL was added to the treatment arm while 250 μL sterile 0.9% NaCl was added to the control arm.

→

Time 0: Quantitative culture was performed prior to the US treatment

Quantitative culture was performed after US treatment at different time points

→

For quantitative culturing:

1. 100 μL of the treated media was added to 900 μL PBS.

2. centrifugation 9888 *g* for 5 minutes.

3. The supernatent was removed and 900 μL PBS was added.

4. 8-fold serial dilution was performed in PBS

5. 100 μL of each dilution was added to CAMH Agar.

6. the plates were incubated overnight and the colonies were counted after 24 hours.

Figure 3-8: Colony counting procedure

Air

Direction of US

1 mL LMB + 9 mL saline 0.9% w/v in 15 mL falcon tube

Nitrile sheath

US probe
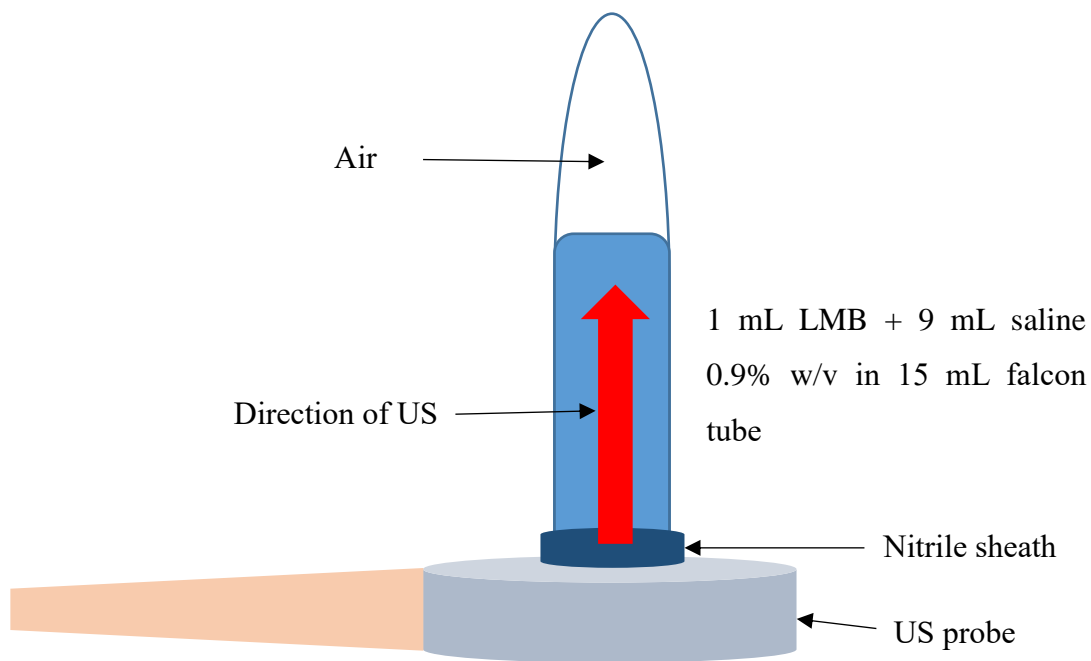
Figure 3-9: Experiment design, the Falcon tube was sealed with nitrile sheath and US was applied through the sheath
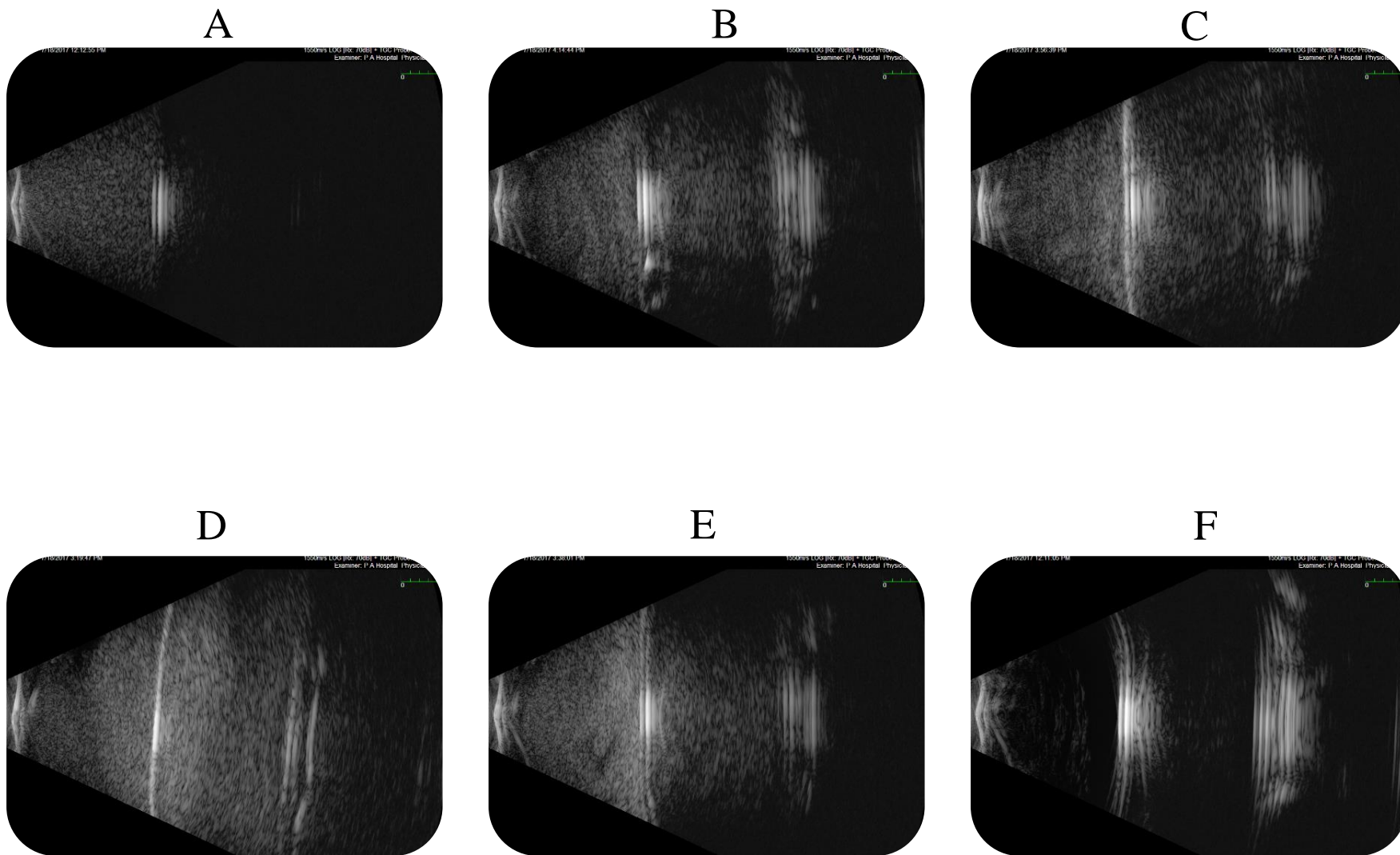
Figure 3-10: Effect of US on echogenicity of 1 mL LMBs (11 mM, made of DSPC:DSPEmPEG-2000 (94:6) and PFP) added to 9 mL saline 0.9% w/v using the setup detailed in the Figure 3-9, the echograms (A-E) are from: before US (A) and after 45 seconds sonication with B) 1 MHz, 50% duty cycle and intensity of 3 W/cm², C) 1 MHz, 100% duty cycle and intensity of 2.5 W/cm², D) 3 MHz, 50% duty cycle and intensity of 3 W/cm², E) 3 MHz, 100% duty cycle and intensity of 2.5 W/cm², only 30 seconds bath sonication with power = 100 W/L and the frequency = 32 – 38 kHz resulted in the loss of echogenicity (F)
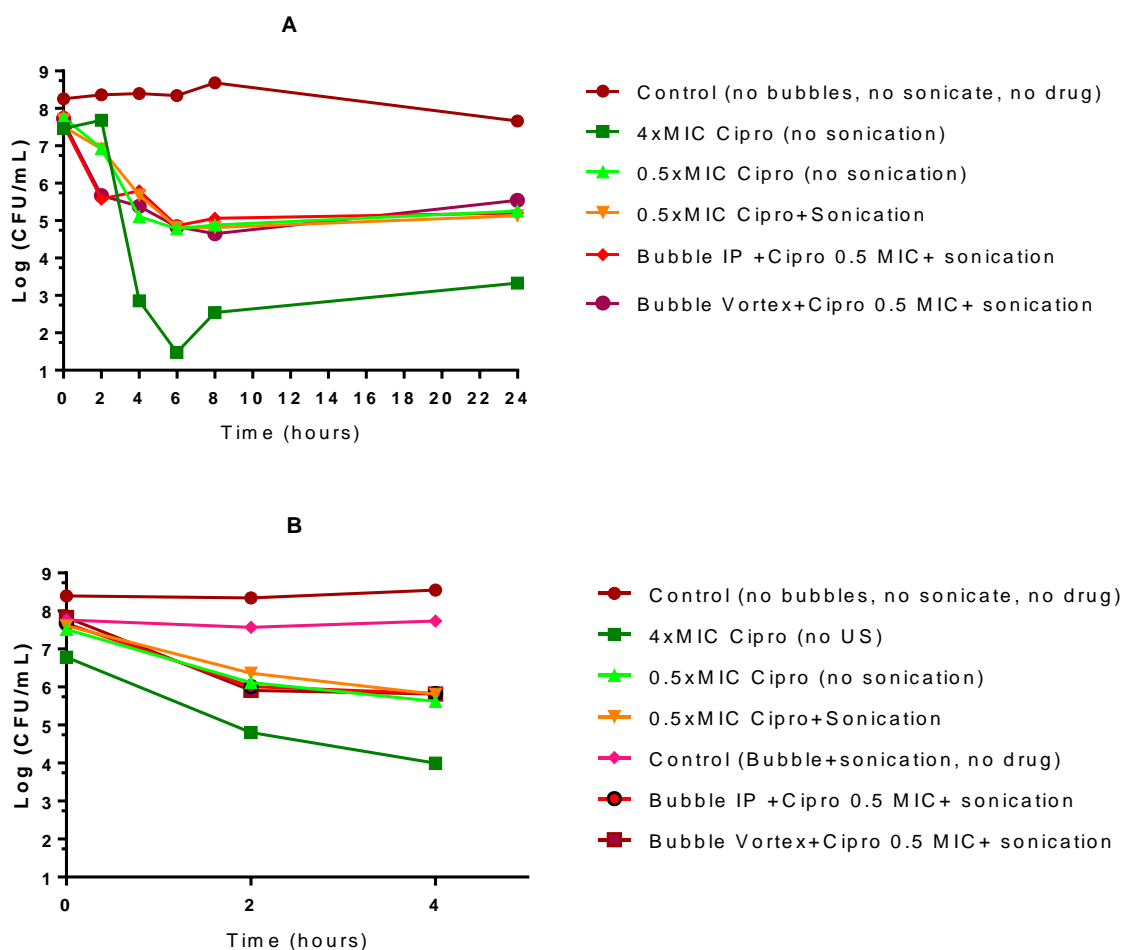
Figure 3-11: Observed viable counts of two independent experiments, P. aeruginosa ATCC® 27853™ treated with ciprofloxacin HCl (0.5 MIC) and LMBs using 30 seconds bath sonication, power100 W/L and frequency 32 – 38 kHz. LMBs were made of DSPC:DSPEmPEG-2000 (94:6) and PFP, the cells were cultured in MH cationic adjusted broth and plated on MH cationic adjusted agar, viability was counted at the indicated time points by 8 serial dilution and plating each arm at each time points (504 agar plates in total), the arms containing ciprofloxacin HCl were washed via centrifugation (9888 g for 5 min) before plating, the Y-axis starts from 1 (the limit of detection), Cipro= ciprofloxacin HCl, A) the time points were 0 min (i.e. before treatment with US), 5 min after US treatments (for the sonicated arms), 2,4,6,8 and 24 hours after US treatment B) the time points 0 min (before treatment with US), 2 and 4 hours after the sonication

3.4.3. Effect of cavitation of LMBs on intracellular uptake of solutes

In order to confirm the results of the bacterial time kill study and determine whether cavitation can enhance/facilitate the penetration of solutes across the cell wall of *P. aeruginosa*, a further Trypan blue exclusion assay study was performed.

Trypan blue is known to be impermeable to live cells (140), hence, was chosen so that would only penetrate the bacteria via external assistance, which in this study refers to US-mediated cavitation.

For this purpose, *P. aeruginosa* was cultured in 40 mL MH cationic adjusted broth at 37º C for 24 hours using a shaker incubator at 230 rpm. Next, the inoculum was centrifuged at 5000 *g* for 20 min and the supernatant was removed. Fresh Muller Hinton cationic adjusted broth was added and the volume was adjusted to the final volume of 20 mL. In this experiment the arms were:

1. 200 µL LMBs (prepared by vortexing) + 750 µL bacteria + 50 µL Trypan blue
2. 200 µL LMBs (in-house, provisionally patented method) + 750 µL bacteria + 50 µL Trypan blue
3. 200 µL liposome + 750 µL bacteria + 50 µL Trypan blue (control)

Each sample was transferred to a 15 mL falcon tubes and was exposed to bath sonication (power100 W/L frequency 32 – 38 kHz at 37 º C) followed by centrifugation for 10 min at 4500 *g*. next:

1. 900 µL of the supernatant was carefully collected (labelled as A in Figure 3-12)
2. 900 µL of fresh broth was added and the tubes were vortex shaken to resuspend the pellets. Next, the samples were centrifuged again (4500 *g*, 10 min) and 900 µL of the supernatant was collected (labelled as B in Figure 3-12).

The final colourless pellets were resuspended in 900 µL fresh broth and were subjected to probe sonication (amplitude 60 for 60 seconds (1 sec on 1 sec off)) to lyse the bacteria and the absorbance was recorded at 585 nm (labelled as C in Figure 3-12). Before the readings at 585 nm: 1st, 2nd wash and lysed cells were centrifuged at 9888 *g* for 5 minutes to remove any remaining cells and/or debris interfering with UV visible reads.
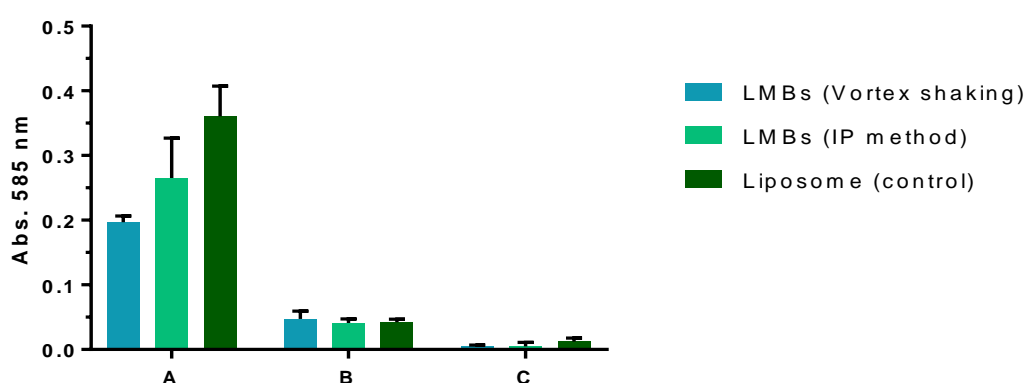
Figure 3-12: Trypan blue exclusion assay, absorbance at 585 nm, the cells were treated by 200 µL LMBs (11 mM, made of DSPC:DSPEmPEG-2000 (94:6) and PFP)and bath sonication, power100 W/L frequency 32 – 38 kHz, after the sonication the cells were centrifuged at 4500 g for 10 min A) Trypan blue in the supernatant after the first centrifugation B) *Trypan blue in* the supernatant after the 2nd centrifugation C) Intracellular Trypan blue after the lysis of the washed cells by probe sonication and centrifugation at 9888 *g* for 5 minutes, the average means of absorbance for C is 0.005, 0.005 and 0.012 for the blue, light green and dark green arms respectively *(the data shown are mean ± SD)*

3.5. Discussion

It has been reported that US as well as US assisted cavitation of LMBs have synergistic effects in increasing the susceptibility of *in vitro* derived *Staphylococcus epidermis* biofilms to vancomycin and therefore has been suggested as an efficient non-invasive adjunct treatment of such biofilm related infections (141). In another study, the efficacy of vancomycin against *in-vitro* biofilms of methicillin-resistant *Staphylococcus aureus* has been enhanced using acoustic cavitation of bubbles (142). Moreover, cavitation of nanobubbles and doxycycline have been shown to have synergistic bactericidal effects on intracellular C*hlamydia trachomatis* (143). This effect is reported to be due to higher cellular uptake of the drug, caused by cavitation of the bubbles, leading to higher concentrations of intracellular doxycycline. Therefore, bacteria present inside host mammalian cells are exposed to a higher dose of doxycycline, correlating with previous reports of enhanced cellular uptake of different drugs using US-induce cavitation (144-147).

The experiments in this chapter were trialled to determine the efficacy of ciprofloxacin against *P. aeruginosa*. The OD results could not show any synergism between the drug and cavitation due to the overlap of the dose response curves. The overlap could be a result of:

- The interference of the LMBs (made of phospholipids) with absorbance reads at 620 nm. Although the observed interferences ($\cong$ 0.054) have been subtracted from all the absorbance reads in the arms containing LMBs, but such issue limits the accuracy of the assay

- The gradual evaporation of the media through condensate formation during the 8-hour incubation at 37 ℃. Since the total volume of sample per each vial was 2.25 mL at the start of the study evaporation of the media would increase concentration of the drug hence resulting in increased bactericidal efficacy bias over the duration of the assay.

In light of the drawbacks presented by these former experiments, a quantitative culture study, which is a direct and accurate technique in assessing bacterial kill was performed next, to investigate possible synergism between cavitation of LMBs and activity of ciprofloxacin HCl against *P. aeruginosa*. However, once again this colony counting study did not show any synergism between cavitation of the LMBs and the bactericidal effects of ciprofloxacin HCL on *P. aeruginosa* ATCC® 27853™ within the technique's limit of detection i.e. 1 log10 CFU/mL (148).

In a final attempt to assess whether there was any measurable detrimental effect to the bacteria a Trypan blue exclusion assay was performed to explore the effect of cavitation on

facilitating the penetration of molecules across the bacterial cell wall and also to corroborate the outcome from the colony counting method. Trypan blue is a cell impermeable dye (149) and therefore deemed to be a suitable candidate to determine any enhancement in cellular uptake of the dye by US mediated cavitation of LMBs. Here, *P. aeruginosa* was exposed to the dye and then treated by LMBs and US (using XUB-5 bath sonicator). Next, the intracellular dye was determined using the protocol described earlier in this chapter. However, the absorbance readings for intracellular dye shown in Figure 3-12 (above) were negligible, indicating the limitation of this assay in identifying the cellular uptake of the dye therefore an inconclusive result was recorded.

4. Chapter 4: Overall conclusions and future directions and outlook

4.1. Overall conclusions

It is estimated that each year around 433,000 Australians are afflicted by chronic wounds, costing around A$2.8 billion to the Australian healthcare system. The Australian Bureau of Statistics have predicted that the number of patients with chronic wounds will triple from around 2.8 million in 2007 to around 7.5 million in 2050, driven by an aging population. Thus, there is an unmet clinical need for more efficacious interventional approaches to treating chronic wounds, given it is inadequately managed by currently available therapies. Chronic wounds share a range of features such as having high levels of proinflammatory cytokines, reactive oxygen species (ROS), which results in premature aging of cells i.e. senescence (150, 151). In addition, excessive levels of protease, persistence of infection, lack of stem cells (69) and presence of biofilms (152) are other common features observed in these wounds. As described earlier, the most efficient approach to managing chronic wounds is debridement, which can be performed via surgery, the bio-debridement by maggots (153), or using dressings for a gradual auto-debridement of slough and crusts. The latter is preferred particularly in patients with ischaemia who cannot tolerate surgical debridement (69). In addition, reports suggest that using LMBs and US can increase the susceptibility of *in vitro Staphylococcus epidermis* biofilms to vancomycin (141, 142) and therefore this platform has been suggested as an effective non-invasive adjunct treatment of such biofilm related infections. However, the aforesaid studies were performed *in vitro* without the other physical barriers that typically exist in chronic wounds, such as coating and slough of the wound, which could further hinder access of LMBs to biofilms.

The potential enhancement in delivery/efficacy of drugs using this platform could decrease the number of cycles of debridement via tackling the biofilms embracing bacteria, which are present in majority of chronic wounds (154), therefore leading to a faster rate of healing, lower treatment cost and improved patient comfort.

In the design and development of nanomedicine, one of the major challenges is the reproducibility of formulation preparation methods. To this end, and for the first time a reproducible method for preparing CLMBs with high loading efficiency (i.e. $\geq 90\%$), high echogenicity with acceptable stability and desired uniformity (i.e. PDI ≤ 0.1) was successfully developed and optimized.

The first challenge in this research was to develop a preparation method for liposomal ciprofloxacin with high loading efficiency. Therefore, a systematic review of the literature was performed to find a biocompatible agent capable of entrapping ciprofloxacin inside liposomes, the main component of LMBs, using a well-established remote loading protocol. Next, this preparation method was optimised to achieve the highest loading efficiency via remote loading performed using a range of loading times. Then, with this aspect addressed the next challenge was to combine the aforesaid optimised preparation method with an already-developed supercharging method to achieve the final echogenic CLMBs with an acceptable stability profile. All the characterisation studies along with the results from the stability studies confirmed the successful combination of the two preparation methods (as depicted in Figure 2-11) paving way for the next phase where *in vitro* characterisation studies were developed and optimized.

Based on a previously published observational study on bubbles and their collapse characteristics (155), loss of bubbles was deemed to occur as a consequence of bubble cavitation. Accordingly, the first task here involved a study of US parameters able to cause bubble loss via cavitation while having negligible hyperthermic effects. Thus, a series of optimisation studies were performed to determine such US parameters and these were then applied in . different US-induced cavitation experiments along with the prepared LMBs in line with the hypotheses to ascertain whether it was possible to:

1. Increase the penetration of a model agent (dye) into barrier models of infectious disease;
2. Enhance the ingress of antibiotic in a gram negative bacteria, leading to reduced bacterial burden.

However, using a low intensity ultrasound unit, and over the course of the systematic studies presented in this thesis i.e. a range of barrier models such as agarose-based barrier model, Franz cell diffusion model as well as *in vitro* studies such as optical density, quantitative bacterial kill assay and Trypan blue assay, it became apparent that the cavitation of LMBs, although achieved as observed under optical microscopy and by echograms, did not show any statistically significant enhancement on depth of penetration of any agent nor did it appear to impact the burden of *P. aeruginosa*.

This could be due to a multitude of factors which are elaborated on below:

1. The off-the-shelf US apparatus used (i.e. JUS2 and XUB-5 bath sonicator): As discussed earlier in chapter one, mechanical index (MI) is a key parameter in US-induced cavitation of LMBs driven by wave amplitude, this being defined as the difference in pressure between peak and baseline in a sound wave. The piezoelectric crystal used in

any US probe dictates its amplitude and consequently MI. Most of the published work in this area have used a device with a MI ranging from 0.4 to 1.6. However, the MI for the devices used in this research remained unknown.

2. The greater relative thickness in bacterial cell walls *c.f.* eukaryotes: Unlike eukaryotes, prokaryotes have a meshlike peptidoglycan envelope which is known to act as a barrier protecting them from their harsh environment (156). Therefore, this layer might serve to prevent ingress of antibiotic assisted by cavitation of the bubbles and therefore make the phenomenon inconsequential to the bacterial cells.

3. The limitation of the assays such as:

    a. The gradual auto-diffusion of rhodamine B into the agarose disks resulting in a fading dye border pattern preventing accurate measurements of the dye's depth of penetration into the disks.

    b. The interference of the LMBs with absorbance at 620 nm in OD studies and/or gradual evaporation of the media during the incubation period resulting in a relative increase in concentration of the drug.

Therefore, the following alternative experiments were performed to gauge whether the negative results from the abovementioned experiments could be overcome by:

1. Franz cell diffusion apparatus studies with desired rhodamine B diffusion pattern across the barrier model.

2. Quantitative culture method to avoid the UV interference issues observed during OD studies.

3. Trypan blue studies as a second alternative to the OD method.

The alternative experiments here did not show the anticipated effects contradicting the numerous published studies in enhanced drug delivery to eukaryotes using this platform (please refer to section 1.5). Therefore, the following factors can potentially play role in this regard:

1. Limitations of these assays such as:

    a. The thickness of dialysis membranes (20 – 45 µm) (157) used in Franz cell diffusion apparatus could act as a physical barrier and absorb the shockwaves generated by cavitation of bubbles in microscale.

    b. The limit of detection in quantitative culture method (i.e. 1 log10 CFU/mL)(please refer to section 3.5 Discussion) therefore this assay was not able to show any enhancement in efficacy of antibiotic using US assisted cavitation of LMBs within this range.

c. The small intracellular space within the bacteria result in inadequate accumulation of Trypan blue inside the cell therefore UV vis plate reader cannot detect the dye.

2. The structural difference between the two class of cells which is detailed later in this chapter (please see Figure 4-1 below).
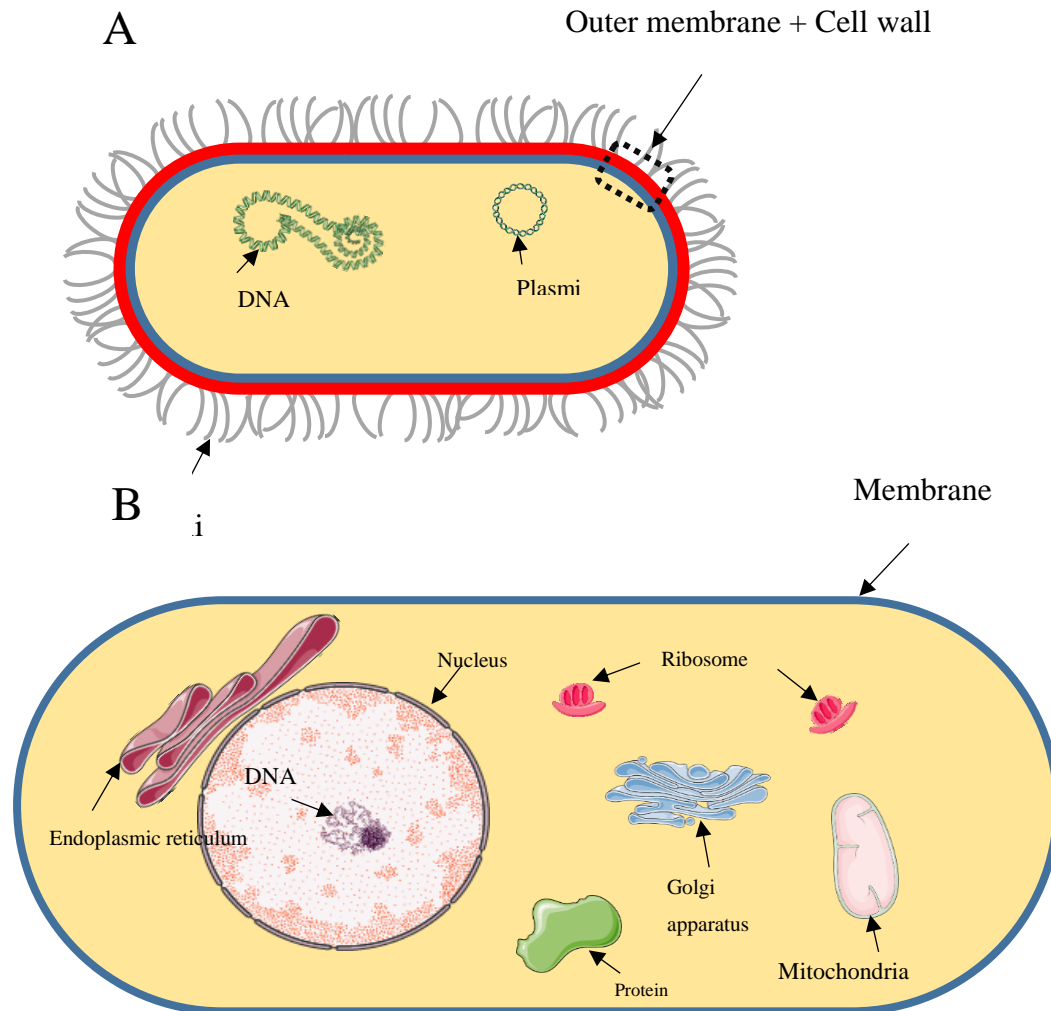
Figure 4-1: Prokaryote cell (A) vs eukaryote cell (B) P. aeruginosa has an outer membrane (defined in red) made of lipopolysaccharides and porins (158) + thick cell wall (defined in blue) consisting of plasma membrane + periplasmic space + peptidoglycan (159) (Fig. A), whereas eukaryote cells have a 'single' membrane with lipid molecules in a bilayered configuration (Fig. B), (160). The organelles inside the cells are simplified for a better demonstration, intracellular organelles images are taken with permission from Servier Medical Art (http://smart.servier.com/)

4.2. Future directions and outlook

US-mediated cavitation of echogenic microbubbles has been reported to create transient pores in the membrane of eukaryotes resulting in increase of cellular uptake of encapsulated therapeutics (147). Therefore from a different perspective, LMBs might benefit patients via an indirect synergism with antibiotics which could consequently reduce the treatment courses in these patients. For example in the tuberculoid form of leprosy, *Mycobacterium leprae* usually starts to multiply in skin through invading and colonizing inside Schwann cells (161). This

consequently leads to appearance of large skin patches via induction of immunological responses (162). In this case, LMBs could increase the delivery of the chemotherapeutics into Schwann cells thus eradicating *M. leprae*, the underlying cause of leprosy. Moreover, LMBs might be able to augment the bactericidal efficacy of antibiotics in patients with lepromatous, another form of leprosy, via the same strategy. In this case, LMBs can expose the *M. leprae*, proliferating inside macrophages (163), to higher levels/dose of intracellular antibiotics, therefore improving the efficacy of antibiotics used in this form of leprosy resulting in shorter period of treatments.

From a bacteriology point of view, the relatively thick cell wall in prokaryotes might play a key role in impeding the effects sought from using LMBs and ultrasound in this class of cells (i.e. enhancing ingress of therapeutic agents). These cells are generally classified into two subgroups based on existing architectural differences in their cell walls (164) (Figure 4-2 (156)):

1. Gram-negative bacteria with three principal layers including an outer membrane, a peptidoglycan cell wall, and cytoplasmic membrane. The thickness of peptidoglycan in this class of bacteria is reported to be 7.5 to 10 nm (165).
2. Gram-positive bacteria with a thick (30–100 nm) multilayered peptidoglycan meshwork membrane.

Hence, optimising a pre-treatment protocol using antibiotic(s) that diminish/weaken the cell wall (e.g. β-Lactams and/or glycopeptide antibiotics (166)) prior to application of LMBs has the potential to enhance the cellular uptake of antibiotics using LMBs overcoming the resistance caused by the lack of penetration of these agents such as the acquired resistance to β-Lactams in *P. aeruginosa* (167) . In addition, the aforesaid combination strategy has the potential to increase the efficacy of antibiotics, which could consequently obviate the need for higher doses.
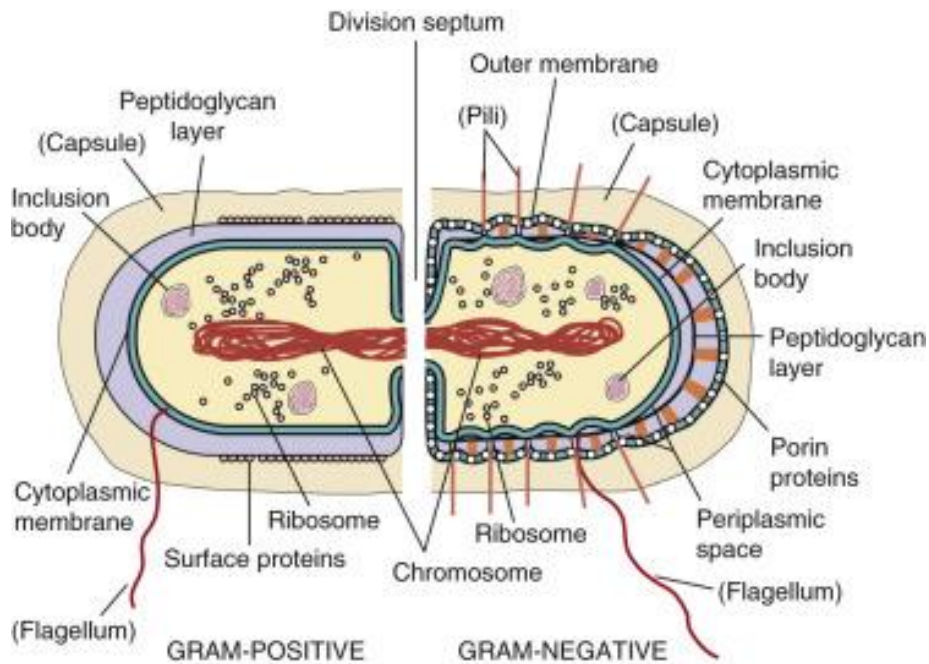
Figure 4-2: Gram-positive with thick peptidoglycan layer (left) vs. Gram-negative with three layers: outer membrane, peptidoglycan cell wall, and cytoplasmic membrane (right) Reprinted from (156), Copyright (2016), with permission from Elsevier

From a practical perspective, access to a 'tunable' US device allowing wider modulation of parameters such as frequency, intensity, duty cycle, and mechanical index is imperative to further optimising the cavitation of LMBs. Moreover, despite the challenges in the measurement of cavitation, the phenomenon has been scrutinized in different studies. For example in one study, using an in house needle-type hydrophone, US-mediated cavitation of bubbles was reported to decrease sound pressures (168) suggesting the method's potential in correlating/quantifying the resulting energy with the decrease in sound pressure. It has also been shown that MBs create acoustic emissions during cavitation and these broadband acoustic emissions can be recorded by hydrophones connected to an amplifier and oscilloscope, (Figure 4-3; (169)) therefore such a set-up can be proposed as a measurement device to quantify the cavitation of LMBs.
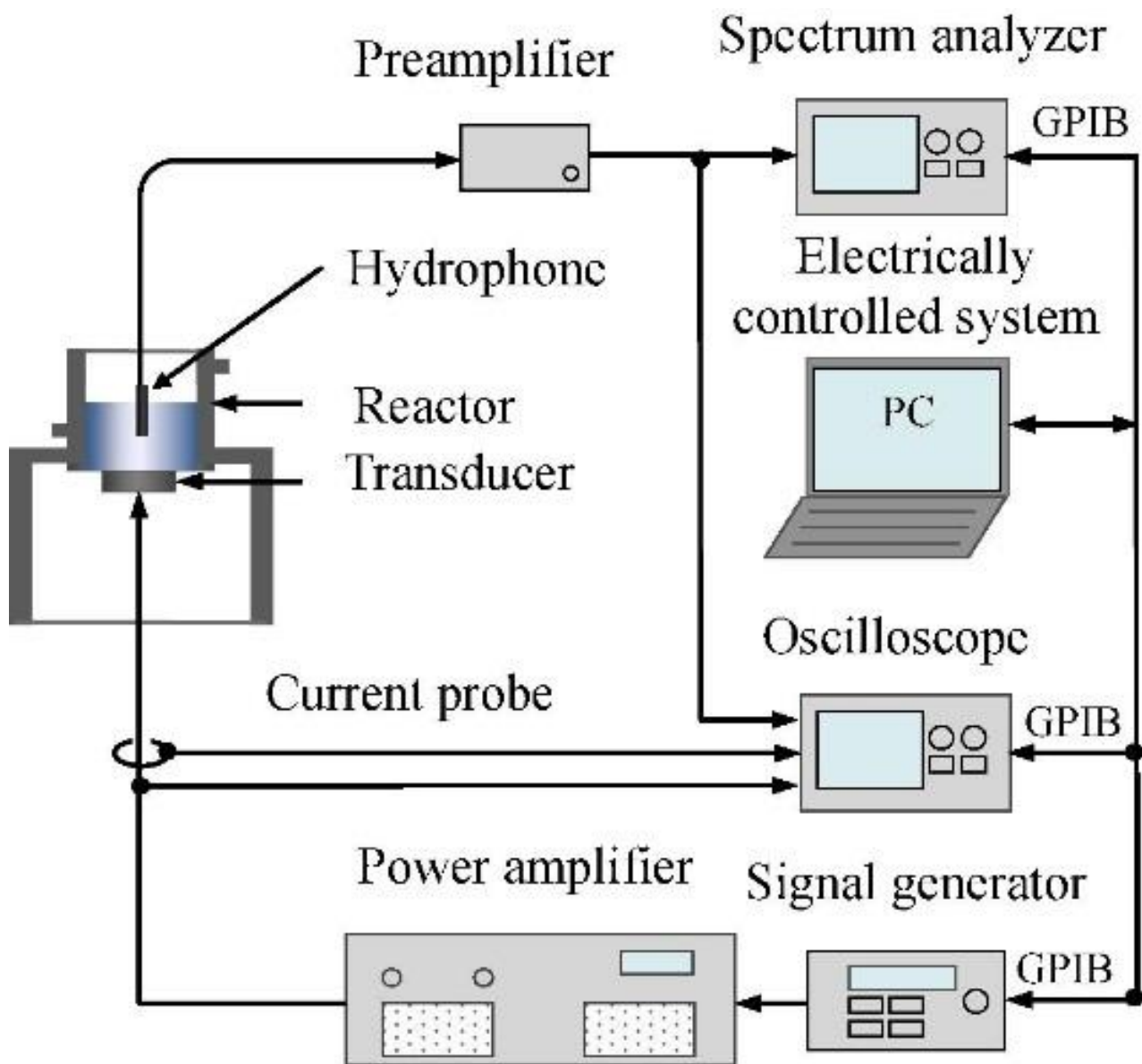
Figure 4-3: Detection and quantification of MBs cavitation in medium using hydrophone, reprinted with permission from (169) Elsevier, copyright 2017

Another important approach that could facilitate our understanding of cavitation is a chemiluminescence assay. Here, conversion of US from sound-to-light energy can be used to quantify the energy released from cavitation of microbubbles. During cavitation, a high amount of energy is released and the temperature of the cavitating bubbles is reported to reach up to 5000 K (4727 °C). This energy is believed to create hydroxyl radicals in the media, which reacts with luminol resulting in emission of light (170). Data obtained from generated chemiluminescence can be used to validate the data obtained from the abovementioned assays.

The assays can be further scrutinized by characterising the physicochemical properties of the media in which LMBs reside, and correlating them to the energy released from cavitation, which is quantified by the hydrophone setup and chemiluminescence assay mentioned earlier. This approach includes an appreciation of viscosity, density and surface tension, which is claimed to play important role in the collapse of bubbles (171, 172). This can be expected to vastly improve the understanding of the complex interrelationships at play and so serve to advance the field of MB-US assisted chemotherapy.

Another important method which can shed more light on the US assisted cavitation of LMBs, is to image/record the bubble(s) during cavitation using high speed cameras. These cameras have been used to record the formation and collapse of bubbles using shock-induced waves (173) therefore, the resulting videograms, if combined with the data from the aforementioned assays, can potentially assist in correlating the influence of US parameters and surrounding media on the behaviour of bubbles during the cavitation e.g. the magnitude and the rate of growth of bubble in different media and different US parameters.

On a final note, the aforementioned studies which can be expected extend our understanding of LMB-US based cavitation require highly specialised instrumentation, which would not be typically present in a pharmaceutics lab, therefore in any future work of this nature the need to collaborate with an engineering faculty is likely required, so more elaborate studies as alluded to above can be comprehensively undertaken.

5. References

1. Roden DM. Principles of Clinical Pharmacology. In: Kasper D, Fauci A, Hauser S, Longo D, Jameson JL, Loscalzo J, editors. Harrison's Principles of Internal Medicine, 19e. New York, NY: McGraw-Hill Education; 2015.

2. de Souza PC, Ranjan A, Towner RA. Nanoformulations for therapy of pancreatic and liver cancers. Nanomedicine (Lond). 2015;10(9):1515-34.

3. Janssen Products L. Doxil full prescribing information 2015 [updated 22/06/2015. Available from: https://www.doxil.com/shared/product/doxil/doxil-prescribing-information.pdf.

4. Miele E, Spinelli GP, Miele E, Tomao F, Tomao S. Albumin-bound formulation of paclitaxel (Abraxane(®) ABI-007) in the treatment of breast cancer. International Journal of Nanomedicine. 2009;4:99-105.

5. Heldin CH, Rubin K, Pietras K, Ostman A. High interstitial fluid pressure - an obstacle in cancer therapy. Nat Rev Cancer. 2004;4(10):806-13.

6. Stone NRH, Bicanic T, Salim R, Hope W. Liposomal Amphotericin B (AmBisome®): A review of the pharmacokinetics, pharmacodynamics, clinical experience and future directions. Drugs. 2016;76(4):485-500.

7. Adler-Moore J. AmBisome targeting to fungal infections. Bone Marrow Transplant. 1994;14 Suppl 5:S3-7.

8. Spector MS, Zasadzinski JA, Sankaram MB. Topology of Multivesicular Liposomes, a Model Biliquid Foam. Langmuir. 1996;12(20):4704-8.

9. Gorfine SR, Onel E, Patou G, Krivokapic ZV. Bupivacaine extended-release liposome injection for prolonged postsurgical analgesia in patients undergoing hemorrhoidectomy: a multicenter, randomized, double-blind, placebo-controlled trial. Diseases of the colon and rectum. 2011;54(12):1552-9.

10. Wei A, Mehtala JG, Patri AK. Challenges and opportunities in the advancement of nanomedicines. Journal of Controlled Release. 2012;164(2):236-46.

11. Scheinberg DA, Villa CH, Escorcia FE, McDevitt MR. Conscripts of the infinite armada: systemic cancer therapy using nanomaterials. Nature Reviews Clinical Oncology. 2010;7:266.

12. Champion JA, Walker A, Mitragotri S. Role of Particle Size in Phagocytosis of Polymeric Microspheres. Pharmaceutical research. 2008;25(8):1815-21.

13. Horne RW, Bangham AD, Whittaker VP. NEGATIVELY STAINED LIPOPROTEIN MEMBRANES. Nature. 1963;200:1340.

14. Bangham AD, Horne RW. Negative staining of phospholipids and their structural modification by surface-active agents as observed in the electron microscope. Journal of Molecular Biology. 1964;8(5):660-IN10.

15. Bangham AD, Standish MM, Watkins JC. Diffusion of univalent ions across the lamellae of swollen phospholipids. J Mol Biol. 1965;13(1):238-52.

16. Torchilin VP. Recent advances with liposomes as pharmaceutical carriers. Nat Rev Drug Discov. 2005;4(2):145-60.

17. Uchegbu IF, Schätzlein AG, Cheng WP, Lalatsa A. Fundamentals of Pharmaceutical Nanoscience: Springer New York; 2013.

18. Doxorubicin MedicinesComplete: Martindale: The Complete Drug Reference; [updated 16/03/2011. Available from: https://www.medicinescomplete.com/mc/martindale/current/ms-21514-e.htm?q=doxorubicin&t=search&ss=text&tot=337&p=1#m1831-a5-y.

19. Octavia Y, Tocchetti CG, Gabrielson KL, Janssens S, Crijns HJ, Moens AL. Doxorubicin-induced cardiomyopathy: From molecular mechanisms to therapeutic strategies. Journal of Molecular and Cellular Cardiology. 2012;52(6):1213-25.

20. Immordino ML, Dosio F, Cattel L. Stealth liposomes: review of the basic science, rationale, and clinical applications, existing and potential. Int J Nanomedicine. 2006;1(3):297-315.

21. The Pharmaceutical Press RPS. Martindale: The Complete Drug Reference 2016 [Available from: https://www.medicinescomplete.com/mc/martindale/2009/.

22.   Barenholz Y. Doxil® — The first FDA-approved nano-drug: Lessons learned. Journal of Controlled Release. 2012;160(2):117-34.

23.   Green AE, Rose PG. Pegylated liposomal doxorubicin in ovarian cancer. International Journal of Nanomedicine. 2006;1(3):229-39.

24.   Jain RK. Normalization of tumor vasculature: an emerging concept in antiangiogenic therapy. Science (New York, NY). 2005;307(5706):58-62.

25.   McIntosh TJ. The effect of cholesterol on the structure of phosphatidylcholine bilayers. BBA - Biomembranes. 1978;513(1):43-58.

26.   Allen TM, Cleland LG. Serum-induced leakage of liposome contents. BBA - Biomembranes. 1980;597(2):418-26.

27.   Cullis PR. Lateral diffusion rates of phosphatidylcholine in vesicle membranes: Eeffects of cholesterol and hydrocarbon phase transitions. FEBS Letters. 1976;70(1-2):223-8.

28.   Allen TM, Cullis PR. Liposomal drug delivery systems: From concept to clinical applications. Advanced Drug Delivery Reviews. 2013;65(1):36-48.

29.   Chang H-I, Yeh M-K. Clinical development of liposome-based drugs: formulation, characterization, and therapeutic efficacy. International Journal of Nanomedicine. 2012;7:49-60.

30.   Meunier F, Prentice HG, Ringden O. Liposomal amphotericin B (AmBisome): safety data from a phase II/III clinical trial. J Antimicrob Chemother. 1991;28 Suppl B:83-91.

31.   US AP. Ambisome [Available from: http://www.ambisome.com/.

32.   Immordino ML, Dosio F, Cattel L. Stealth liposomes: review of the basic science, rationale, and clinical applications, existing and potential. International Journal of Nanomedicine. 2006;1(3):297-315.

33.   Wasan KM, Lopez-Berestein G. Characteristics of lipid-based formulations that influence their biological behavior in the plasma of patients. Clin Infect Dis. 1996;23(5):1126-38.

34.   Denning DW, Lee JY, Hostetler JS, Pappas P, Kauffman CA, Dewsnup DH, et al. NIAID mycoses study group multicenter trial of oral itraconazole therapy for invasive aspergillosis. The American Journal of Medicine. 1994;97(2):135-44.

35.   Fassas A, Anagnostopoulos A. The use of liposomal daunorubicin (DaunoXome) in acute myeloid leukemia. Leuk Lymphoma. 2005;46(6):795-802.

36.   Tomkinson B, Bendele R, Giles FJ, Brown E, Gray A, Hart K, et al. OSI-211, a novel liposomal topoisomerase I inhibitor, is active in SCID mouse models of human AML and ALL. Leukemia research. 2003;27(11):1039-50.

37.   Hoarau D, Delmas P, David S, Roux E, Leroux JC. Novel long-circulating lipid nanocapsules. Pharm Res. 2004;21(10):1783-9.

38.   Park JW. Liposome-based drug delivery in breast cancer treatment. Breast cancer research : BCR. 2002;4(3):95-9.

39.   RL H. Liposomal anti-cancer drug researches the myth of long circulation. J Chinese Oncol Soc. 2004;20(2):10–21.

40.   Gardikis K, Tsimplouli C, Dimas K, Micha-Screttas M, Demetzos C. New chimeric advanced Drug Delivery nano Systems (chi-aDDnSs) as doxorubicin carriers. Int J Pharm. 2010;402(1-2):231-7.

41.   Novartis Ophthalmics, Inc [homepage on the Internet] Visudyne® (verteporfin for injection) [Available from: http://www.bauschretinarx.com/visudyne/ecp/about.

42.   Chowdhary RK, Shariff I, Dolphin D. Drug release characteristics of lipid based benzoporphyrin derivative. Journal of pharmacy & pharmaceutical sciences : a publication of the Canadian Society for Pharmaceutical Sciences, Societe canadienne des sciences pharmaceutiques. 2003;6(1):13-9.

43.   DepoCyt® (cytarabine liposome injection) Prescribing Information [Available from: https://www.drugs.com/pro/depocyt.html.

44.   DepoDur (morphine sulfate extended-release liposome injection) Prescribing Information [Available from: https://www.drugs.com/pro/depodur.html.

45.   Burgess DJ. Injectable dispersed systems : formulation, processing, and performance: Boca Raton : Taylor&Francis; 2005.

46. Usonis V, Bakasenas V, Valentelis R, Katiliene G, Vidzeniene D, Herzog C. Antibody titres after primary and booster vaccination of infants and young children with a virosomal hepatitis A vaccine (Epaxal). Vaccine. 2003;21(31):4588-92.

47. Herzog C, Hartmann K, Kunzi V, Kursteiner O, Mischler R, Lazar H, et al. Eleven years of Inflexal V-a virosomal adjuvanted influenza vaccine. Vaccine. 2009;27(33):4381-7.

48. J. Lasch VW, and M.Brandl. In: Vladimir P. Torchilin VW, editor. Liposomes (Practical Approach): Oxford University Press; 2003.

49. Wagner A, Vorauer-Uhl K. Liposome Technology for Industrial Purposes. Journal of Drug Delivery. 2011;2011.

50. Schubert R. Liposome Preparation by Detergent Removal. Methods in Enzymology. Volume 367: Academic Press; 2003. p. 46-70.

51. Charcosset C, Juban A, Valour J-P, Urbaniak S, Fessi H. Preparation of liposomes at large scale using the ethanol injection method: Effect of scale-up and injection devices. Chemical Engineering Research and Design. 2015;94:508-15.

52. Turánek J, Kašná A, Záluská D, Neča J. Preparation of Sterile Liposomes by Proliposome– Liposome Method. Methods in Enzymology. Volume 367: Academic Press; 2003. p. 111-25.

53. Pons M, Foradada M, Estelrich J. Liposomes obtained by the ethanol injection method. International Journal of Pharmaceutics. 1993;95(1):51-6.

54. Perrett S, Golding M, Williams WP. A simple method for the preparation of liposomes for pharmaceutical applications: characterization of the liposomes. J Pharm Pharmacol. 1991;43(3):154-61.

55. Drummond DC, Noble CO, Guo Z, Hong K, Park JW, Kirpotin DB. Development of a highly active nanoliposomal irinotecan using a novel intraliposomal stabilization strategy. Cancer Research. 2006;66(6):3271-7.

56. Mayer LD, Tai LCL, Bally MB, Mitilenes GN, Ginsberg RS, Cullis PR. Characterization of liposomal systems containing doxorubicin entrapped in response to pH gradients. BBA - Biomembranes. 1990;1025(2):143-51.

57. Bolotin EM, Cohen R, Bar LK, Emanuel N, Ninio S, Barenholz Y, et al. Ammonium sulfate gradients for efficient and stable remote loading of amphipathic weak bases into liposomes and ligandoliposomes. Journal of Liposome Research. 1994;4(1):455-79.

58. Duong AD, Collier MA, Bachelder EM, Wyslouzil BE, Ainslie KM. One Step Encapsulation of Small Molecule Drugs in Liposomes via Electrospray-Remote Loading. Mol Pharm. 2016;13(1):92-9.

59. Juliano RL, Stamp D. The effect of particle size and charge on the clearance rates of liposomes and liposome encapsulated drugs. Biochemical and Biophysical Research Communications. 1975;63(3):651-8.

60. Kimelberg HK, Tracy Jr TF, Biddlecome SM, Bourke RS. The effect of entrapment in liposomes on the in vivo distribution of [3H]methotrexate in a primate. Cancer Research. 1976;36(8):2949-57.

61. Gregoriadis G, Neerunjun DE. Control of the rate of hepatic uptake and catabolism of liposome entrapped proteins injected into rats. Possible therapeutic applications. European Journal of Biochemistry. 1974;47(1):179-85.

62. Johnston MJW, Semple SC, Klimuk SK, Edwards K, Eisenhardt ML, Leng EC, et al. Therapeutically optimized rates of drug release can be achieved by varying the drug-to-lipid ratio in liposomal vincristine formulations. Biochimica et Biophysica Acta - Biomembranes. 2006;1758(1):55-64.

63. Laginha KM, Verwoert S, Charrois GJR, Allen TM. Determination of doxorubicin levels in whole tumor and tumor nuclei in murine breast cancer tumors. Clinical Cancer Research. 2005;11(19 I):6944-9.

64. Hyodo K, Yamamoto E, Suzuki T, Kikuchi H, Asano M, Ishihara H. Development of Liposomal Anticancer Drugs. Biological and Pharmaceutical Bulletin. 2013;36(5):703-7.

65.   Forssen EA, Tokes ZA. Use of anionic liposomes for the reduction of chronic doxorubicin-induced cardiotoxicity. Proceedings of the National Academy of Sciences of the United States of America. 1981;78(3):1873-7.

66.   Gabizon AA. Selective tumor localization and improved therapeutic index of anthracyclines encapsulated in long-circulating liposomes. Cancer Res. 1992;52(4):891-6.

67.   Abraham SA, Edwards K, Karlsson G, Hudon N, Mayer LD, Bally MB. An evaluation of transmembrane ion gradient-mediated encapsulation of topotecan within liposomes. Journal of Controlled Release. 2004;96(3):449-61.

68.   Boman NL, Cullis PR, Mayer LD, Bally MB, Webb MS. Liposomal Vincristine: The Central Role of Drug Retention in Defining Therapeutically Optimized Anticancer Formulations. In: Woodle MC, Storm G, editors. Long Circulating Liposomes: Old Drugs, New Therapeutics. Berlin, Heidelberg: Springer Berlin Heidelberg; 1998. p. 29-49.

69.   Frykberg RG, Banks J. Challenges in the Treatment of Chronic Wounds. Advances in Wound Care. 2015;4(9):560-82.

70.   Stojadinovic A, Carlson JW, Schultz GS, Davis TA, Elster EA. Topical advances in wound care. Gynecologic Oncology. 2008;111(2, Supplement):S70-S80.

71.   Woo K, Ayello EA, Sibbald RG. The Edge Effect: Current Therapeutic Options to Advance the Wound Edge. Advances in Skin & Wound Care. 2007;20(2):99-117.

72.   Henry Zheng NG. Modelling the direct health care costs of chronic wounds in Australia. Wound Practice & Research: Journal of the Australian Wound Management Association.22(No. 1):20-4, 6-33.

73.   Subhas Gupta CA, Joyce Black, Jean de Leon, Caroline Fife, John C. Lantis II, Jeffrey Niezgoda, Robert Snyder, Bauer Sumpio, William Tettelbach, Terry Treadwell, Dot Weir, Ronald P. Silverman. Management of Chronic Wounds: Diagnosis, Preparation, Treatment, and Follow-up. WOUNDS. 2017;29:S19–S36.

74.   Analise B. Thomas WPT. Debridement of Chronic Wounds: A Review of Past & Present Treatment Strategies. Today's woundclinic. 2014;8(5).

75.   Fonder MA, Lazarus GS, Cowan DA, Aronson-Cook B, Kohli AR, Mamelak AJ. Treating the chronic wound: A practical approach to the care of nonhealing wounds and wound care dressings. Journal of the American Academy of Dermatology.58(2):185-206.

76.   Seaman S. Dressing selection in chronic wound management. Journal of the American Podiatric Medical Association. 2002;92(1):24-33.

77.   ENLUXTRA Smart Wound Dressing 2016 [Available from: https://www.enluxtrawoundcare.com/.

78.   Franz MG. Wound Healing. In: Doherty GM, editor. CURRENT Diagnosis & Treatment: Surgery, 14e. New York, NY: McGraw-Hill Education; 2015.

79.   Whittam AJ, Maan ZN, Duscher D, Wong VW, Barrera JA, Januszyk M, et al. Challenges and Opportunities in Drug Delivery for Wound Healing. Advances in Wound Care. 2016;5(2):79-88.

80.   Han G, Ceilley R. Chronic Wound Healing: A Review of Current Management and Treatments. Advances in Therapy. 2017;34(3):599-610.

81.   Clinton A, Carter T. Chronic Wound Biofilms: Pathogenesis and Potential Therapies. Laboratory Medicine. 2015;46(4):277-84.

82.   Melaiye A, Youngs WJ. Silver and its application as an antimicrobial agent. Expert Opinion on Therapeutic Patents. 2005;15(2):125-30.

83.   Gopal A, Kant V, Gopalakrishnan A, Tandan SK, Kumar D. Chitosan-based copper nanocomposite accelerates healing in excision wound model in rats. Eur J Pharmacol. 2014;731:8-19.

84.   Randeria PS, Seeger MA, Wang XQ, Wilson H, Shipp D, Mirkin CA, et al. siRNA-based spherical nucleic acids reverse impaired wound healing in diabetic mice by ganglioside GM3 synthase knockdown. Proceedings of the National Academy of Sciences of the United States of America. 2015;112(18):5573-8.

85.   Zheng H, Dayton PA, Caskey C, Zhao S, Qin S, Ferrara KW. Ultrasound-Driven Microbubble Oscillation and Translation Within Small Phantom Vessels. Ultrasound in Medicine & Biology. 2007;33(12):1978-87.

86.   Marmottant P, Hilgenfeldt S. Controlled vesicle deformation and lysis by single oscillating bubbles. Nature. 2003;423:153.

87.   Turánek J, Miller AD, Kauerová Z, Lukáč R, Mašek J, Koudelka Š, et al. Lipid-Based Nanoparticles and Microbubbles – Multifunctional Lipid-Based Biocompatible Particles for in vivo Imaging and Theranostics. 2015.

88.   Dragicevic N, Maibach HI. Percutaneous Penetration Enhancers Physical Methods in Penetration Enhancement: Springer Berlin Heidelberg; 2017.

89.   Unger EC, Porter T, Culp W, Labell R, Matsunaga T, Zutshi R. Therapeutic applications of lipid-coated microbubbles. Advanced Drug Delivery Reviews. 2004;56(9):1291-314.

90.   Leong T, Ashokkumar M, Kentish S. The fundamentals of power ultrasound—a review. Acoust Aust. 2011;39(2):54-63.

91.   Helfield B, Black JJ, Qin B, Pacella J, Chen X, Villanueva FS. Fluid viscosity affects the fragmentation and inertial cavitation threshold of lipid encapsulated microbubbles. Ultrasound in medicine & biology. 2016;42(3):782-94.

92.   Leong TS, Wooster TJ, Kentish SE, Ashokkumar M. Minimising oil droplet size using ultrasonic emulsification. Ultrason Sonochem. 2009;16(6):721-7.

93.   Crum LA, Mason TJ, Reisse JL, Suslick KS. Sonochemistry and Sonoluminescence: Springer Netherlands; 1998.

94.   Farncombe T, Iniewski K. Medical Imaging: Technology and Applications: CRC Press; 2013.

95.   Brennen CE. Cavitation in medicine. Interface Focus. 2015;5(5):20150022.

96.   Apfel RE, Holland CK. Gauging the likelihood of cavitation from short-pulse, low-duty cycle diagnostic ultrasound. Ultrasound Med Biol. 1991;17(2):179-85.

97.   Apfel RE. Acoustic cavitation: a possible consequence of biomedical uses of ultrasound. The British Journal of Cancer Supplement. 1982;5:140-6.

98.   Graham SM, Carlisle R, Choi JJ, Stevenson M, Shah AR, Myers RS, et al. Inertial cavitation to non-invasively trigger and monitor intratumoral release of drug from intravenously delivered liposomes. Journal of Controlled Release. 2014;178:101-7.

99.   Helfield B, Chen X, Watkins SC, Villanueva FS. Biophysical insight into mechanisms of sonoporation. Proceedings of the National Academy of Sciences. 2016;113(36):9983-8.

100.   Negishi Y, Ishii Y, Shiono H, Akiyama S, Sekine S, Kojima T, et al. Bubble Liposomes and Ultrasound Exposure Improve Localized Morpholino Oligomer Delivery into the Skeletal Muscles of Dystrophic mdx Mice. Molecular Pharmaceutics. 2014;11(3):1053-61.

101.   Kinoshita M, Hynynen K. A novel method for the intracellular delivery of siRNA using microbubble-enhanced focused ultrasound. Biochem Biophys Res Commun. 2005;335(2):393-9.

102.   Li T, Tachibana K, Kuroki M, Kuroki M. Gene transfer with echo-enhanced contrast agents: comparison between Albunex, Optison, and Levovist in mice--initial results. Radiology. 2003;229(2):423-8.

103.   Taniyama Y, Tachibana K, Hiraoka K, Aoki M, Yamamoto S, Matsumoto K, et al. Development of safe and efficient novel nonviral gene transfer using ultrasound: enhancement of transfection efficiency of naked plasmid DNA in skeletal muscle. Gene Ther. 2002;9(6):372-80.

104.   Koebis M, Kiyatake T, Yamaura H, Nagano K, Higashihara M, Sonoo M, et al. Ultrasound-enhanced delivery of Morpholino with Bubble liposomes ameliorates the myotonia of myotonic dystrophy model mice. Scientific reports. 2013;3:2242.

105.   Belcik JT, Davidson BP, Xie A, Wu MD, Yadava M, Qi Y, et al. Augmentation of Muscle Blood Flow by Ultrasound Cavitation Is Mediated by ATP and Purinergic Signaling. Circulation. 2017;135(13):1240-52.

106.   Administration UFaD. Information for Healthcare Professionals: Micro-bubble Contrast Agents (marketed as Definity (Perflutren Lipid Microsphere) Injectable Suspension and Optison (Perflutren

Protein-Type A Microspheres for Injection) 15/08/2013 [cited 2016 22/06/2016]. Available from: http://www.fda.gov/Drugs/DrugSafety/PostmarketDrugSafetyInformationforPatientsandProviders/ucm125574.htm.

107.   Sontum PC. Physicochemical Characteristics of Sonazoid™, A New Contrast Agent for Ultrasound Imaging. Ultrasound in Medicine & Biology. 2008;34(5):824-33.

108.   Galema TW, Geleijnse ML, Vletter WB, de Laat L, Michels M, ten Cate FJ. Clinical usefulness of SonoVue contrast echocardiography: the Thoraxcentre experience. Netherlands Heart Journal. 2007;15(2):55-60.

109.   Agency EM. ANNEX I SUMMARY OF PRODUCT CHARACTERISTICS [cited 2016 03/07]. Available from: http://www.ema.europa.eu/docs/en_GB/document_library/EPAR_-_Product_Information/human/000303/WC500055380.pdf.

110.   Kim J, Lindsey BD, Chang WY, Dai X, Stavas JM, Dayton PA, et al. Intravascular forward-looking ultrasound transducers for microbubble-mediated sonothrombolysis. Scientific reports. 2017;7(1):3454.

111.   Yin T, Wang P, Li J, Zheng R, Zheng B, Cheng D, et al. Ultrasound-sensitive siRNA-loaded nanobubbles formed by hetero-assembly of polymeric micelles and liposomes and their therapeutic effect in gliomas. Biomaterials. 2013;34(18):4532-43.

112.   Wu SK, Chu PC, Chai WY, Kang ST, Tsai CH, Fan CH, et al. Characterization of Different Microbubbles in Assisting Focused Ultrasound-Induced Blood-Brain Barrier Opening. Scientific reports. 2017;7:46689.

113.   Yue T, Xu H-L, Chen P-P, Zheng L, Huang Q, Sheng W-S, et al. Combination of coenzyme Q10-loaded liposomes with ultrasound targeted microbubbles destruction (UTMD) for early theranostics of diabetic nephropathy. International Journal of Pharmaceutics. 2017;528(1–2):664-74.

114.   Zhou Q, Lam KH, Zheng H, Qiu W, Shung KK. Piezoelectric single crystals for ultrasonic transducers in biomedical applications. Progress in materials science. 2014;66:87-111.

115.   Bellew JW, Michlovitz SL, Nolan T. Modalities for therapeutic intervention / [edited by] James W. Bellew, PT, EdD, Professor, Krannert School of Physical Therapy, University of Indianapolis, Indianapolis, IN, Susan L. Michlovitz, PT, PhD, CHT, Adjunct Associate Professor, Rehabilitation Medicine, Columbia University, New York, NY, Thomas P. Nolan Jr., PT, DPT, OCS, Associate Professor, School of Health Sciences, Stockton University, Galloway, NJ. Sixth edition.. ed. ProQuest, editor. Philadelphia, PA: Philadelphia, PA : F.A. Davis Company; 2016.

116.   Steiss JE, McCauley L. Chapter 19 - Therapeutic Ultrasound A2 - Millis, Darryl L. In: Levine D, Taylor RA, editors. Canine Rehabilitation & Physical Therapy. Saint Louis: W.B. Saunders; 2004. p. 324-36.

117.   Pinton G, Pernot M, Bossy E, Aubry JF, Muller M, Tanter M, editors. Mechanisms of attenuation and heating dissipation of ultrasound in the skull bone: Comparison between simulation models and experiments. 2010 IEEE International Ultrasonics Symposium; 2010 11-14 Oct. 2010.

118.   Hangiandreou NJ. AAPM/RSNA physics tutorial for residents. Topics in US: B-mode US: basic concepts and new technology. Radiographics : a review publication of the Radiological Society of North America, Inc. 2003;23(4):1019-33.

119.   S. AJ, B. BS, A. DF, D. EP, H. HK, C. ZM. Fetal Thermal Effects of Diagnostic Ultrasound. Journal of Ultrasound in Medicine. 2008;27(4):541-59.

120.   Afadzi M, Strand SP, Nilssen EA, Masoy SE, Johansen TF, Hansen R, et al. Mechanisms of the ultrasound-mediated intracellular delivery of liposomes and dextrans. IEEE transactions on ultrasonics, ferroelectrics, and frequency control. 2013;60(1):21-33.

121.   Miller DL. Gas body activation. Ultrasonics. 1984;22(6):259-60.

122.   Miller D, Smith N, Bailey M, Czarnota G, Hynynen K, Makin I, et al. Overview of Therapeutic Ultrasound Applications and Safety Considerations. Journal of ultrasound in medicine : official journal of the American Institute of Ultrasound in Medicine. 2012;31(4):623-34.

123.   Şen T, Tüfekçioğlu O, Koza Y. Mechanical index. Anatolian Journal of Cardiology. 2015;15(4):334-6.

124.   Conner-Kerr T, Oesterle ME. Current perspectives on therapeutic ultrasound in the management of chronic wounds: a review of evidence. Chronic Wound Care Management and Research. 2017:89-98.

125.   Ultrasound in Wound Healing: Physiopedia; [cited 2018 10/02/2018]. Available from: https://www.physio-pedia.com/Ultrasound_in_Wound_Healing.

126.   Webb MS, Boman NL, Wiseman DJ, Saxon D, Sutton K, Wong KF, et al. Antibacterial efficacy against an in vivo Salmonella typhimurium infection model and pharmacokinetics of a liposomal ciprofloxacin formulation. Antimicrobial agents and chemotherapy. 1998;42(1):45-52.

127.   Zhang H. Thin-Film Hydration Followed by Extrusion Method for Liposome Preparation. Methods Mol Biol. 2017;1522:17-22.

128.   Torchilin VP, Weissig V. Liposomes : a practical approach / edited by Vladimir Torchilin and Volkmar Weissig. 2nd ed.. ed. Oxford ; New York: Oxford ; New York : Oxford University Press; 2003.

129.   Thakur SS, Ward MS, Popat A, Flemming NB, Parat MO, Barnett NL, et al. Stably engineered nanobubbles and ultrasound - An effective platform for enhanced macromolecular delivery to representative cells of the retina. PloS one. 2017;12(5):e0178305.

130.   Smolen JE. Liposomes in the Study of Membrane Fusion in Neutrophils. Methods in Enzymology. 372: Academic Press; 2003. p. 300-19.

131.   Diamond JP, White L, Leeming JP, Bing Hoh H, Easty DL. Topical 0.3% ciprofloxacin, norfloxacin, and ofloxacin in treatment of bacterial keratitis: a new method for comparative evaluation of ocular drug penetration. The British Journal of Ophthalmology. 1995;79(6):606-9.

132.   Conley J, Yang H, Wilson T, Blasetti K, Di Ninno V, Schnell G, et al. Aerosol delivery of liposome-encapsulated ciprofloxacin: aerosol characterization and efficacy against Francisella tularensis infection in mice. Antimicrobial agents and chemotherapy. 1997;41(6):1288-92.

133.   Oh YK, Nix DE, Straubinger RM. Formulation and efficacy of liposome-encapsulated antibiotics for therapy of intracellular Mycobacterium avium infection. Antimicrobial agents and chemotherapy. 1995;39(9):2104-11.

134.   Hoffmann G. Improvement of Wound Healing in Chronic Ulcers by Hyperbaric Oxygenation and by Waterfiltered Ultrared a Induced Localized Hyperthermia. In: Vaupel P, Zander R, Bruley DF, editors. Oxygen Transport to Tissue XV. Boston, MA: Springer US; 1994. p. 181-8.

135.   Siddiqui AR, Bernstein JM. Chronic wound infection: facts and controversies. Clinics in dermatology. 2010;28(5):519-26.

136.   Lipsky BA, Hoey C. Topical Antimicrobial Therapy for Treating Chronic Wounds. Clinical Infectious Diseases. 2009;49(10):1541-9.

137.   Dobrynin D, Fridman G, Friedman G, Fridman AA. Deep Penetration into Tissues of Reactive Oxygen Species Generated in Floating-Electrode Dielectric Barrier Discharge (FE-DBD): An In Vitro Agarose Gel Model Mimicking an Open Wound. 2012;2(1-3):71-83.

138.   Serra R, Grande R, Butrico L, Rossi A, Settimio UF, Caroleo B, et al. Chronic wound infections: the role of Pseudomonas aeruginosa and Staphylococcus aureus. Expert review of anti-infective therapy. 2015;13(5):605-13.

139.   Buchanan K, Heimbach DM, Minshew BH, Coyle MB. Comparison of quantitative and semiquantitative culture techniques for burn biopsy. Journal of Clinical Microbiology. 1986;23(2):258-61.

140.   Strober W. Trypan blue exclusion test of cell viability. Current protocols in immunology. 2001;Appendix 3:Appendix 3B.

141.   Dong Y, Chen S, Wang Z, Peng N, Yu J. Synergy of ultrasound microbubbles and vancomycin against Staphylococcus epidermidis biofilm. J Antimicrob Chemother. 2013;68(4):816-26.

142.   Guo H, Wang Z, Du Q, Li P, Wang Z, Wang A. Stimulated phase-shift acoustic nanodroplets enhance vancomycin efficacy against methicillin-resistant Staphylococcus aureus biofilms. Int J Nanomedicine. 2017;12:4679-90.

143.   Ikeda-Dantsuji Y, Feril LB, Jr., Tachibana K, Ogawa K, Endo H, Harada Y, et al. Synergistic effect of ultrasound and antibiotics against Chlamydia trachomatis-infected human epithelial cells in vitro. Ultrason Sonochem. 2011;18(1):425-30.

144.   Larina IV, Evers BM, Esenaliev RO. Optimal drug and gene delivery in cancer cells by ultrasound-induced cavitation. Anticancer research. 2005;25(1a):149-56.

145.   Thakur SS, Ward MS, Popat A, Flemming NB, Parat M-O, Barnett NL, et al. Stably engineered nanobubbles and ultrasound - An effective platform for enhanced macromolecular delivery to representative cells of the retina. PloS one. 2017;12(5):e0178305.

146.   Pitt WG, Husseini GA, Staples BJ. Ultrasonic Drug Delivery – A General Review. Expert opinion on drug delivery. 2004;1(1):37-56.

147.   Ohl C-D, Arora M, Ikink R, de Jong N, Versluis M, Delius M, et al. Sonoporation from Jetting Cavitation Bubbles. Biophysical Journal. 2006;91(11):4285-95.

148.   Steed ME, Werth BJ, Ireland CE, Rybak MJ. Evaluation of the novel combination of high-dose daptomycin plus trimethoprim-sulfamethoxazole against daptomycin-nonsusceptible methicillin-resistant Staphylococcus aureus using an in vitro pharmacokinetic/pharmacodynamic model of simulated endocardial vegetations. Antimicrobial agents and chemotherapy. 2012;56(11):5709-14.

149.   Tran S-L, Puhar A, Ngo-Camus M, Ramarao N. Trypan Blue Dye Enters Viable Cells Incubated with the Pore-Forming Toxin HlyII of Bacillus cereus. PloS one. 2011;6(9):e22876.

150.   Ben-Porath I, Weinberg RA. The signals and pathways activating cellular senescence. The International Journal of Biochemistry & Cell Biology. 2005;37(5):961-76.

151.   Demidova-Rice TN, Hamblin MR, Herman IM. Acute and impaired wound healing: pathophysiology and current methods for drug delivery, part 1: normal and chronic wounds: biology, causes, and approaches to care. Adv Skin Wound Care. 2012;25(7):304-14.

152.   Panuncialman J, Falanga V. The science of wound bed preparation. Clinics in plastic surgery. 2007;34(4):621-32.

153.   Sherman RA. Maggot versus conservative debridement therapy for the treatment of pressure ulcers. Wound repair and regeneration : official publication of the Wound Healing Society [and] the European Tissue Repair Society. 2002;10(4):208-14.

154.   Attinger C, Wolcott R. Clinically Addressing Biofilm in Chronic Wounds. Advances in Wound Care. 2012;1(3):127-32.

155.   Outi S, Danail O, Philippe K, Mohamed F. Detailed Jet Dynamics in a Collapsing Bubble. Journal of Physics: Conference Series. 2015;656(1):012038.

156.   Murray PRP, Rosenthal KSP, Pfaller MAMD. Bacterial Classification, Structure, and Replication. In: Murray PRP, Rosenthal KSP, Pfaller MAMD, editors. Medical Microbiology2016. p. 105-18.e2.

157.   Sakai K. Dialysis membranes for blood purification. Frontiers of medical and biological engineering : the international journal of the Japan Society of Medical Electronics and Biological Engineering. 2000;10(2):117-29.

158.   Ryan KJ. Pseudomonas and Other Opportunistic Gram-negative Bacilli. Sherris Medical Microbiology, 7e. New York, NY: McGraw-Hill Education; 2017.

159.   Beveridge TJ. Structures of Gram-Negative Cell Walls and Their Derived Membrane Vesicles. Journal of Bacteriology. 1999;181(16):4725-33.

160.   Chen A, Moy VT. Cross-linking of cell surface receptors enhances cooperativity of molecular adhesion. Biophys J. 2000;78(6):2814-20.

161.   Spierings E, De Boer T, Zulianello L, Ottenhoff TH. The role of Schwann cells, T cells and Mycobacterium leprae in the immunopathogenesis of nerve damage in leprosy. Leprosy review. 2000;71 Suppl:S121-9.

162.   SUZUKI K, AKAMA T, KAWASHIMA A, YOSHIHARA A, YOTSU RR, ISHII N. Current status of leprosy: Epidemiology, basic science and clinical perspectives. The Journal of Dermatology. 2012;39(2):121-9.

163.   Yang D, Shui T, Miranda JW, Gilson DJ, Song Z, Chen J, et al. Mycobacterium leprae-Infected Macrophages Preferentially Primed Regulatory T Cell Responses and Was Associated with Lepromatous Leprosy. PLoS Neglected Tropical Diseases. 2016;10(1):e0004335.

164.   Silhavy TJ, Kahne D, Walker S. The Bacterial Cell Envelope. Cold Spring Harbor Perspectives in Biology. 2010;2(5):a000414.

165.   Salton MRJ KK. Structure. S B, editor: Medical Microbiology. 4th edition. Galveston (TX): University of Texas Medical Branch at Galveston; 1996.

166.   Kohanski MA, Dwyer DJ, Collins JJ. How antibiotics kill bacteria: from targets to networks. Nature reviews Microbiology. 2010;8(6):423-35.

167.   Delcour AH. Outer Membrane Permeability and Antibiotic Resistance. Biochimica et biophysica acta. 2009;1794(5):808-16.

168.   Tam Thanh N, Yoshiyuki A, Nagaya O, Shinobu K, Keiji Y. Effect of ultrasonic cavitation on measurement of sound pressure using hydrophone. Japanese Journal of Applied Physics. 2017;56(7S1):07JE6.

169.   Thanh Nguyen T, Asakura Y, Koda S, Yasuda K. Dependence of cavitation, chemical effect, and mechanical effect thresholds on ultrasonic frequency. Ultrasonics Sonochemistry. 2017;39:301-6.

170.   Podbevsek D, Colombet D, Ledoux G, Ayela F. Observation of chemiluminescence induced by hydrodynamic cavitation in microchannels. Ultrasonics Sonochemistry. 2018;43:175-83.

171.   Levkovskii YL, Il'in VP. Effect of surface tension and viscosity on the collapse of a cavitation bubble. Journal of engineering physics. 1968;14(5):478-80.

172.   Kuvshinov GI. Effect of surface tension on the collapse of a cavitation bubble. Journal of engineering physics. 1991;60(1):34-7.

173.   Pan Z, Kiyama A, Tagawa Y, Daily DJ, Thomson SL, Hurd R, et al. Cavitation onset caused by acceleration. Proceedings of the National Academy of Sciences. 2017;114(32):8470-4.